



University
of Glasgow

<https://theses.gla.ac.uk/>

Theses Digitisation:

<https://www.gla.ac.uk/myglasgow/research/enlighten/theses/digitisation/>

This is a digitised version of the original print thesis.

Copyright and moral rights for this work are retained by the author

A copy can be downloaded for personal non-commercial research or study,
without prior permission or charge

This work cannot be reproduced or quoted extensively from without first
obtaining permission in writing from the author

The content must not be changed in any way or sold commercially in any
format or medium without the formal permission of the author

When referring to this work, full bibliographic details including the author,
title, awarding institution and date of the thesis must be given

Enlighten: Theses

<https://theses.gla.ac.uk/>
research-enlighten@glasgow.ac.uk

INTERACTION OF THE EFFECTS OF HYPERTHERMIA
AND IONIZING RADIATION ON CELL SURVIVAL

Thesis presented to the University of Glasgow
for the Degree of Ph.D.

September, 1976

David D. Loshek, B.S., M.S.,
Department of Clinical Physics and Bio-engineering,
West of Scotland Health Boards,
11 West Graham Street,
Glasgow.

ProQuest Number: 10647512

All rights reserved

INFORMATION TO ALL USERS

The quality of this reproduction is dependent upon the quality of the copy submitted.

In the unlikely event that the author did not send a complete manuscript and there are missing pages, these will be noted. Also, if material had to be removed, a note will indicate the deletion.



ProQuest 10647512

Published by ProQuest LLC (2017). Copyright of the Dissertation is held by the Author.

All rights reserved.

This work is protected against unauthorized copying under Title 17, United States Code
Microform Edition © ProQuest LLC.

ProQuest LLC.
789 East Eisenhower Parkway
P.O. Box 1346
Ann Arbor, MI 48106 – 1346

Thesis
4632
Copy 2.



CONTENTS

	<u>Page</u>
ILLUSTRATIONS	vii
TABLES	xi
ACKNOWLEDGEMENTS	xii
SUMMARY	xiii
<u>Chapter 1</u> THE FIELD OF INVESTIGATION	
1.1 Cellular Survival	1
1.2 The Effect of Radiation on Cell Survival	3
1.2.1 Single Cell Survival Curves	3
1.2.2 The Effect of Oxygen	5
1.2.3 The Effect of LET	7
1.3 The Effect of Hyperthermia on Cell Survival	9
1.3.1 Single Cell Survival curves	9
1.3.2 The Effect of Oxygen	11
1.3.3 Selective Effects of Hyperthermia	12
1.3.4 The Effects of Cell Cycle Progression	14
1.4 The Interaction of Radiation and Hyperthermia	16
1.4.1 Interaction in Non- Mammalian Systems	16
1.4.2 Interaction in Mammalian Systems	18
1.4.3 Selective Effects of Interaction	19
1.5 Recovery Phenomena	21
1.5.1 Sublethal Damage	21
1.5.2 Interaction Sensitizing Damage	25
1.5.3 Potentially Lethal Damage	26
1.5.4 The Effect of Treat- ment Order	28
1.6 Conclusion	29

<u>Chapter 2</u>	MATERIALS AND METHODS	
2.1	Materials	30
	2.1.1 Cell Line	30
	2.1.2 Media	30
	2.1.3 Cell Maintenance	32
2.2	Experimental Procedures	34
2.3	Hyperthermia Techniques	36
	2.3.1 Heating Techniques	36
	2.3.2 Thermometry	39
2.4	Irradiation Techniques	39
	2.4.1 ^{60}Co Gamma Radiation	39
	2.4.2 X-radiation	40
	2.4.3 Neutron Radiation	41
	2.4.4 Dosimetry	42
<u>Chapter 3</u>	PRELIMINARY EXPERIMENTS	
3.1	Introduction	43
3.2	Experimental Stability	44
3.3	The Effects of Hyperthermia on Cell Survival	46
	3.3.1 Hyperthermia Survival Curves	46
	3.3.2 The Effect of Temperature on Thermal- Sensitivity	46
	3.3.3 Discussion	48
3.4	The Interaction of Radiation and Hyperthermia	49
	3.4.1 Sensitization of Radiation Response by Hyperthermia	49
	3.4.2 Interaction Relaxation	51
	3.4.3 Sensitization of Hyperthermia Response by Radiation	53
	3.4.4 The Effect of Hyperthermia Dose on Radiation Sensitivity	53
	3.4.5 The Effect of Temperature on Sensitization of Radiation Response	54
	3.4.6 The Effect of Temperature on Sensitization of Hyperthermia Response	55
	3.4.7 Discussion	55

<u>Chapter 4</u>	SURVIVAL SURFACE AND THE MATRIX EXPERIMENT	
4.1	Introduction	58
4.2	Theory	59
	4.2.1 A Minimal Model of Interaction	59
	4.2.2 The Survival Surface	65
	4.2.3 First Order Inter- action Model	68
4.3	Matrix Experiment	70
	4.3.1 Experimental Procedure	70
	4.3.2 Data Analysis	72
	4.3.3 Experimental Results	74
	4.3.4 Discussion	76
	4.3.5 Conclusion	80
<u>Chapter 5</u>	THE EFFECT OF RADIATION QUALITY	
5.1	Introduction	81
5.2	The Experiment	82
	5.2.1 Experimental Procedure	82
	5.2.2 Results	83
5.3	Discussion	86
	5.3.1 Comparison of Analytical Methods	86
	5.3.2 Comparison of Radiation Qualities	87
	5.3.3 The Effect of Dose Rate	88
	5.3.4 A Theory of High LET Radiation Action in Relation to Interaction	89
<u>Chapter 6</u>	THE EFFECT OF TEMPERATURE	
6.1	Introduction	93
6.2	The Experiment	94
	6.2.1 Experimental Procedure	94
	6.2.2 Experimental Results	96
	6.2.3 Limitations of the Experimental Data	98
	6.2.4 Discussion	98
6.3	Thermodynamics of Thermal Sterilization	103
	6.3.1 Theory of Absolute Reaction Rates	103

6.3.2	A Model for Protein Denaturation	106
6.3.3	Compensation Phenomena	109
6.3.4	The Effect of Water on Conformation Reactions	113
6.3.5	The Effect of Pressure on Conformation Reactions	115
6.3.6	Summary of the Evidence for the Implication of Protein Denaturation in The Thermal Inactivation of Living Organisms	116
6.4	The Thermodynamics of Hyperthermia and Ionizing Radiation Interaction	118
6.4.1	Comparison of the Observed Thermodynamic Parameters	118
6.4.2	Interaction as a Compensation Phenomenon	123
6.4.3	Conclusion	127
<u>Chapter 7</u>	CONCLUSION	
7.1	Introduction	129
7.2	A Final Experiment	130
7.2.1	Experiment Design	130
7.2.2	Results	132
7.2.3	Discussion	133
7.3	Conclusions	135
7.3.1	Firm Conclusions	135
7.3.2	Supported Conclusions	135
7.4	Future Developments	136
7.4.1	High LET Interaction	136
7.4.2	Temperature Sensitivity of Interaction	137
7.4.3	Interaction Relaxation	137
7.4.4	The Oxygen Effect	138
7.5	The Application of the Component Approach to the In Vivo Situation	138
<u>Appendix I</u>		
I 1	The Effects of Hyperthermia at the Subcellular Level	143

I 1.1	The Effects of Hyperthermia on Cellular Respiration	143
I 1.2	The Effects of Hyperthermia on Nucleic Acid and Protein Synthesis	147
I 1.3	The Effects of Hyperthermia on Membranes and Lysosomes	154
I 1.4	The Effects of Hyperthermia on the Mitotic Cycle and Mitosis	157
I 2	The Effects of Hyperthermia on Chromosomes and the Repair of DNA Damage	

Appendix II MATERIALS AND METHODS

II 1	Cell Media and Reagents
II 2	Trypsinization Procedure
II 3	Chromosome Preparations
II 4	Labelling Index

Appendix III MISCELLANEOUS OBSERVATIONS

III 1	The Effect of Hyperthermia on Elkind Repair
III 2	The Effect of Cell Age on Interaction

Appendix IV SIMPLEX PROGRAM

ILLUSTRATIONS

Chapter 1

- Figure 1.1 X-ray survival curve for HeLa cells.
- Figure 1.2 X-ray survival curves for Chinese hamster cells in the presence of various oxygen concentrations.
- Figure 1.3 Survival curves for Chinese hamster cells exposed to neutrons of various energy.
- Figure 1.4 Hyperthermia survival curves for pig kidney cells.
- Figure 1.5 Temperature dependence of the deuteron inactivation for dry catalase.
- Figure 1.6 Temperature dependence of x-radiation inactivation for *Bacillus megaterium*.
- Figure 1.7 Survival of Chinese hamster cells x-irradiated at different temperatures.
- Figure 1.8 Survival curve and split dose recovery curve.
- Figure 1.9 A fractionated survival curve for Chinese hamster cells.
- Figure 1.10 Cell survival curves for Chinese hamster ovary cells given heat treatments in two exposures.

Chapter 2

- Figure 2.1 Perspex rack for holding T30 flasks submerged.
- Figure 2.2 Configuration for simultaneous heating and irradiation technique.

Chapter 3

- Figure 3.1 CHO hyperthermia survival curve, method A.

- Figure 3.2 CHO hyperthermia survival curve, method B.
- Figure 3.3 Arrhenius plot of mammalian cell inactivation rates.
- Figure 3.4 Heating and irradiation schedule for the data of figure 3.5.
- Figure 3.5 CHO survival after simultaneous and separated heating and radiation.
- Figure 3.6 CHO cell survival and radiation inactivation rate against time separating radiation and hyperthermia dose.
- Figure 3.7 CHO survival after hyperthermia (44°) alone or followed 5 minutes later by 3.5 Gy ^{60}Co .
- Figure 3.8 Heating and irradiation schedule for the data in figures 3.9 and 3.10.
- Figure 3.9 Relative radiosensitivity and relative plating efficiency for a hyperthermia exposure for t minutes at 42°C .
- Figure 3.10 Relative radiosensitization and relative plating efficiency for irradiation during a seven minute exposure at a temperature T .
- Figure 3.11 Relative thermal-sensitization for a radiation dose of 4 Gy at a temperature T .

Chapter 4

- Figure 4.1 Hypothetical iso-survival plot assuming no interaction.
- Figure 4.2 Hypothetical survival surface.
- Figure 4.3 CHO survival H-3min.- Y.

- Figure 4.4 Survival curve parameters H-3min.- γ .
- Figure 4.5 Iso-survival contours H-3min.- γ .
- Figure 4.6 Survival curve slopes for CHL cells as a function of time at 42°C.

Chapter 5

- Figure 5.1 CHO survival γ -100min.-H (42°).
- Figure 5.2 CHO survival X-100min.-H (42°).
- Figure 5.3 CHO survival n-100min.-H (42°).
- Figure 5.4 Radiation survival curve parameters radiation - 100min.-H.
- Figure 5.5 Hyperthermia survival curve parameters radiation - 100min.-H.
- Figure 5.6 Iso-survival contours radiation - 100min.-H.

Chapter 6

- Figure 6.1 CHO survival X-100min.-H (42°).
- Figure 6.2 CHO survival X-100min.-H (43°).
- Figure 6.3 CHO survival X-100min.-H (44°)
- Figure 6.4 CHO survival X-100min.-H (45°)
- Figure 6.5 Radiation inactivation rate X-100min.-H (T°).
- Figure 6.6 Hyperthermia inactivation rate X-100min.-H (T°).
- Figure 6.7 Activation enthalpy for hyperthermia inactivations X-100min.-H (T°).
- Figure 6.8 Arrhenius plot of the temperature dependent parameters of equation 6.1.

- Figure 6.9 | Schematic representation of the mechanism of protein denaturation.
- Figure 6.10 Iso-kinetic plots for protein and living organism inactivation by heat.

Chapter 7

- Figure 7.1 Hyperthermia survival 100 minutes after three Gy radiation at high and low dose rate.
- Figure 7.2 Hypothetical iso-response curve for in vivo test system.

Appendix III

- Figure III.1 The effect of hyperthermia on Elkind repair.
- Figure III.2 Radiation and hyperthermia interaction as a function of cell age.
- Figure III.3 Sensitization curves with sensitivity dependent on cell age.
- Figure III.4 Sensitization curves with extrapolation number dependent on cell age.
- Figure III.5 Sensitization curves with both extrapolation number and sensitivity dependent on cell age.
- Figure III.6 Sensitization curves with sensitivity dependent on cell age to varying degrees.

TABLES

Table 3.1	Long term stability of radiation and hyperthermia survival response.
Table 3.2	Radiation survival curve parameters for simultaneous and separated interaction.
Table 4.1	Interaction parameters for H-3min-Y.
Table 5.1	Interaction parameters (eqn 4.11) radiation-100min-H.
Table 5.2	Interaction parameters (unbiased) radiation-100min-H.
Table 6.1	Interaction parameters x-100min-H.
Table 6.2	Activation enthalpy for interaction parameters.
Table 6.3	Thermodynamic parameters for Sindbis virus inactivation denaturation.
Table 6.4	Thermodynamic parameters for protein denaturation.
Table 6.5a	Thermodynamic parameters for mammalian cell inactivation.
Table 6.5b	Thermodynamic parameters for protein and virus.
Table 6.6	Thermodynamic parameters for virus inactivation by heat and ionizing radiation.
Table 6.7	CHO cell inactivation by heat and ionizing radiation.
Table 7.1	Hyperthermia survival curve parameters 100 minutes after 3 Gy radiation at high and low dose rate.

Acknowledgements

This thesis is the result of a collaborative effort. Professor J.M.A. Lenihan and Mr. J. McKie (Department of Clinical Physics and Bio-Engineering, Glasgow) provided support and encouragement. Dr. K.E. Halnan (Glasgow Institute of Radiotherapeutics) provided the research premises. The work was inspired by Dr. J.S. Orr (D.C.P.B.). Drs. R. Lawson and D. Porter (D.C.P.B.) provided the neutron irradiations and performed the neutron dosimetry. Useful discussions were had with Drs. H. Porter (G.I.R.), R. Lawson, D. Porter, J. Kirk, T. Wheldon (D.C.P.B.), A.H.W. Nias, (G.I.R.), I. Szumiel (Institute for Nuclear Research, Warsaw), and Mr. R. Hamlet (G.I.R.). Mr. D. Craig (D.C.P.B.) assisted in the literature search. Mrs. S. McEwan (G.I.R.) assisted in technical aspects. Mrs. M. Findlayson did the photographic work. My wife prepared the diagrams and was responsible for the layout. Mrs. M. Donnelly typed the thesis. Parts of the thesis were read by Mrs. E. Solomonidis (D.C.P.B.) and Dr. R. Lawson.

The author is grateful for all of the above and especially for the long hours devoted by Mrs. E. Solomonidis to this project.

Summary

Chapter one contains a brief review of the literature concerning the effects of hyperthermia and radiation on cellular reproductive integrity.

Chapter two describes the cell line used and the physical and biological aspects of the experiments.

The preliminary experiments of chapter three revealed that the experimental stability was adequate for inter-experiment comparisons, provided that sufficient control data were obtained. Further experiments provided a cursory examination of several aspects of the interaction between radiation and hyperthermia.

In chapter four, a simple sensitization model that would account for the observed results for any single value of the perturbing radiation or hyperthermia dose is developed. Using the concept of the survival surface, this simple model is expanded to simultaneously describe survivals for any combination of the radiation and hyperthermia dose. The resulting first order interaction model, while only approximately describing the survival surface, is nevertheless useful in providing a coherent picture of the results of chapter three.

The interaction component of this model is first order in both hyperthermia exposure and radiation dose. The mechanism by which radiation contributes to the interaction was investigated by altering the radiation quality. The results of this investigation, presented in chapter five, suggest that high LET events contribute to the interaction.

The mechanism by which hyperthermia contributes to the interaction was investigated by altering the hyperthermia temperature. A thermodynamic analysis of the data, presented in chapter six, reveals parallels with the effects of hyperthermia and radiation on protein, suggesting a possible involvement of protein denaturation in cell inactivation.

Chapter seven contains concluding remarks and suggestions for extended applications of the survival surface approach. These include an in vivo application of the theory that might provide the data required for clinical application.

CHAPTER ONE

THE FIELD OF INVESTIGATION

1.1 Cellular Survival

A review of the biochemical and biophysical effects of hyperthermia and radiation on a variety of living organisms is contained in Appendix I. These observations can best be described as dynamic phenomena in that the time of observation is a critical factor in the observation. All of these effects will, however, be expected to be resolved either as a return to the control behaviour, possibly after repeated cell divisions, or entrance to a permanent state of malfunction, either as a cause of, or caused by, the cellular failure to reproduce.

In contrast, the state of cellular reproductive integrity, of crucial importance in cancer therapy, can be demonstrated to be a deterministic state of which observations are theoretically time independent after a sufficient interval. These ideal properties of time independence and determinism have led to the application of many stochastic models of cellular reproductive integrity.

In this thesis, the theoretical end point for most experiments is the loss of reproductive integrity. The experimental end point is the loss of ability to form a macroscopic colony of cells in a specified period of time.

The individual cells that are not able to form a macroscopic colony fall into three categories. In the first place, there are cells that are "killed" immediately upon, or shortly after radiation or heating. The term "interphase death" has been applied and implies a rapid lysis of the cell. Secondly, there are those cells that remain metabolically active, but are only capable of a limited number of cell divisions. Finally, there are those cells both metabolically active and clonegenically competent, but only capable of substantially reduced or delayed cell division.

Experimentally as well as clinically, the third category of cells presents problems and experiments and treatments must be designed to minimise these problems. The first class of cells, cells affected by interphase death, are of minor importance in successful radiotherapy, but may present genuine problems when hyperthermic treatments are used.

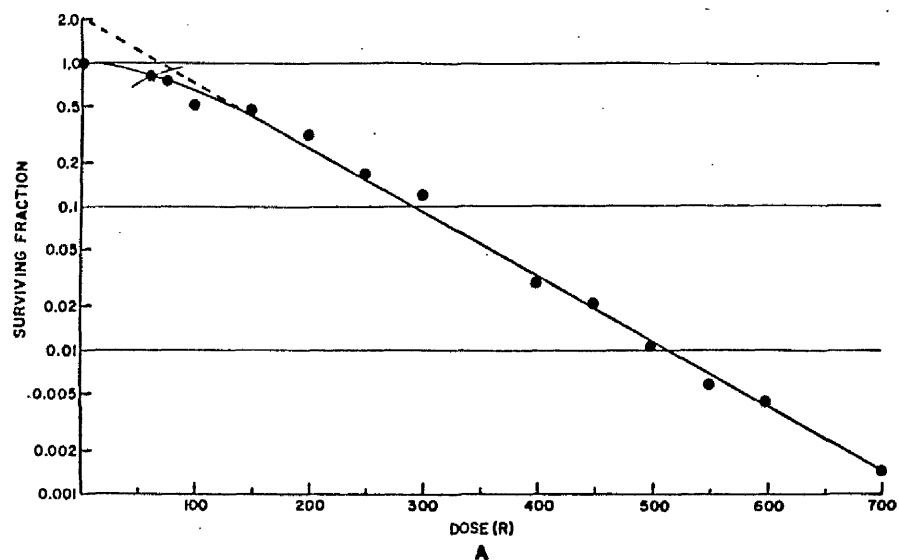


Fig. 1.1 X-ray survival curve for HeLa cells in culture. (from Puck and Markus 1956)

1.2 The Effect of Radiation on Cell Survival

1.2.1 Single Cell Survival Curves

The first in vitro single mammalian cell survival curve was provided by Puck and Markus (1956). This is illustrated in figure 1.1 and displays the features observed in most, but by no means all, mammalian cell survival curves. For survivals below about 20%, the plot of the logarithm of survival against dose is linear indicating an exponential decrease in the probability of survival. The extrapolation of the straight line portion to zero dose intersects the ordinate at a value characteristically greater than unity, called the extrapolation number.

The parameters and symbols used in this thesis to describe the survival curve will be;

K_R the slope of the exponential portion of the survival curve. The dimension of K_R is Gray^{-1} (Gy^{-1})

M_R the extrapolation number, a dimensionless unit

D_q the quasi-threshold dose, the dose at which the extrapolate of the straight line portion of the survival curve intersects the unity survival

level. The dimension of D_q is the Gray (Gy)

The subscripts R on the parameters M and K designate the parameters of the radiation survival curve as opposed to that of the hyperthermia survival curve.

Where no ambiguity will arise these will be omitted.

Survival for a radiation dose D much larger than D_q can be represented by

$$\text{or } S(D) = me^{-DK} \quad 1.1$$

$$S(D) = e^{-(D-D_q)K} \quad 1.2$$

where D is the absorbed dose in Gray units.

Cell survival in the low dose region requires more elaborate expressions which are the subject of a great deal of controversy and will not be dealt with to any extent here.

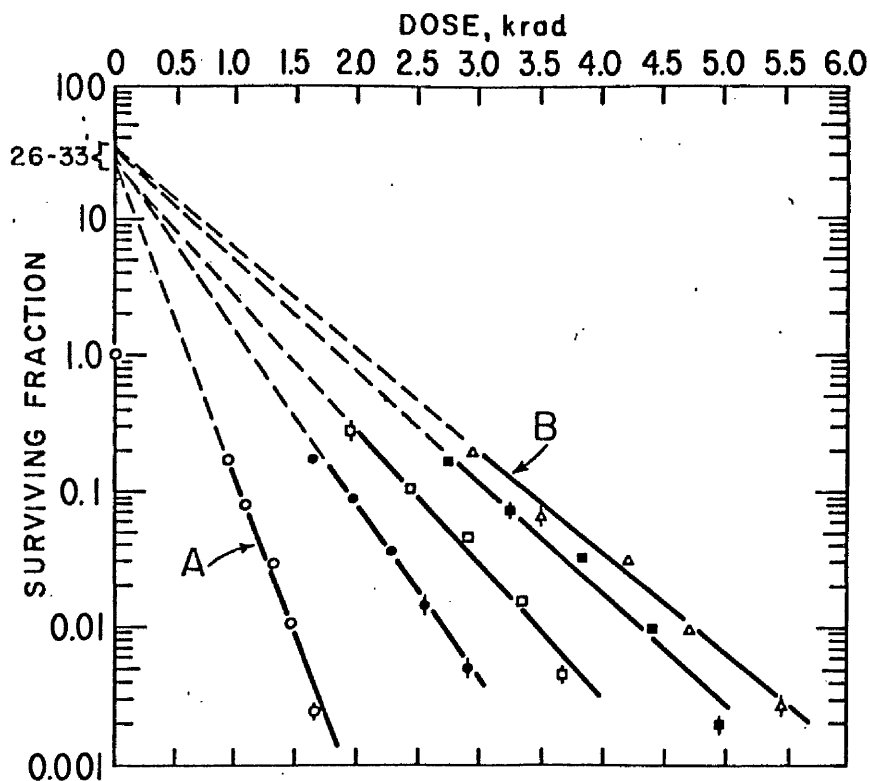


Fig. 1.2. Survival curves for Chinese hamster cells exposed to x-rays in the presence of various oxygen concentrations. Open circles, air; closed circles, 2200 parts per million (ppm) of oxygen or a partial pressure of oxygen of 1.7 mm of mercury; open squares, 355 ppm of oxygen or a partial pressure of 0.25 mm of mercury; closed squares, 100 ppm of oxygen, or a partial pressure of 0.075 mm of mercury; open triangles, 10 ppm of oxygen or a partial pressure of 0.0076 mm of mercury which corresponded to the lowest level of hypoxia which could be obtained. (From Elkind, Swain, Alescio, Sutton, Moses 1963)

1.2.2 The Effect of Oxygen

The effect of oxygen concentration on radio-sensitivity is possibly of critical importance in the clinical situation and offers the radiobiologist additional insight into the nature of the radiolesion. While the different mechanisms involved and effects observed are not fully understood, the presence of molecular oxygen during, or within a very short interval after, irradiation increases the lethal effect of the radiation dose.

Figure 1.2 illustrates survival curves for V79 cells irradiated at various oxygen concentrations. (Elkind et.al. 1965). At these concentrations the effect is primarily on the slope of the survival curve so that oxygen appears to directly modify the damage due to a given dose of radiation. This simple effect of oxygen is characterised in the literature by the parameter OER, oxygen enhancement ratio, which is the ratio of the radiation survival curve slope for the well oxygenated situation to that of the anoxic situation.

At lower concentrations, e.g. less than 2 parts per million, an additional effect on the extrapolation number has been observed (Littbrand and Revesz 1969)

If hypoxia is maintained for long periods similar effects occur. After 24 hours storage at 37° under hypoxic conditions, a reduction of the survival curve extrapolation number to unity has been observed for HeLa cells (Hall, Bedford, and Oliver 1966).

1.2.3. The Effect of LET

The presence of an extrapolation number greater than unity for x-rays indicates a multiple event phenomenon, that is seen to be greatly affected by the ionization density of the charged particles associated with the photon beam. The ionization density is related to the rate of energy loss per unit distance of particle travel, to which is referred to as the linear energy transfer coefficient, LET. As the LET increases, the slopes of the survival curves increase and the extrapolation number decreases until it is unity. Increasing LET eventually results in a decrease in the slope of the survival curve.

A simplistic explanation of these phenomena is that as the LET increases, the probability of registering more than one event in a given volume increases. If the active events require at least a minimum amount of energy, the probability of an event being active increases with LET. The result of this is that for increasing LET, the extrapolation number decreases and the sensitivity, the slope of the survival curve, increases. The sensitivity continues to increase with LET until the LET is high enough to provide, on the average, one active event per particle traversing the target. For LET higher than this, an "overkill"

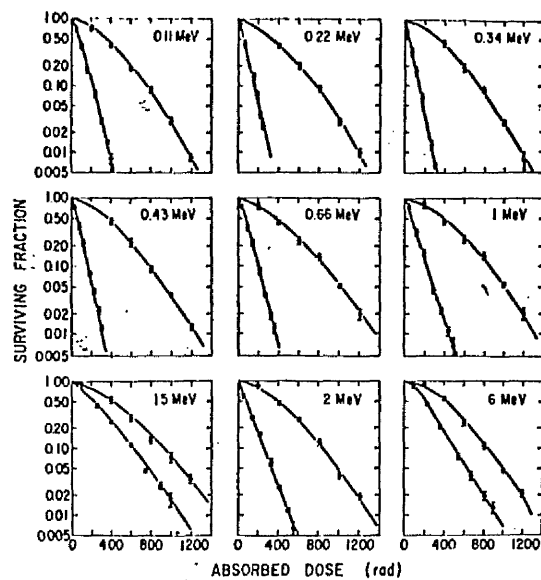


Fig. 1.3. Survival curves for Chinese hamster cells exposed to neutrons of various energy. Each set of data includes a 250 kVp x-ray survival curve. (from Hall et.al. 1975).

situation occurs and more than one active event per particle is registered so that the sensitivity falls.

Figure 1.3 demonstrates the effect on the shape of the neutron survival curve as the LET is increased.

As the direct effect of the radiation energy transfer becomes more effective, the influence of the indirect effect decreases. Therefore the oxygen enhancement ratio decreases for increasing LET, finally reaching a minimum value marginally greater than one.

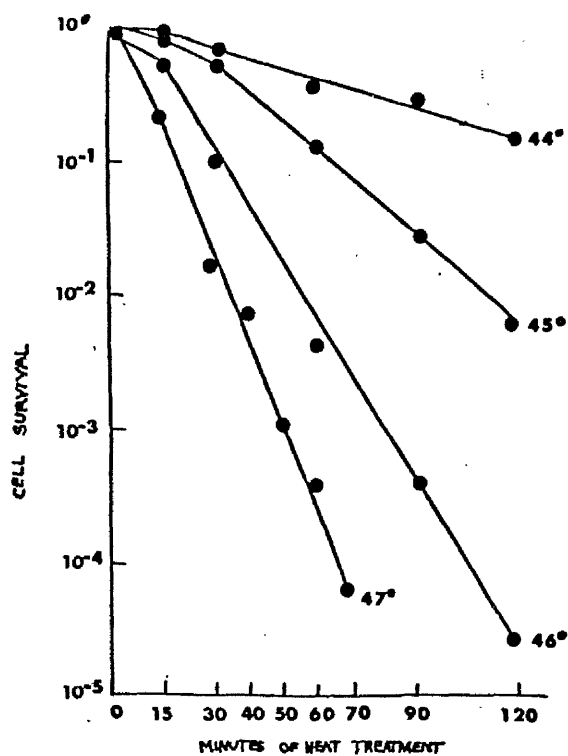


Fig. 1.4. Hyperthermia survival curves for pig kidney cells in culture. (from Harris 1967)

1.3 The Effect of Hyperthermia on Cell Survival

1.3.1. Single Cell Survival Curves

Figure 1.4 illustrates hyperthermia survival curves for pig kidney cells (Harris 1967). For each temperature, the survival as a function of time at the elevated temperature exhibits features similar to those observed for low LET radiation. That is, there exists a shoulder followed by an exponential slope.

While there are exceptions, most of the published survival curves could be characterised by the following parameters;

K_H the slope of the exponential portion of the hyperthermia survival curve. The dimension of K_H is min^{-1} .

M_H the extrapolation number, a dimensionless unit.

t_q the quasi-threshold time, the time at which the extrapolate of the straight line portion of the survival curve intersects the unity survival level. The dimension of t_q is that of time (min).

Survival for exposure times much greater than t_q is described by

$$S = M_H e^{-t K_H}$$

or

$$S = e^{-(t - t_q) K_H}$$

The slope of the hyperthermia survival curve exhibits a strong temperature dependence, roughly doubling for every degree centigrade rise in temperature. (Suit and Shwayder 1974).

This simple behaviour of an exponential decrease in survival following an initial shoulder, has not been observed by all workers. Both Palzer and Heidelberger (1973) and Hall (1976) reported that the survival curves exhibited a biphasic nature, possessing a significantly reduced terminal slope for survivals below the 10% level. Hall further observed that if the dose was fractionated with 21 hours separating the two doses, then the resulting survival curve exhibited a single slope comparable to the initial slope observed in the single dose experiments.

1.3.2. The Effect of Oxygen

Decreased oxygen concentration, possibly a limiting factor in successful radiotherapy due to the increased radioresistance of hypoxic cells, was observed to slightly sensitize cells to hyperthermia inactivation (Gerweck, Gillette, and Dewey 1974). Schulman and Hall(1974) and Harisiadis et.al. (1975) observed a marked protective effect of oxygen on hyperthermia survival, but this was discovered subsequently to be due to insufficient control of pH (Hall 1976). More rigorous control produced results comparable to those observed by Gerweck et.al. (1974).

Crile (1963)observed that tumours implanted in the feet of mice were more heat sensitive when they were large, whereas they were more radiation sensitive when they were small. In the light of the previous OER effects reviewed this behaviour might reflect an oxygen effect.

1.3.3. Selective Effects of Hyperthermia

Lambert (1912) provided probably the first in vitro demonstration of thermal selectivity. Using the hanging plasma drop method of culture, he observed that rat or mouse sarcoma cells were more susceptible than normal connective tissue to temperatures of $42.5^{\circ} - 46^{\circ} \text{ C}$. Levine and Robbins (1970) observed similar responses for several human cell lines. Schrek (1966) observed that leukemic lymphocytes were more susceptible to hyperthermia than normal lymphocytes. Dietzel (1975) reported destruction of Erlich ascites tumour at temperatures which had little effect on normal tissues.

Chen and Heidelberger (1969), Giovanella et.al., (1973), and Kase and Hahn (1975) observed that chemical or virus induced transformations resulted in the transformed cells being more susceptible to hyperthermia.

In contrast there have been a number of negative reports. Harisiadis et.al. (1975) observed almost identical hyperthermia response for a number of normal and neoplastic cell lines that exhibited widely different x-ray survival characteristics.

Ossovski and Sachs (1967) isolated a temperature resistant mutant polyoma virus that could synthesize viral DNA at 41.5° C , and induce cellular DNA synthesis at 41° C . Cells transformed by this virus were able

to multiply at 41^o, whereas normal or non-viral carcinogen transformed cells could not. Kachani and Sabin (1969) similarly observed that virus transformed hamster cell lines were more resistant than normal or physico-chemical transformed lines. However, if the transformation occurred in vivo, or the cells were passaged in vivo, then the differential disappeared.

Harris (1967, 1969) and Reeves (1972) observed thermal resistant strains that had developed from thermal sensitive parents. Thermotolerance, induced by a previous heat treatment, was observed by SeLawry, Goldstein, and McCormick (1957), Gerner and Schneider (1975), Hall (1976) and Henle and Leeper (1976).

Induced thermotolerance or a selection process may have been responsible for the recurrence in hyperthermia resistant forms of previously thermal sensitive tumours observed by Pettigrew et.al. (1974) after whole body hyperthermia.

1.3.4. The Effects of Cell Cycle Progression

Cellular progression through the mitotic cycle has been reported to affect hyperthermia sensitivity. Levine and Robbins(1970) observed increased susceptibility of human diploid lines that were in exponential growth. Dickson and Shah(1972) similarly found exponentially growing SDB cells were more susceptible to hyperthermia than cells in lag phase, that period of intense metabolic activity before growth is resumed after a cellular insult, which in this case was trypsinization. Giovanella and Heidelberger (1968) found dividing L1210 cells more sensitive than static ascites cells. Kase and Hahn (1975) found exponentially growing lung fibroblasts more sensitive than their contact-inhibited counterparts. However, Hahn (1974) observed that Chinese hamster HAl cells were less sensitive in exponential growth than contact-inhibited cells.

Position in the cell cycle influences the effect of hyperthermia. For simplicity, the usual terms described by Howard and Pelc (1953) will be used. Westra and Dewey (1971) observed that Chinese hamster cells in S and M phase were the most sensitive to hyperthermia sterilization. Palzer and Heidelberger(1973) observed similar results with HeLa cells.

Radiation sensitivity as a function of cell age is complementary to that observed in connection with hyperthermia. While M phase is very sensitive to radiation, G_1 phase is more sensitive than S phase (Elkind and Whitmore 1967).

Mitosis is delayed after sublethal doses of radiation or hyperthermia. Division delay after radiation for CHO cells varied from 23 to 80 min/Gy depending on the position in the cell cycle at the time of radiation (Leeper, Schneiderman, and Dewey 1972). Leeper and Henle (1974) found that division delay after hyperthermia on CHO cells was 28.6 min/(min at 45°). Correcting for relative sensitivity, the division delay for a dose giving a reduction of e^{-1} on the exponential portion of the survival curve yields a division delay for hyperthermia nearly twice as long as for radiation. Kal, Hatfield and Hahn (1975) observed similar results for EMT-6 cells.

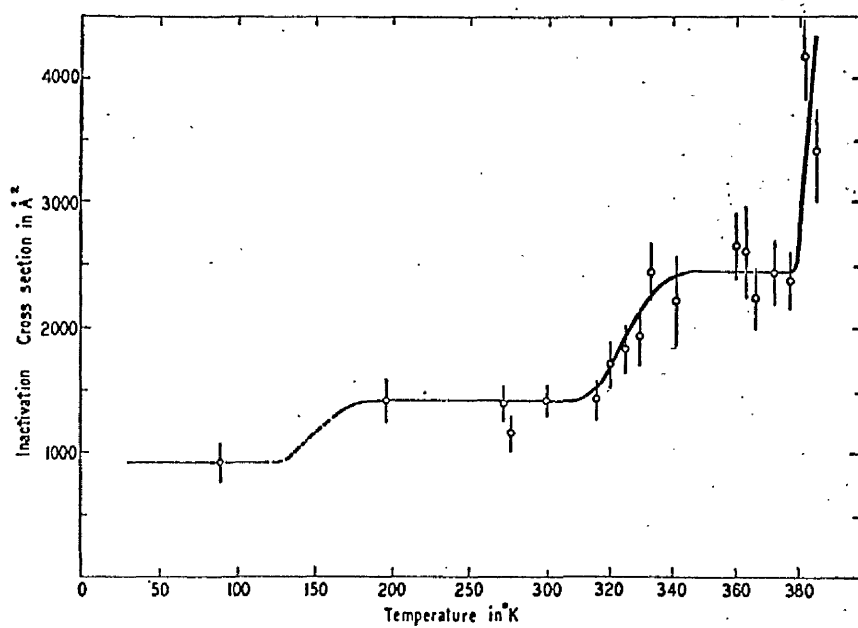


Fig. 1.5. The inactivation cross-section for 3.8-m. e. v. deuterons vs. the temperature during irradiation for dry catalase. (from Setlow 1952b).

1.4 The Interaction of Radiation and Hyperthermia

1.4.1 Interaction in Non-Mammalian Systems

An interaction between temperature and radiation has been reported for biological macromolecules (Setlow 1952 a, b; Pollard, Powell, Reaume 1952; Sanner and Kovacs-Proszt 1972), for bacteria and bacterial spores (Webb, Powers and Ehret, 1960; Emborg 1974), and for viruses (DiGioia et.al., 1970; Trujillo and Dugan, 1972; DeFlora and Badolati 1973), in addition to mammalian cells.

Probably the most striking demonstration of an effect of temperature on radiation sensitivity was presented by Setlow (1952b). He determined the inactivation cross section of dry catalase for a deuteron beam. His data are illustrated in figure 1.5. The plot of the cross section against temperature exhibits three flat regions and three rising regions. Setlow postulated that at very low temperatures a single hit in one of the four heme groups was sufficient to inactivate that group. Above 150°K a single hit in a heme group would inactivate both that group and one adjacent group. Above 320°K a single hit would inactivate all three active heme groups, the fourth group being inactive.

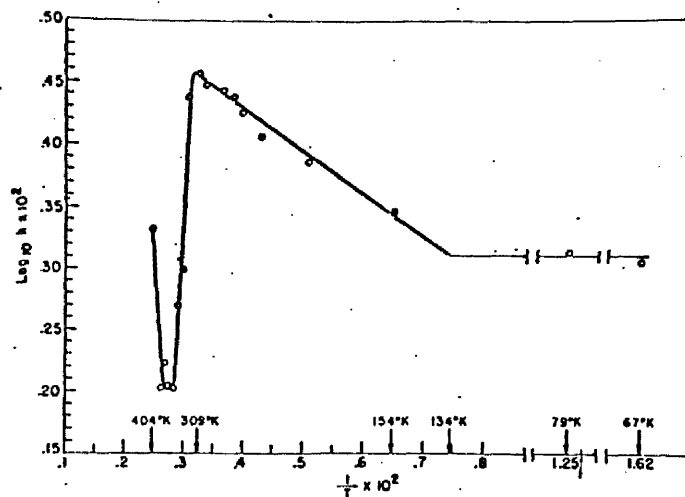


Fig. 1.6. X-radiation inactivation constant as a function of irradiation temperature for dry spores of *Bacillus megaterium*. (from Powers, Webb, and Ehret 1959).

One is tempted to generalize and say that, as the temperature is raised, so too is the radiosensitivity. However, there are exceptions. Maxwell, Kempton and Mosley (1942) observed that maize seed was most radio-sensitive between 0° and 25°C , the radiosensitivity dropping above and below this temperature range.

Powers, Webb and Ehret (1959) observed the unusual temperature dependence of dry spores of *Bacillus megaterium* illustrated in figure 1.6. The radiation sensitivity is independent of temperature up to 152°K , whereupon it rises until, at 309°K , it suddenly falls to below the original temperature-independent level. At 404°K the sensitivity again starts to increase.

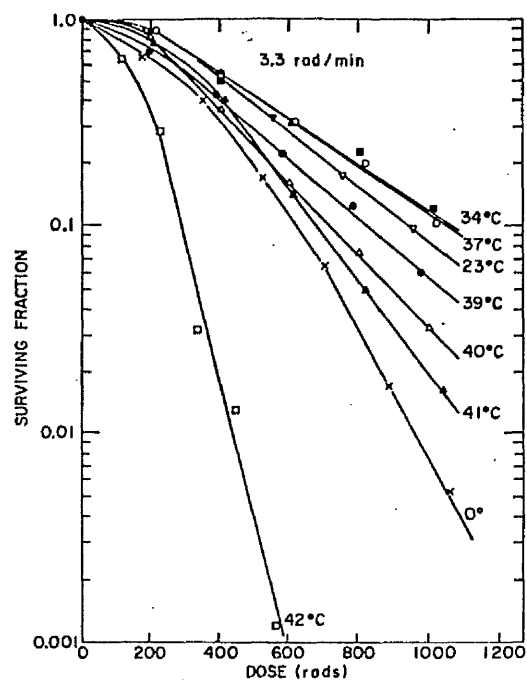


Fig. 1.7. Survival of Chinese hamster cells x-irradiated at different temperatures (250 kVp, 3.3 rad/min). (from Ben-Hur et.al. 1972)

1.4.2 Interaction in Mammalian Systems

Possibly the earliest demonstration of a synergistic interaction between hyperthermia and radiation was provided by Rohdenburg and Prime(1921) using an in vitro/in vivo assay on mouse sarcomas. More recently an in vivo synergistic effect has been suggested, but not demonstrated unequivocally, for rat hepatoma (Cater, Silver, and Watkinson 1964), dog bladder, (Cockett et.al., 1967), rabbit VX-2 carcinoma, (Muckle and Dickson 1973), mouse mammary tumour (Overgaard and Overgaard 1974) mouse osteosarcoma (Hahn, Alfieri, and Kim 1974), and mouse fibrosarcoma (Yerushalmi: 1974, 1975).

Synergistic action has been observed in vitro (Belli and Bonte, 1963; Ben - Hur et.al. 1972, 1974, 1975; Robinson and Wizenberg 1974; Philips et.al. 1975). Survival data for low dose rate (.033 Gy/min) x-rays (Ben - Hur et.al 1972) is illustrated in figure 1.7. Chinese hamster cells were exposed to the indicated temperatures for 5 hours (3 hours at 42°C) starting with the irradiation. As the temperature was increased, the survival curve terminal slope increased the quasi-threshold dose decreased, but the extrapolation number increased.

1.4.3 Selective Effects of Interaction

The observation that hyperthermia sensitized the radiation response of certain tissues would not be of such clinical significance if normal tissues were sensitized as much as, or more than, neoplastic tissue.

Robinson, Wizenberg, and McCready (1974) observed the response of skin and C3H mammary tumour of the mouse to radiation and hyperthermia. For both tissues, there was enhanced radiosensitivity at elevated temperatures, but the mammary tumour radiosensitivity was increased more than that of skin, indicating a favourable therapeutic ratio which increased with increasing temperature.

Hahn, Feingold, and Kim (1974) found that the radiation enhancement factor for growth retardation in bones of the mouse was 1.04 to 1.08, compared to a figure of 4 for the radiation enhancement factor for mouse tumour.

Thrall, Gillette, and Dewey (1975) however, observed that hyperthermia (44°C) increased the radiosensitivity of skin more than C3H mammary tumour in the mouse, although they could not rule out the possibility of this being due to slightly increased temperatures in the skin, as opposed to the tumours. They also observed that hyperthermia increased, rather

than decreased, the oxygen enhancement factor for radiation of both skin and tumour.

Kim, Kim, and Hahn(1974)reported that hyperthermia (42°C) radiosensitized HeLa cells more than 3T3 mouse fibroblasts, a contact-inhibited "normal" line. They further reported that 2 hours at 42°C , after gamma radiation, significantly lowered the oxygen enhancement ratio of HeLa cells.

Robinson et.al. (1974) and Philips et.al. (1975) observed similar results for the spleen colony bone marrow system and the EMT6 mammary tumour in vitro respectively.

1.5 Recovery Phenomena

The possibility of a living organism reversing damage is of fundamental importance to the clinician and radiobiologist alike. For the clinician, recovery necessarily affects fractionation schedules and for the biologist, recovery considered as an "undoing of damage" provides additional information about the damage mechanism.

1.5.1 Sublethal Damage

The term sublethal damage may take on a variety of definitions particularly if one considers the damage element responsible for sensitization to be itself a form of sublethal damage. In order to avoid confusion a working definition for this thesis shall be,

Sublethal damage (SLD) due to a particular agent is a form of damage that is not lethal of itself but contributes to the cumulative lethal effect of that same agent.

In this way a distinction is made between hyperthermia SLD and radiation SLD.

If reproductive integrity is the end point in question, the existence of SLD is suggested by the shape of the survival curve in the low dose region, but is without doubt demonstrated by the recovery or repair of SLD for split dose recovery experiments.

Fig. 1.8
Survival curve
(closed circles)
and 2-dose fract-
ionation curve
(open squares) of
"Clone A" cultured
Chinese hamster
cells. (from
Elkind and Sutton
1959)

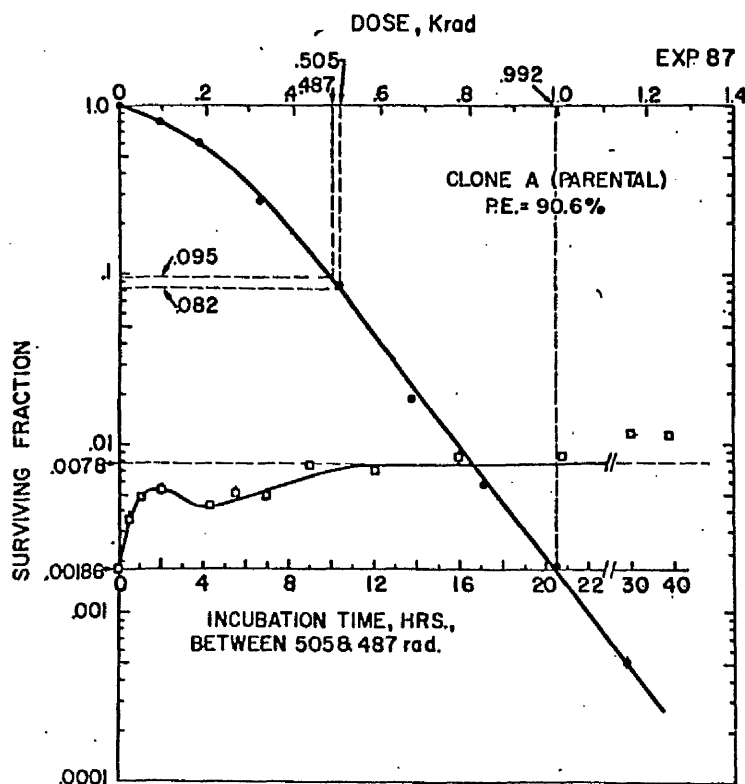
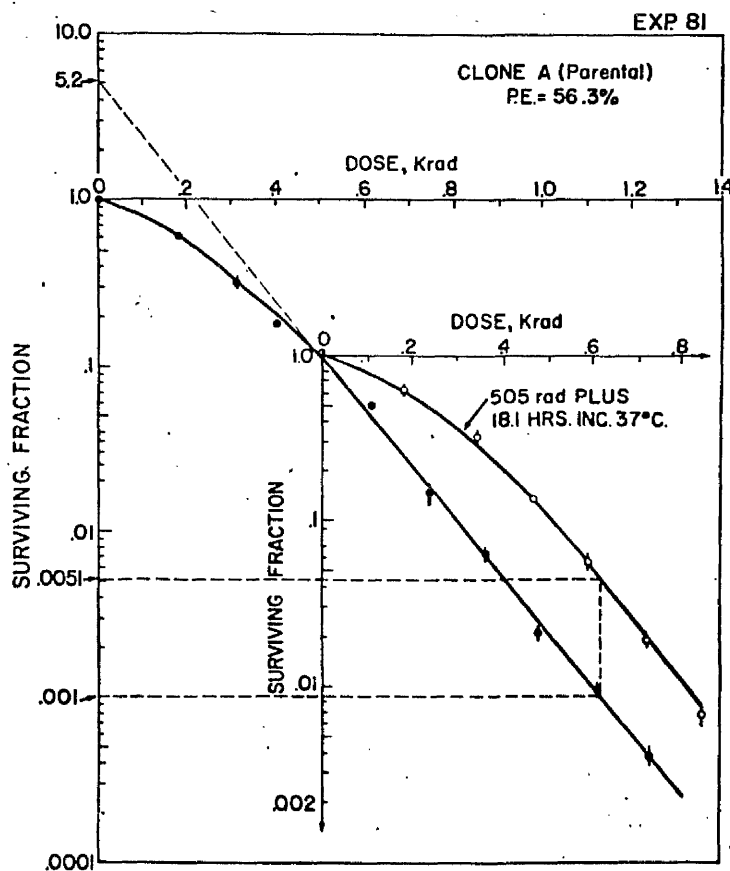


Fig. 1.9
Initial survival
curve (closed
circles) and
fractionation
survival curve
(open circles)
for "clone A"
cultured Chinese
hamster cells.
The
fractionation
survival curve
was determined
18.1 hours after
505 rad, and
the curve is
normalized to
the survival
corresponding
to 505 rad.
(from Elkind and
Sutton 1960)



Elkind and Sutton (1959, 1960) provided the first demonstration of recovery from SLD in mammalian cells. Figure 1.8 illustrates the radiation survival curve and recovery curve for chinese hamster cells obtained by Elkind and Sutton. The recovery curve is a graph of cell survival as a function of the time separating two approximately equal doses of radiation. At zero separation, the survival is as predicted from the survival curve but rises sharply for a time interval between doses. The dip in recovery at 4 hours is thought to be due to progression of the cells to a more sensitive position in the cell cycle. After about 12 hours the survival has risen to a plateau that is approximately the survival level for the product of survivals for each dose separately. Figure 1.9 is the fractionated survival curve obtained by Elkind and Sutton (1960). The curve on the right was obtained by administering graded doses after 18 hours at 37°C following a radiation dose of 5.05Gy. The fractionated curve exhibits very nearly the same survival characteristics indicating a more or less complete recovery with regard to radiosensitivity.

Evidence for repair of hyperthermia sublethal damage has been presented, (Palzer and Heidelberger, 1973; Leeper and Henle, 1974; Henle and Leeper 1975; Gerweck, Gillette, and Dewey 1975), however, the phenomenon of induced thermoresistance, mentioned previously, complicates the picture.

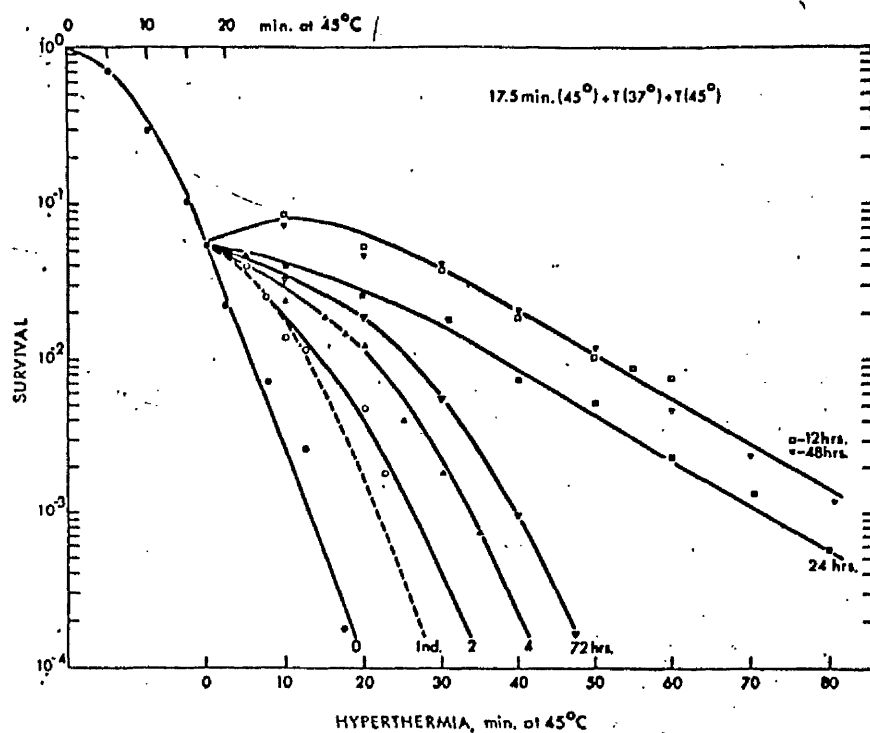


Fig. 1.10. Cell survival curves for Chinese hamster ovary cells given heat treatments in two equal exposures ($45^{\circ}\text{C} \times 17 \text{ min}$) with intertreatment intervals of 2, 4, 12, 24, 48, and 72 hours. (from Henle and Leeper 1976)

Figure 1.10 illustrates a fractionated hyperthermia survival curve for CHO cells (Henle and Leeper 1976). In addition to any effect on the shoulder due to repair of hyperthermia SLD, the survivors of the first dose have distinctly different thermal sensitivities.

The effect of hyperthermia on cellular ability to recover from radiation SLD has been investigated, although the interpretation of the results is less clear than the conventional split dose experiment as a result of the interaction of the hyperthermia exposure with either or both radiation doses.

That hyperthermia interferes with the ability to accumulate sublethal damage is demonstrated by the survival curves in figure 1.7. At the low dose rate used, the cells are capable of a concurrent repair of damage at 20°C to 37°C but not at 0°C. At temperatures above the normal environmental range, this capacity is reduced, but at 42°C there is an additional effect since the killing effect, being greater than that at 0°C, cannot be attributed solely to the inhibition of repair. Ben Hur et.al. (1974) carrying out further investigations, irradiated V79 cells at 0°C, incubated the cells at 41.2°C for 2 hours, and then gave graded radiation doses at 0°C after varying time periods at 37°C. They observed that unlike the

normal SLD repair which was complete in a few hours, repair modified by the hyperthermia dose occurred very much more slowly and was not complete at 190 hours separation.

Lai and Ducoff (1975) similarly report that incubation of Flour beetles for 2 hours at 43°C after a radiation dose of 720 Gy irreversibly suppressed repair of radiation SLD as measured by the conventional split dose technique. Henle and Leeper (1975), however, observed that CHO cells could repair radiation SLD at 40°C.

1.5.2 Interaction Sensitizing Damage

In order to avoid confusion the damage from one agent responsible for sensitizing a second agent will be defined separately from sublethal damage.

Interaction Sensitizing Damage (ISD) due to a particular agent is a form of damage, not lethal of itself, which however increases the sensitivity of the system to a different agent.

It should be noted that, for instance, hyperthermia SLD and ISD might possibly be biochemically indistinguishable and that the artificial distinction made here relates to the way in which the two damage types are realized. For an experiment in which radiation is given first and then probed at successive time intervals by a hyperthermia dose, any repair will be attributed to the repair of radiation ISD. Similarly hyperthermia probed by radiation will provide information on the repair of hyperthermia ISD.

The existence of radiation or hyperthermia ISD is unambiguously demonstrated by radiation and hyperthermia interaction in situations in which the two stimuli are not presented simultaneously.

Crile (1963) observed that if heat and radiation were applied to normal feet, or tumours implanted in the feet of mice, there was a marked interaction between the agents, which gradually disappeared for increasing time separation between the agents.

Robinson and Wizenberg (1974) observed a gradual recovery of the increased slope of the radiation survival curve for Chinese hamster cells, for increasing time intervals between the hyperthermia and radiation dose.

That radiation ISD and hyperthermia ISD are not similar damage states is suggested by the different recovery kinetics observed. Gerweck et.al (1975) observed that radiation ISD in synchronous CHO cells was repaired with a half time of 30 minutes for both G_1 or S phase cells, whereas the repair of hyperthermia ISD did not begin until after 6 hours, for exposure during G_1 , or after 12 hours for S phase cells.

1.5.3 Potentially Lethal Damage(PLD)

is that damage due to a lethal agent that is lethal only in the presence of an otherwise nonlethal agent.

The existence of PLD is demonstrated by recovery from or fixation of PLD. PLD phenomena have been demonstrated by a wide variety of effects on radiation survival measurements, the most common however is the effect of incubation temperature. Winans, Dewey, and Dettor (1972) demonstrated that, if CHO cells were left at room temperature after radiation for increasing lengths of time, before being incubated at 37°C, the

survival increased with the period of time at room temperature. They also demonstrated the reciprocal effect of fixation of PLD by irradiating the cells at 37° and incubating them at this temperature for increasing times before a 2 hour period at 20°C.

PLD was rapidly converted to lethal damage, as evidenced by the survival falling by a factor of 5 within 40 minutes, at which time fixation was complete.

Henle and Leeper (1975) observed that CHO cells exhibited a similar repair of PLD due to a hyperthermic exposure at 45° for 20 minutes.

Evans, Li, and Hahn (1975) investigated the effects of hyperthermia on the repair of radiation PLD. HA1 cells were irradiated (16Gy), and either assayed immediately or incubated at hyperthermic temperatures and then allowed to repair PLD at room temperature for 5 hours. If the cells were not exposed to elevated temperatures, repair of PLD increased survival by a factor of 10 to 20.

41° for 1 hour reduced the factor to 4 to 5 and

43° for 45 minutes gave a recovery factor of 1 to 2.

1.5.4 The Effect of Treatment Order

The effect of treatment order on the extent of the interaction must be associated with the deposition or more probably the repair of ISD. There is little agreement on this point between different workers and different systems.

Crile (1963), Hahn, Alfieri, and Kim (1974), and Robinson and Wizenberg (1974) report that order makes no apparent difference in mice feet, Ridgeway osteogenic sarcoma in vivo, and in CHL cells in vitro.

Gerwyck, Gillette and Dewey (1975) and Lai and Ducoff (1975) find that hyperthermia before radiation is more effective than during or after for the killing of CHO cells in vitro and Flour beetles in vivo.

Ben-Hur, Elkind and Bronk (1974), however, found that hyperthermia before radiation was without effect on the radiation sensitivity of V79 cells.

Hofer (1975) found hyperthermia after radiation more effective than during or before for L1210 and Erlich ascites cells in vivo. Thrall, Gillette and Dewey (1975) found that C₃H mammary tumours responded similarly, but that for normal mouse skin, hyperthermia before radiation was slightly more effective.

1.6 Conclusion

From the published work it can be seen that the interaction of radiation and hyperthermia occurs. The variety of the expressions observed and the apparent contradictions suggest a somewhat complex mechanism, which has so far been elucidated only to a very limited extent. The interaction phenomena, occurring when additional agents such as drugs or oxygen, and other forms of ionizing radiation, are used, are a field in which few observations have been made, and little coherent analysis presented. Although in the work for this thesis, only a small part of the field can be covered, an attempt is made, within the circumscribed area of in vitro cell survival, to develop an approach which may be found useful in further studies.

CHAPTER TWO

MATERIALS AND METHODS

2.1 Materials

2.1.1 Cell Line

Chinese Hamster Ovary Clone A, a fibroblast-like line, was first obtained from Mr. T. R. Munro, Strangeways Laboratory in 1970. Since then the behaviour of these cells has been well documented in two laboratories at this institute. (Railton, Lawson, Porter, and Hannan 1973; Railton, Porter, Lawson, and Hannan 1974; Malone, Porter, and Hendry 1974; Railton, Lawson, and Porter 1975; Szumiel and Nias 1975; Szumiel and Nias 1976). In addition, the short doubling time and the absence of a cell feeder effect made this cell line desirable for the observations required.

The majority of experiments described in this thesis were performed with cells derived from a single subcloning and frozen in liquid nitrogen in March of 1973. These cells exhibited a modal chromosome number of 21.

2.1.2 Media

All media and components were supplied by Gibco-Biocult. Appendix II details catalogue numbers and formulations used. Hams F10, supplemented with 2 mM glutamine and 15% calf serum and buffered with a 5% CO₂-air mixture, yielded plating efficiencies of 60 to 75% and a cell number doubling time of 11 to 11.5 hours.

Hams F12 supplemented with non-essential amino acids, 2mM Glutamine, and 15% calf serum, and buffered with 20mM Hepes buffer yielded plating efficiencies of 50 to 65% and a doubling time of 10.5 to 11 hours.

The observed plating efficiencies, comparable in both laboratories, are perhaps low for this cell line and are indeed lower than those previously observed at the commencement of this project. The effect of pH and serum concentration and type on plating efficiency was determined. The optimum pH was 7.2 for both media, plating efficiency dropping only marginally in the range 7.10 to 7.35. Similarly an investigation into the effect of calf serum concentration from 5 to 30% revealed the plating efficiency to be relatively insensitive to this parameter. Foetal bovine serum marginally increased the plating efficiency, but the improvement did not seem to warrant the extra cost.

The most valid criticism of techniques yielding less than 100% plating efficiencies is that the plating efficiency may be cell age dependent, thereby perturbing the natural distribution of cells about the cell cycle. That this perturbation is not severe is suggested by the similarity of survival curve parameters obtained in both laboratories compared to those previously obtained by the above mentioned authors. Indeed,

Elkind and Sutton (1959) reported that variations in plating efficiency of Chinese Hamster cells from 10 to 90% produced similar radiation survivals.

The low plating efficiencies prompted a re-examination of any feeder effects. Concentrations of 200, 1000, 5000, and 1×10^4 per ml of cells, previously irradiated to 20Gy, did not increase the plating efficiency of unirradiated cells plated at a concentration of 160/ml or 80/ml in Hams F12 or Hams F10 respectively, confirming the observations made earlier by Malone (1972).

To ensure uniformity, medium for any experiment was mixed from the same batch of ingredients. Unlike Hams F10, Hams F12 media required eight components in the mixture thus allowing a greater bottle to bottle variation in media. To prevent this variation, this media was in addition subsequently mixed and pooled in 1 or 1.5 litre batches for each experiment.

2.1.3 Cell Maintenance

The cells were maintained in exponential growth as a monolayer in T75 plastic flasks (Sterilin). Cultures were split twice weekly and reseeded with 3×10^4 or 1×10^5 cells. After any change of media (e.g. from Hams F10 to Hams F12), or after thawing from liquid nitrogen, the cells were allowed

one week in culture before they were used experimentally.

The cultures were handled in a class 100 laminar flow cabinet which was itself contained in a clean air room equipped with an airlock changing area and maintained at positive pressure with a class 100 filter-fan unit. These working conditions and stringent aseptic techniques allowed an exclusive use of antibiotic-free media for stock cultures.

Mycoplasma contamination was not thought to be a problem due to the ability to maintain the cultures without antibiotics (Hayflick 1965). On occasion when doubt arose, cultures were checked for mycoplasma contamination by the Department of Virology of the University of Glasgow and mycoplasma were never reported.

2.2 Experimental Procedures

Twenty four hours prior to an experiment 3×10^6 cells were seeded into a T75 flask yielding 6×10^6 cells in exponential growth at a cell density of 8×10^4 cells/cm² on the experimental day. Growth curves revealed that when flasks were seeded at this level, exponential growth could be attained to cell densities in excess of 13×10^4 cells/cm². This procedure ensured that the immediate histories of the cells for each experiment were similar and that the nutritional and other environmental factors for all of the cells in the culture were identical, perhaps unlike that for cultures in which 5 to 10 doubling times have elapsed between seeding and the experiment.

Two basic experimental techniques were used. Method A utilized the less expensive CO₂ buffered F10 and plastic petri dishes (Sterilin), while method B utilized Hepes buffered F12 and plastic T30 Flasks (Nuncclon).

Method A required that the experimental culture bottle be trypsinized, counted on an electronic counter, and resuspended in medium at a concentration of 1.25×10^5 cells/ml. This suspension was divided among replicate treatment vessels, either glass tubes or plastic flasks. The cells, having been treated with radiation and/or hyperthermia, were returned to

the aseptic laboratory and then recounted, diluted and dispensed into 90 mm petri dishes to give, generally, a fixed number of cells per plate. Increasing numbers of plates partially compensated for the decrease in clones/plate. Generally, the minimum number of clones per experimental point was 400.

These plates were incubated for six days at 37°C , rinsed in tap water and stained with 1:10 Carbol Fuchsin (Gurr). Macroscopic colonies, determined by random counts to contain more than about 50 cells, were counted manually.

Method B required that the experimental culture be trypsinized counted and resuspended at the final concentration. This suspension was plated into T30 plastic flasks and then either treated immediately or after a two hour interval at 37° during which time the cells had attached to the plastic surface. These plates were maintained for 1 hour (except where noted) at room temperature before incubation at 37° . The plates were rinsed, stained, and counted as described above.

Due to the expense, and in some cases limited experimental capacity, extra plates were not generally plated at the high dose points. The resulting increased statistical uncertainty was allowed for

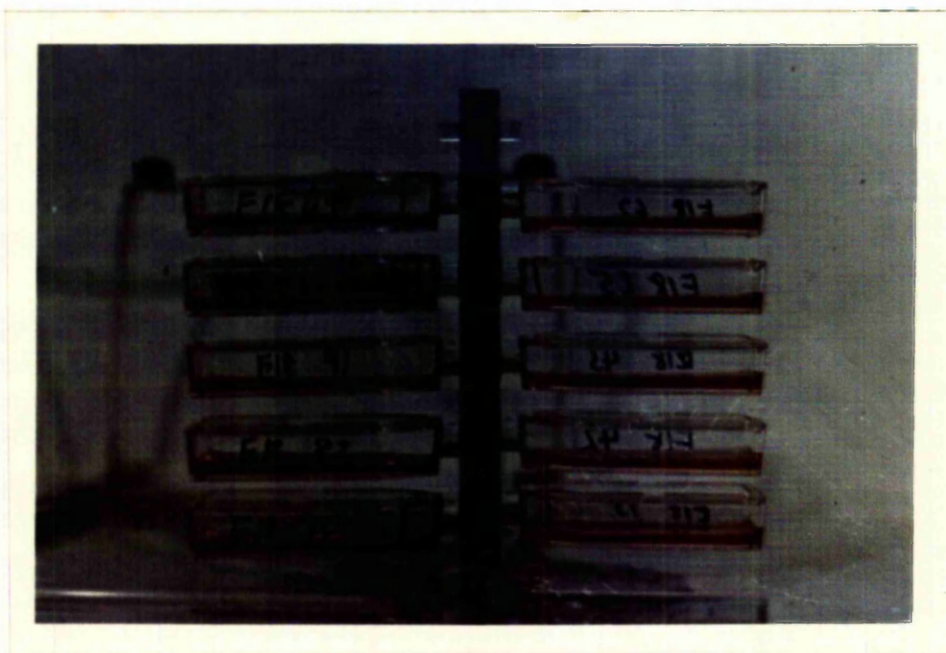
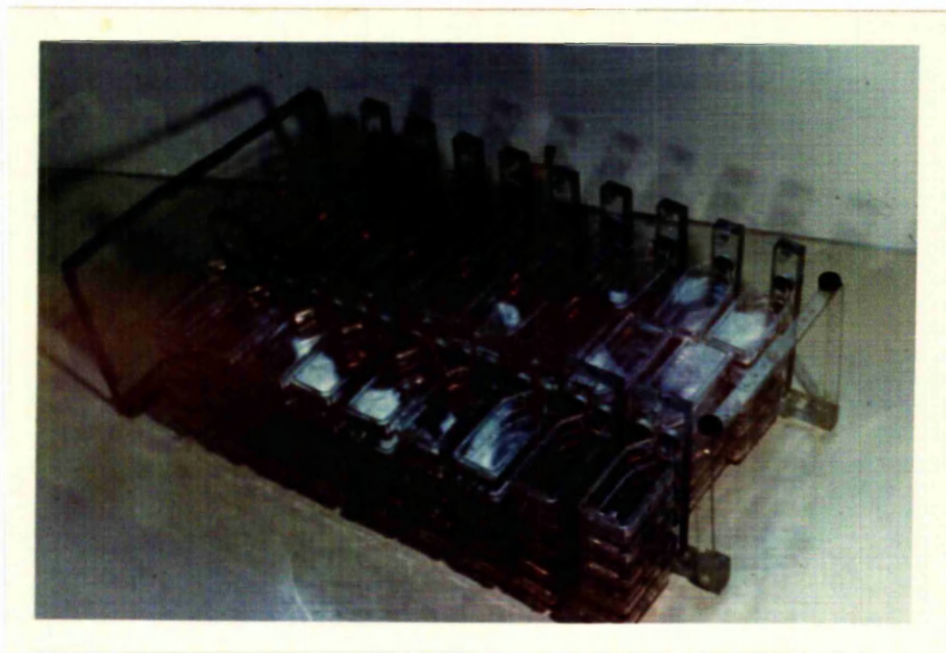


Fig. 2.1 Perspex rack for holding T30 flasks submerged. Upper - rack with full complement of 150 flasks - lower - removable stem holding 10 flasks.

in the experimental fits by a weighting equal to the theoretical inverse variance.

Method C is a hybrid of method A and B and requires that the cells be suspended at a concentration of 1.25×10^5 cells/ml, given graded doses of radiation and then resuspended at different plating concentrations to yield 500 clones/T30 flask if they were not further treated. The separate suspensions were dispensed into T30 flasks and then these flasks were treated as described in method B.

2.3 Hyperthermia Techniques

2.3.1. Heating Techniques

Two thermostatically controlled waterbaths (SX-35, Grant Instruments) served as heating devices. These were controlled by a contact thermometer and variable power controller, yielding 24 hour stability, under optimum conditions, of $\pm 0.01^\circ\text{C}$, as advertised and confirmed by precision resistance thermometry.

Cells were heated in screw stoppered glass test tubes or in plastic T30 flasks. T30 flasks were held by the screw caps in groups of 5 or 10 in a perspex rack constructed to accommodate 150 flasks. This rack, illustrated in figure 2.1, allowed all of the flasks to be submerged simultaneously and then removed in groups of 5 or 10 at a time.

All of the flasks were maintained at 1cm separation for all surfaces except for the flask ends, at which the separation was only 0.2cm. The waterbath circulation was via a circulation chamber underneath a metal tray, supporting the rack, and then back through the spaces between the flasks. Full temperature stability for a fully loaded situation was better than $\pm .02^{\circ}\text{C}$ over the experimental period after an initial recovery period.

The temperature in the flasks, heated in this way, rose exponentially with a half time of 30 seconds. To minimise the initial depression of the waterbath temperature, which recovered slowly, the rack and complement of flasks were first heated for 15 minutes in another waterbath maintained at 37° . At a hyperthermic temperature of 42° , the rack and 120 flasks transferred from 37° lowered the temperature by 0.3°C . The waterbath temperature typically recovered in 5 to 8 minutes.

Cells that were to be heated and then returned to the aseptic area were heated in glass test tubes. Initially, to prevent the cells from plating on the test tubes, these were siliconized with either "Repelcote" or "1107 fluid" (Dow Corning, Hopkins and Williams.) Despite the fact that the Dow Corning

1107 fluid was a heat-cured agent, both of these agents proved susceptible to the cleaning and sterilising process, resulting in non-uniform coatings. To maintain optimum uniformity, siliconized tubes were replaced by plain glass tubes without any apparent adverse effects for the short hyperthermia exposures.

The glass tubes containing 2.5 ml of cell suspension were held in light metal racks and were sunk to the necks of the tubes under their own weight. Usually no more than 12 tubes were heated at one time, so that the temperature depression was minimal. Once again, the tubes heated with a half time of 30 seconds, the increased thermal conductivity of the glass over the plastic apparently being compensated for by the decrease in surface area.

The plastic screw cap was further sealed to the glass by plastic tape to prevent the waterbath water entering under the threads of the cap. These tubes were rinsed in spirit savlon before returning to the aseptic area.

To minimise gross contamination of the waterbath water, a broad spectrum antibiotic (Panabath, BDH Chemicals Ltd) was initially used. This was, however, of limited effect and eventually a 0.25M solution of Cu SO_4 was implemented as the heating fluid.

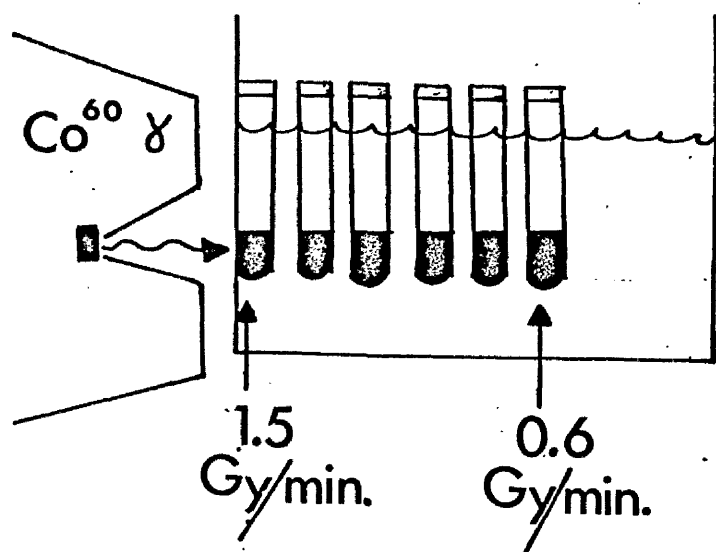


Fig. 2.2. Configuration for simultaneous heating and irradiation technique.

2.3.2 Thermometry

Static thermometry was determined using precision, total-immersion, mercury in glass thermometers graded at $.05^{\circ}\text{C}$ intervals (268/0040, Baird and Tatlock), with a calibration traceable to the National Physical Laboratory. The usual corrections for partial immersion were made. The estimated accuracy was $\pm 0.02^{\circ}\text{C}$.

Dynamic thermometry was determined using thermistors (type F, ITT Electronic Services) connected in an unbalanced bridge arrangement or, for the stability measurements, connected to a precision resistance bridge (type B331, Wayne Kerr).

2.4 Irradiation Techniques

2.4.1 ^{60}Co Gamma Radiation

Three irradiation techniques were used with a ^{60}Co teletherapy unit. Simultaneous irradiation and heating was accomplished by positioning the waterbath adjacent to the horizontally orientated cobalt unit, as depicted in fig.2.2. The SCD, surface to cell distance, was 40.5 to 50.5 cm, corresponding to dose rates of 1.5 to 0.4 Gy/min. The maximum dose gradient across a cell suspension was estimated to be 10% by interpolation of the dose rate data. The dosimetry was determined by ionization chamber and LiF techniques.

With the beam positioned vertically upwards, a double stack of 10 T30 flasks (20 flasks) was placed within the field defining jaws, held on a perspex jig that provided dose build-up. Over the first 6 positions most commonly used, the SCD varied from 27 to 36 cm, corresponding to dose rates of 2.90 to 1.45 Gy/min. Dose uniformity for the bottom flask was better than 15%, as indicated by LiF dosimetry. Relative and absolute dosimetry was determined by both ionization chamber and LiF techniques.

With the beam positioned vertically downwards, a single T30 flask containing a suspension of cells was irradiated at an SCD of 46 cm and a dose rate of 0.96 Gy/min. One half centimeter of perspex was used to provide the necessary build up. Dose uniformity was better than 2%, estimated by geometrical considerations.

2.4.2 X-radiation

Cells were irradiated in single T30 flasks on an x-ray unit operating at 250 kVp and 15 ma and filtered to a half value thickness of 1.8 mm of copper. The FCD was 30 cm, corresponding to a dose rate of 1.35 Gy/min.

Ionization chamber and LiF dosimetry were employed.

Cells were irradiated in multiple (30) T30 flasks on a 4MeV clinical linear accelerator at a FCD of 160 cm and a dose rate of 0.95 Gy/min. A five centimeter thick presswood block was placed over the flasks to optimise the flask to flask uniformity, determined to be better than 5% by ionization chamber dosimetry.

2.4.3 Neutron Radiation

Cells were irradiated simultaneously in a stack of 6 T30 flasks with neutrons, produced by a sealed generator (type P, Marconi Elliot Avionic Systems Ltd.) utilizing the $^3\text{H}(\text{d},\text{n})$ reaction to produce neutrons with a mean energy of 14.7 MeV. The FCD was 8 to 17 cm, corresponding to dose rates of 0.15 to 0.03 Gy/min. Gamma contamination of the beam was from 5 ± 2 to 7 ± 3 per cent of the total dose, increasing over the distance from the bottom (nearest) to the top of the stack. Uniformity at the highest dose rate was 11% of the total dose based on geometrical considerations. The relative and absolute dose rates were determined by the neutron physics section of this Institute using tissue-equivalent ionization chambers.

2.4.4 Dosimetry

Radiation doses were determined with Baldwin Farmer type dosimeters in addition to a variety of other ionization chambers. All calibrations are traceable to radiation standards maintained at the National Physical Laboratory. γ and x-ray doses were calculated as doses to muscle using the factors from ICRU Handbook 85. Neutron doses were calculated as wet tissue doses using spectrum weighted kerma values (ICRU Report 13, 1969) W values (Dennis 1971) and stopping power ratios, assuming that the stopping powers for solid and gaseous hydrocarbons are the same.

LiF loaded ptfе microrods were supplied and read by the National Radiological Protection Board.

Photon doses were measured to an estimated accuracy of 5%. Neutron doses were measured to an estimated accuracy of 10%.

CHAPTER THREE

PRELIMINARY EXPERIMENTS

3.1 Introduction

It is necessary to determine the unperturbed response to radiation and hyperthermia in order to assess the degree of interaction between the two agents. The survival response was determined and found to be reproducible and comparable to other published data.

The preliminary experiments were designed to probe several aspects of the interaction, in order to provide basic information and facilitate the design of more complex experiments. The importance of sequence and separation of the insults was assessed with a view to optimize experimental stability.

Little has been published to suggest how the degree of interaction varies with radiation or hyperthermia dose. This was investigated by determining the radio-sensitivity during exposure at 42°C for increasing periods of time. The effect of temperature on the interaction was investigated by determining the radiosensitivity during exposure for a fixed period at various temperatures. Another aspect of the temperature dependence of the interaction was investigated by assessing the degree of thermal-sensitization at different temperatures due to a prior radiation dose.

3.2 Experimental Stability

While it is customary to demonstrate the stability of the experimental techniques, it is perhaps more to the point to demonstrate the extremes of instability encountered.

On one occasion after a long series of hyperthermia survival experiments, during which nothing unusual was noted, a neutron survival experiment produced a survival curve slope of $.667 \text{ Gy}^{-1}$ which was at least 30% lower than expected. This same degree of increased radio-resistance was verified for both ^{60}Co and 250 kVp x-radiation. This was confirmed to be a consistent property of this somehow altered cell line by freezing and subsequently thawing the cells and comparing the radiation and hyperthermia survival characteristics simultaneously with freshly thawed parent stock.

An interesting feature of this line, designated CHOZ, is that, in addition to exhibiting unaltered hyperthermia survival characteristics, the plating efficiency was 15 to 20% higher than the normal parent stock.

Hyperthermia survival anomalies also occurred. On two occasions early in the investigations,, deviations from the expected thermal sensitivity of 100% were noted.

These observations demonstrate that for interaction experiments, control survival parameters must be determined within the context of each experiment.

The results of control radiation and hyperthermia survival curves utilizing a single technique and obtained over a period of 9 months are listed in table 3.1.

Table 3.1

Treatment	Expts.	K \pm S.D. (%S.D.)	M \pm S.D. (%S.D.)
Hyperthermia(42°)	11	.0229 \pm .0037 min ⁻¹ (16.2)	1.70 \pm .36 (21.2)
Radiation	17	.548 \pm .056 Gy ⁻¹ (10.3)	1.40 \pm .30 (21.5)

It should be observed that the errors are the standard deviation rather than the standard error. These reflect the experimental stability of a given system, which is considered adequate provided the control survival curves are obtained.

Overall, radiation survival for low LET radiation, using various techniques, has been described by survival curve slopes in the range of .475 to .600 Gy⁻¹ and extrapolation numbers of 1.3 to 3. These values fall within the range of values reviewed by Whitmore and Till (1964) and are in agreement with those reported by the previous workers at this Institute, already cited.

Fig. 3.1
Hyperthermia
survival
curves for
CHO cells
using method
A with Hams
F10. Each
survival
curve represents
a single
experiment.

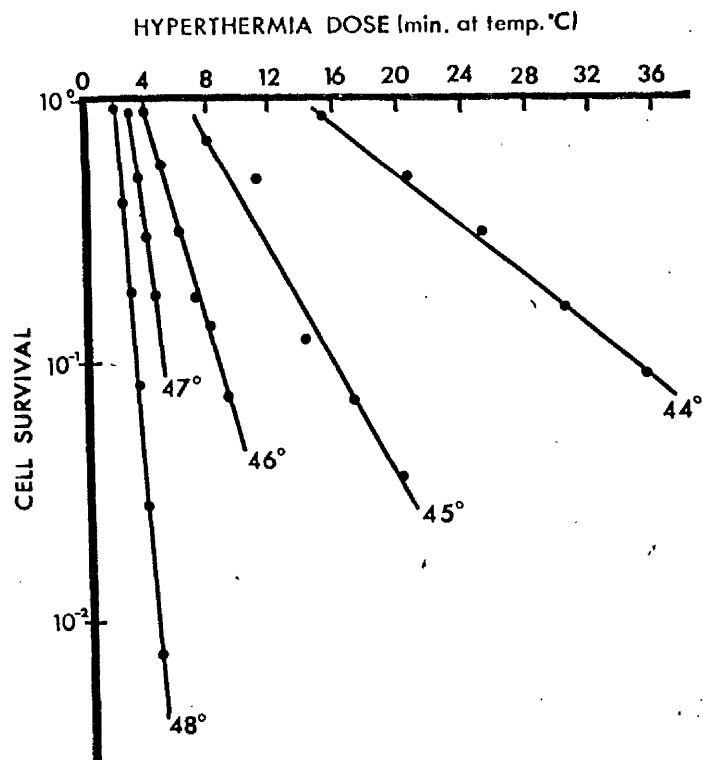
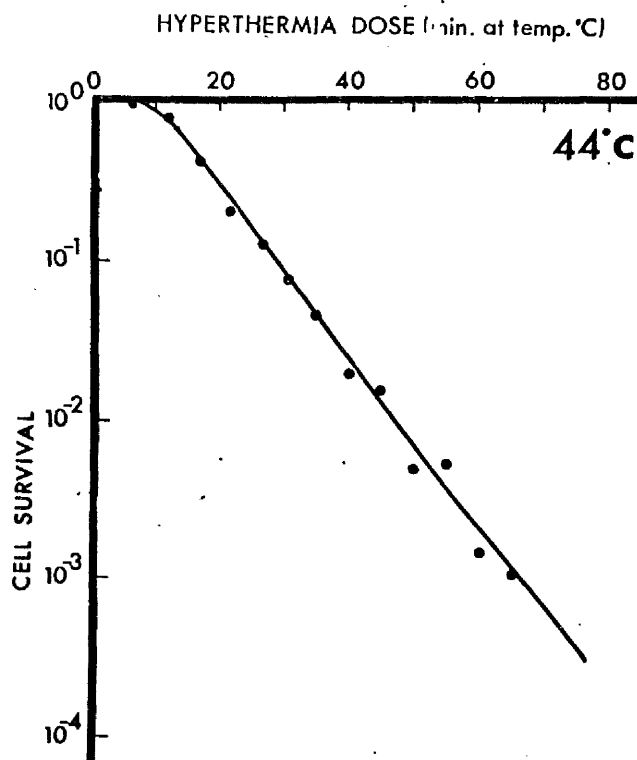


Fig. 3.2
Hyperthermia
survival
curve for CHO
cells using
method B with
Hams F12. The
data points
represent one
simultaneous
observation.



3.3 The Effects of Hyperthermia on Cell Survival

3.3.1 Hyperthermia Survival Curves

Figure 3.1 illustrates hyperthermia survival curves at different temperatures obtained by method A, (suspended-treated-plated), using Hams F10 and unsiliconized glass tubes. In contrast to the radiation survival curves obtained with this cell line, which exhibit large initial slope, the hyperthermia survival curve changes abruptly from the shoulder to the exponential portion. Figure 3.2 illustrates a hyperthermia survival curve at 44°C obtained by method B, (suspended-plated-treated), using Hams F12 and plastic T30 flasks. The slopes of the 44°C survival curve are, within experimental limits, identical. The apparent difference in extrapolation number is difficult to quantify due to the finite time required to raise the temperature to the experimental level. While it has been suggested that this might be allowed for (Westra and Dewey 1972) the times quoted in this thesis are the total heating times.

3.3.2 The Effect of Temperature on Thermal-sensitivity

Examination of figure 3.1 reveals that the thermal sensitivity exhibits a strong temperature dependence. An Arrhenius plot of thermal inactivation rates observed by both methods A and B and for both media is illustrated in figure 3.3a.

Fig. 3.3a

Arrhenius plot of CHO hyperthermia inactivation rate. Standard errors where larger than the displayed point are indicated. The small number above each data point is the number of observations.

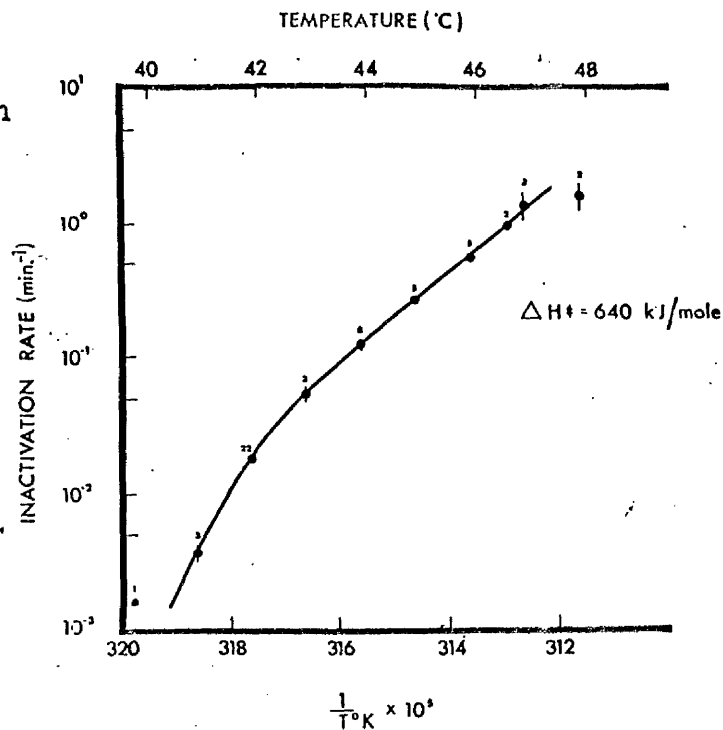


Fig. 3.3b

Arrhenius plot of mammalian cell inactivation rates

- A. CHO (Westra and Dewey 1972)
- B. CHO as in fig. 3.3a
- C. CH (Johnson and Pavelec 1972)
- D. Pig kidney (Harris 1967)

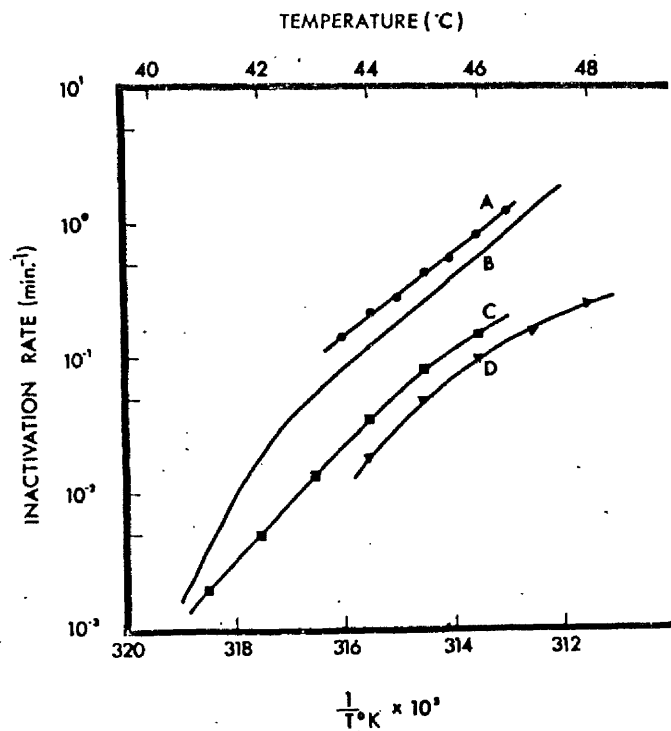


Figure 3.3b illustrates the observed inactivation rates in comparison to those observed by other experimenters on different cell lines. The factor of 20 difference between curve A and D can be compared to a factor of about 2 observed in the range of radiosensitivities for mammalian cells (Whitmore and Till 1964).

The Arrhenius plot in figure 3.3a is linear from 47° to 43° dropping sharply below this temperature. The linear portion of the curve can be described by the Arrhenius equation.

$$K = Ae^{-(\Delta H^\ddagger + RT)/RT} \quad 3.1$$

where

- K = inactivation rate
- A = constant
- ΔH^\ddagger = activation enthalpy
- R = gas constant
- T = absolute temperature in °K

The value of the activation enthalpy was found to be 640 ± 60 kJ/mole. This value, being considerably higher than that observed for most physico-chemical reactions, apart from the denaturation of proteins, has led to a great deal of speculation about the involvement of protein denaturation in thermal killing. This subject will be dealt with in a later chapter.

3.3.3 Discussion

The results presented show that the techniques used result in survival characteristics within the range observed by other authors. Both types of technique and media result in similar inactivation rates and may be directly compared. The temperature coefficient for hyperthermia killing is similar to that observed for other single cell systems and indeed similar to some of the temperature coefficients observed in vivo (Suit and Shwayder, 1974).

It has been suggested that the transition from the straight line portion to the curved portion of the Arrhenius plot represents an activation energy "break", signifying a different process of thermal sterilization occurring below this temperature.

While it seems plausible that more than one mechanism may be responsible for killing and there is some evidence for a dual effect (Harris 1969), the dual mechanism hypothesis is not necessary to explain the observed phenomenon. The downward curvature of the Arrhenius plot may reflect a phenomenon similar to the low dose rate phenomenon observed for radiation.

Johnson and Pavelec (1972) observed the discrepancy between doubling time and generation time at temperatures from 37 to 42°C in order to determine the spontaneous death rate.

Fig. 3.4
Heating and
irradiation
schedule for
the data of
figure 3.5.

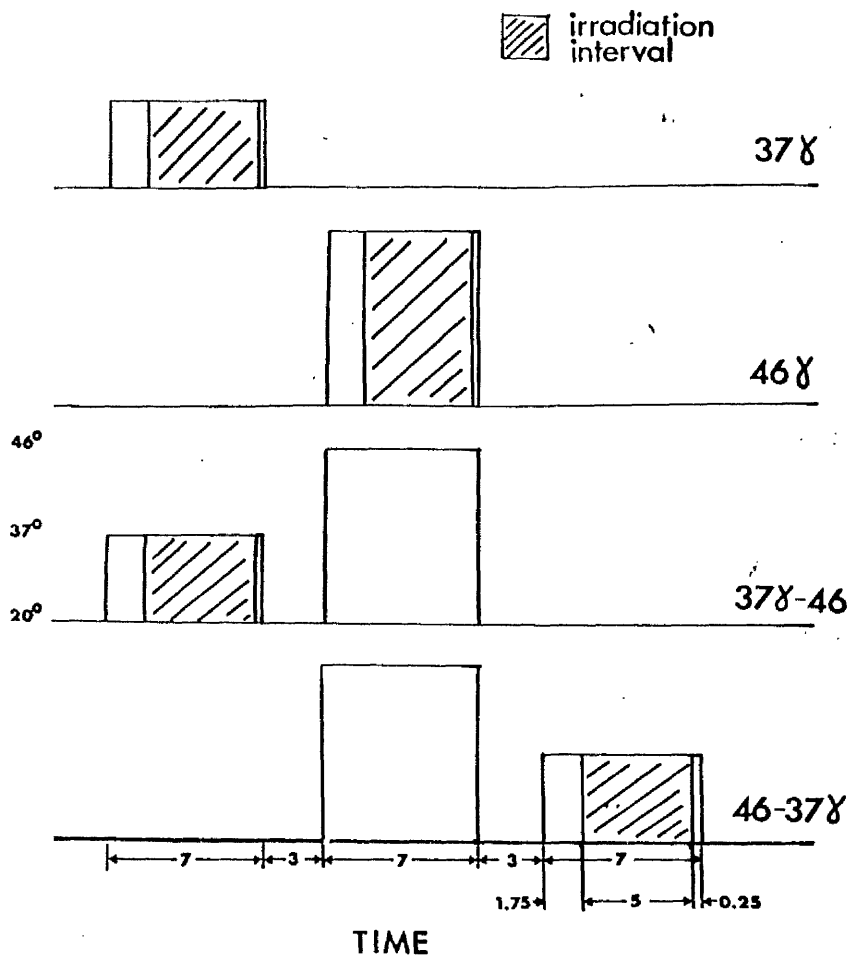
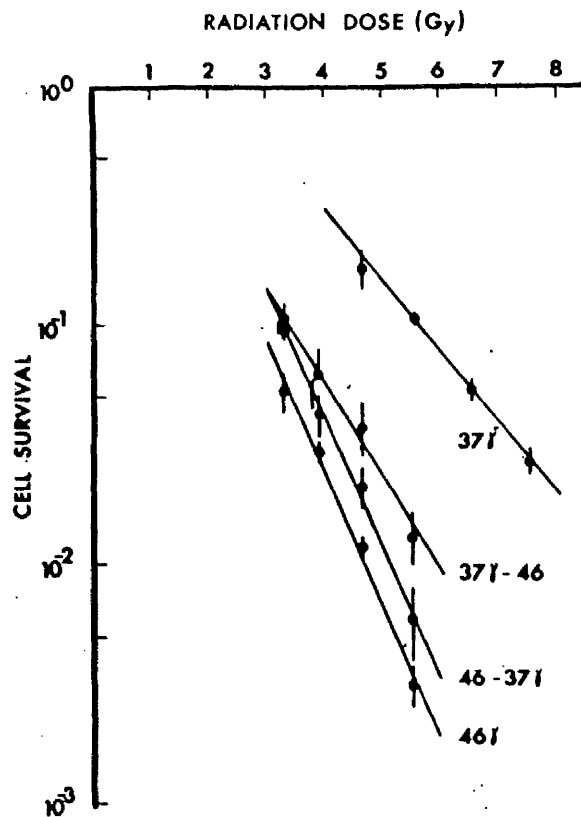


Fig. 3.5
CHO survival
after
simultaneous
and separated
heating and
radiation,
using the
treatment
schedule of
Fig. 3.4 Data
points represent
the mean and
standard error
of 4 expts (37°C-
46, 46-37°C) or
8 expts (46°C, 37°C).



Within experimental limits, these data fall on a straight line extension of the Arrhenius plot of their inactivation data from 42° to 46° suggesting that a single mechanism was responsible for the thermal inactivation from 37° to 46°C

3.4 The Interaction of Radiation and Hyperthermia

3.4.1 Sensitization of Radiation Response by Hyperthermia

Utilising method A (suspending-treating-plating) with Hams F10, the effect of simultaneous and separated interaction was investigated. Cells heated in unsiliconized glass tubes were irradiated through the side of the waterbath by a ^{60}Co teletherapy unit. The test tubes were irradiated in six positions with dose rates ranging from 1.5 Gy/min to 0.6 Gy/min. Figure 3.4 illustrates the treatment schedules used. Exposure at 37° or 46° was for 7 minutes, irradiation starting 1.75 minutes after the heating started and stopping 0.25 minutes before heating was terminated by cooling in room temperature water. The temperature rise was exponential from room temperature with a half time of 30 seconds so exposure at 46° resulted in a temperature of 42.5°C at the start of irradiation and a final temperature of 46°C .

In any single experiment, all of the tubes heated to 46° were heated simultaneously, thereby providing exactly the same hyperthermia dose. Those tubes not irradiated (e.g. hyperthermia controls and tubes to be irradiated at 37°C) were positioned out of the radiation beam and received a total dose of less than .01Gy.

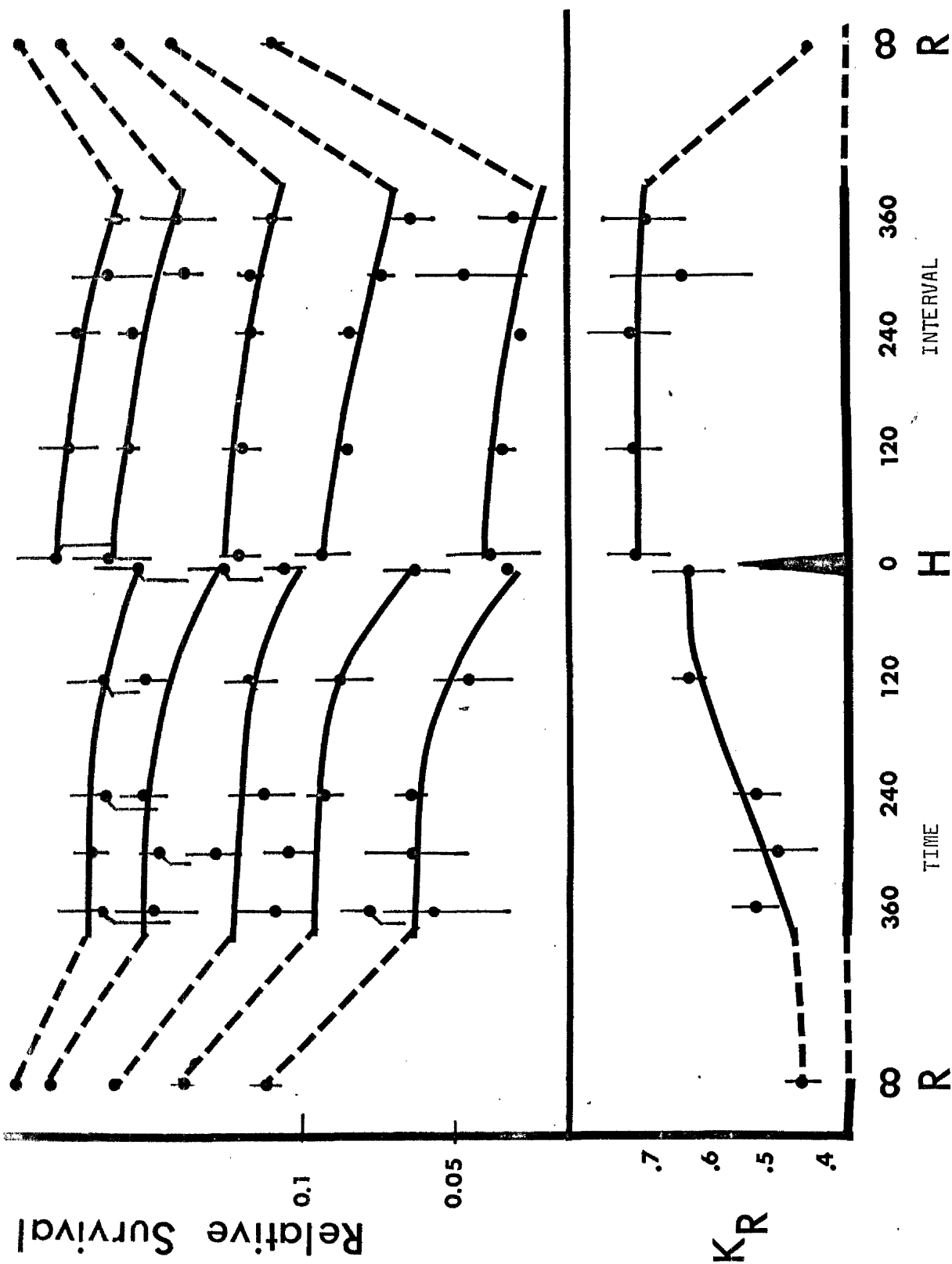
The parameters of these survival curves are listed in table 3.2. It is observed that irradiation

Table 3.2. Radiation survival curve parameters for simultaneous and separated interaction.

Treatment	Radiosensitivity	Extrapolation No.
37Y	.569 \pm .010 Gy ⁻¹	2.95 \pm .09
46Y	1.07 \pm .063	1.78 \pm .04
37Y-46	.834 \pm .058	1.63 \pm .03
46-37Y	1.21 \pm .091	5.05 \pm .14

simultaneously with heating is the most effective in reducing cell survival, reflecting an increased radiosensitivity and decreased extrapolation number compared to the control irradiations at 37°. Irradiating 3 minutes after heating results in an increase in extrapolation number to a level higher than the control extrapolation number without any significant change in

Figure 3.6. Interaction relaxation for separated hyperthermia (20min, 44°C) and radiation doses (3.7, 4.3, 4.8, 5.6, and 6.5Gy). Survival normalization to unity at zero radiation dose and radiosensitivity K_R (Gy⁻¹). Abscissa, separation times in minutes. Hyperthermia dose (0 time). Points to the right of zero represent radiation following hyperthermia. Data points represent the mean and standard error of four experiments.



radiosensitivity. In contrast, heating 3 minutes after irradiation results in an intermediate sensitivity.

3.4.2 Interaction Relaxation

The relaxation of the interaction that occurs when radiation is given at greater intervals before or after hyperthermia is of biological, and technical importance. Figure 3.5 illustrates that a relaxation occurs and that at least for radiation preceding hyperthermia, this cannot be neglected. To determine the magnitude and rate of relaxation, CHO cells were suspended and plated into T30 flasks at a fixed concentration, incubated at 37° for two hours and then cooled to room temperature. They were then either heated to 44° for 20 minutes, cooled to room temperature and groups of 10 flasks irradiated simultaneously at 5 variable dose rates at increasing time intervals; or, irradiated at room temperature and then subsequently heated. The radiation was ⁶⁰Co radiation at dose rates from 2.90 to 1.65 Gy/min. Figure 3.6 illustrates the relaxation survival data and the average slope of the survival curve over this dose range.

Radiation followed by increasing time intervals before hyperthermia results in a recovery in survival, at least partially explained by a decrease in radiosensitivity. In contrast, radiation after

hyperthermia results in a constant radiosensitivity with apparently decreasing survival for increased time intervals. The effects on the radiosensitivity are in agreement with the data in figure 3.5 and in substantial agreement with Gerwylch et.al. (1975) who observed that, unlike radiation ISD, the repair of hyperthermia ISD did not begin until after 6 or 12 hours for CHO cells.

The biological implication is that either radiation and hyperthermia ISD are distinctly different or that the mechanisms by which they are repaired are different. Technically, radiation given within 100 minutes before hyperthermia may represent an unstable experimental situation that should be avoided if consistent results are required.

While the complexities of the relaxation process remain undisclosed, these experiments did suggest the requirements for satisfactory experimental techniques. For short separations of radiation and hyperthermia insults, the timing must be precise and the heating and irradiation should occur simultaneously, as for the data in figure 3.5. Where longer separations are used, the survival is not changing rapidly with time and therefore the above conditions may be relaxed slightly.

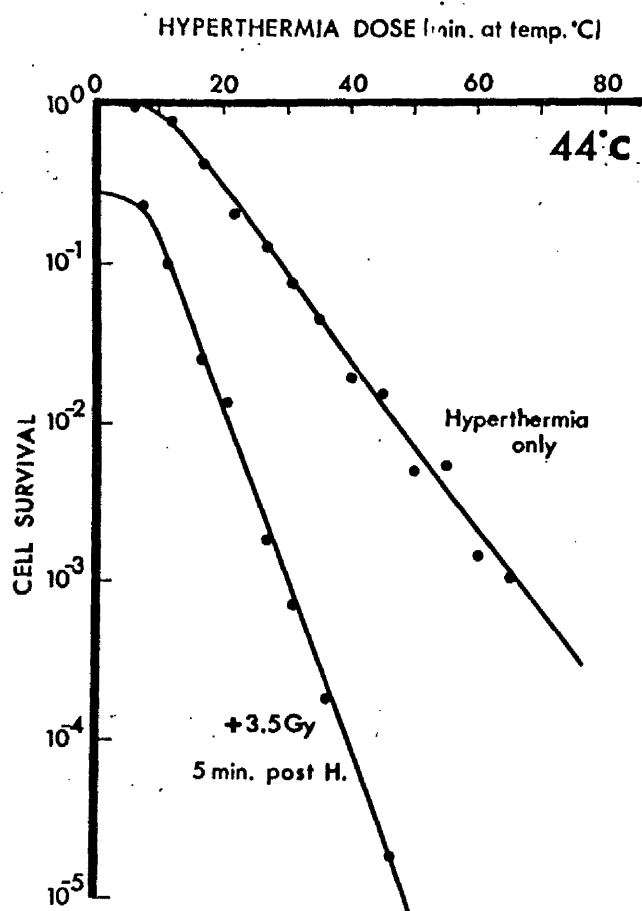


Fig. 3.7 CHO survival after hyperthermia (44°) alone or followed 5 minutes later by 3.5 Gy ^{60}Co at room temperature. The data points represent the result of a single experiment.

3.4.3 Sensitization of Hyperthermia Response by Radiation

Using method B, CHO cells in Hams F12 were plated in T30 flasks at concentrations of 10^3 , 10^4 , 10^5 , cells per flask. These flasks were then heated to 37° for 15 minutes and subsequently to 44° . Samples were withdrawn from the water bath at successive times and half of these were given a total dose of 3.5 Gy of ^{60}Co γ radiation, 5 minutes after being cooled to room temperature.

The survival data for a single experiment are illustrated in Fig 3.7. It is observed that both survival curves exhibit a shoulder followed by an exponential slope, which is increased if heating is followed by a radiation exposure.

3.4.4. The Effect of Hyperthermia Dose on Radiation Sensitivity

In order to provide a clearer picture of the interaction and of the interaction event, the effect of hyperthermia dose on radiation sensitivity was briefly explored. CHO cells suspended in Hams F10 (method A) were heated at 42°C for different times and irradiated with ^{60}Co γ radiation at variable dose rates from 1.5 to 0.6 Gy/min.

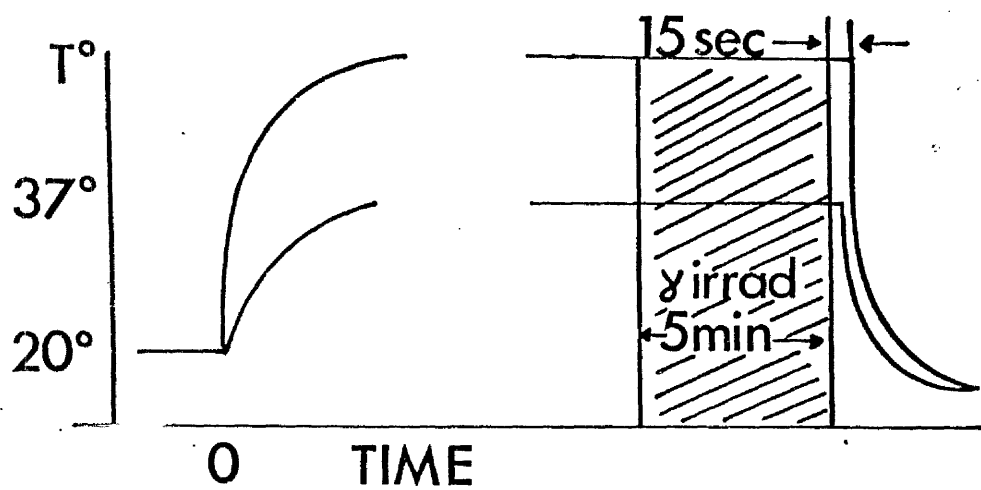


Fig. 3.8 Heating and irradiation schedule for the data presented in figures 3.9 and 3.10.

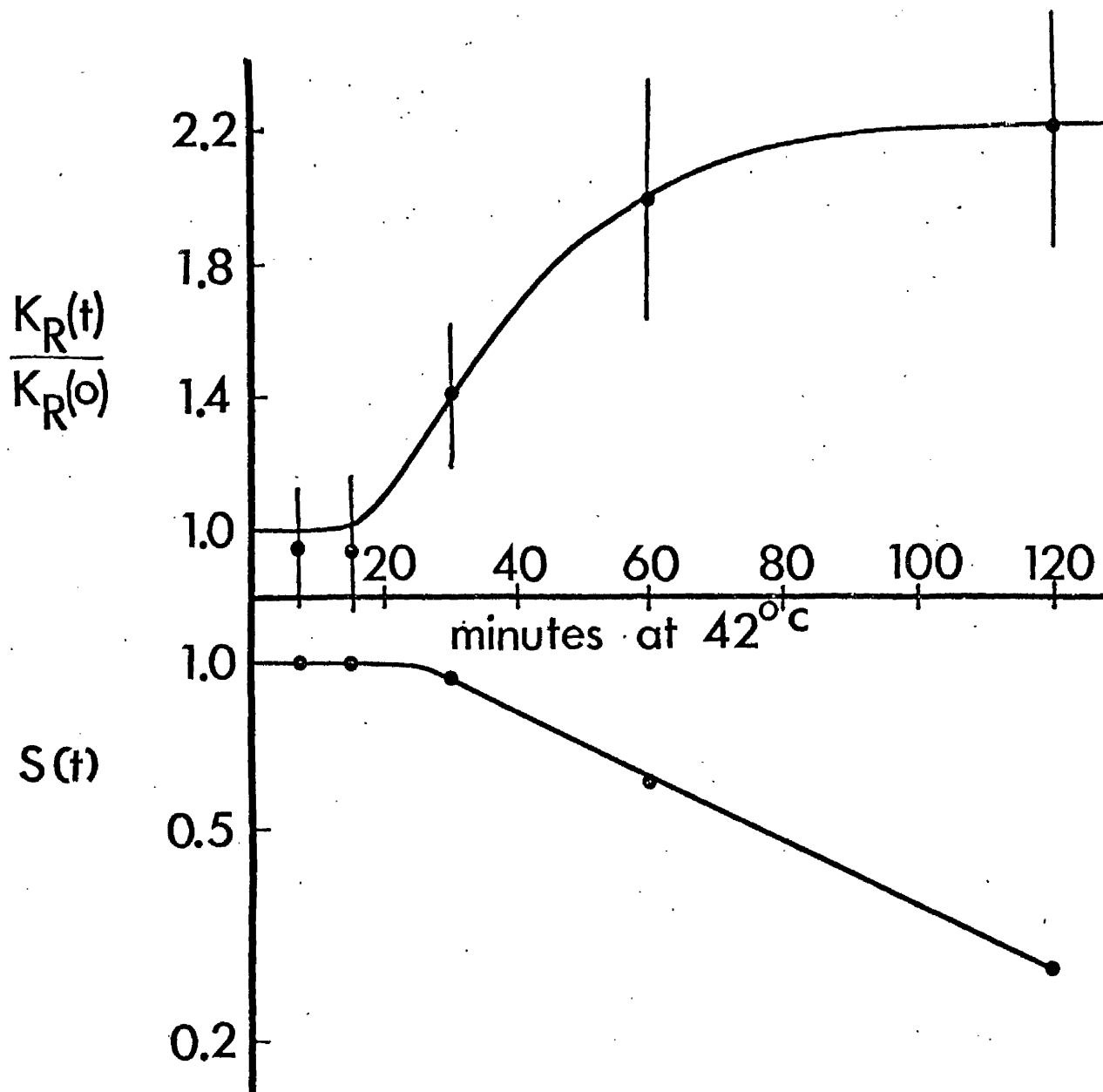


Figure 3.9 Relative radiosensitivity $K_R(t)/K_R(0)$ and relative plating efficiency $S(t)$ for a hyperthermic exposure for t minutes at 42°C. $K_R(0)$ is the radiosensitivity at 37°C. Each point represents the result of a separate experiment and error bars represent the standard errors of the ratio calculated from the observed standard error of the fit.

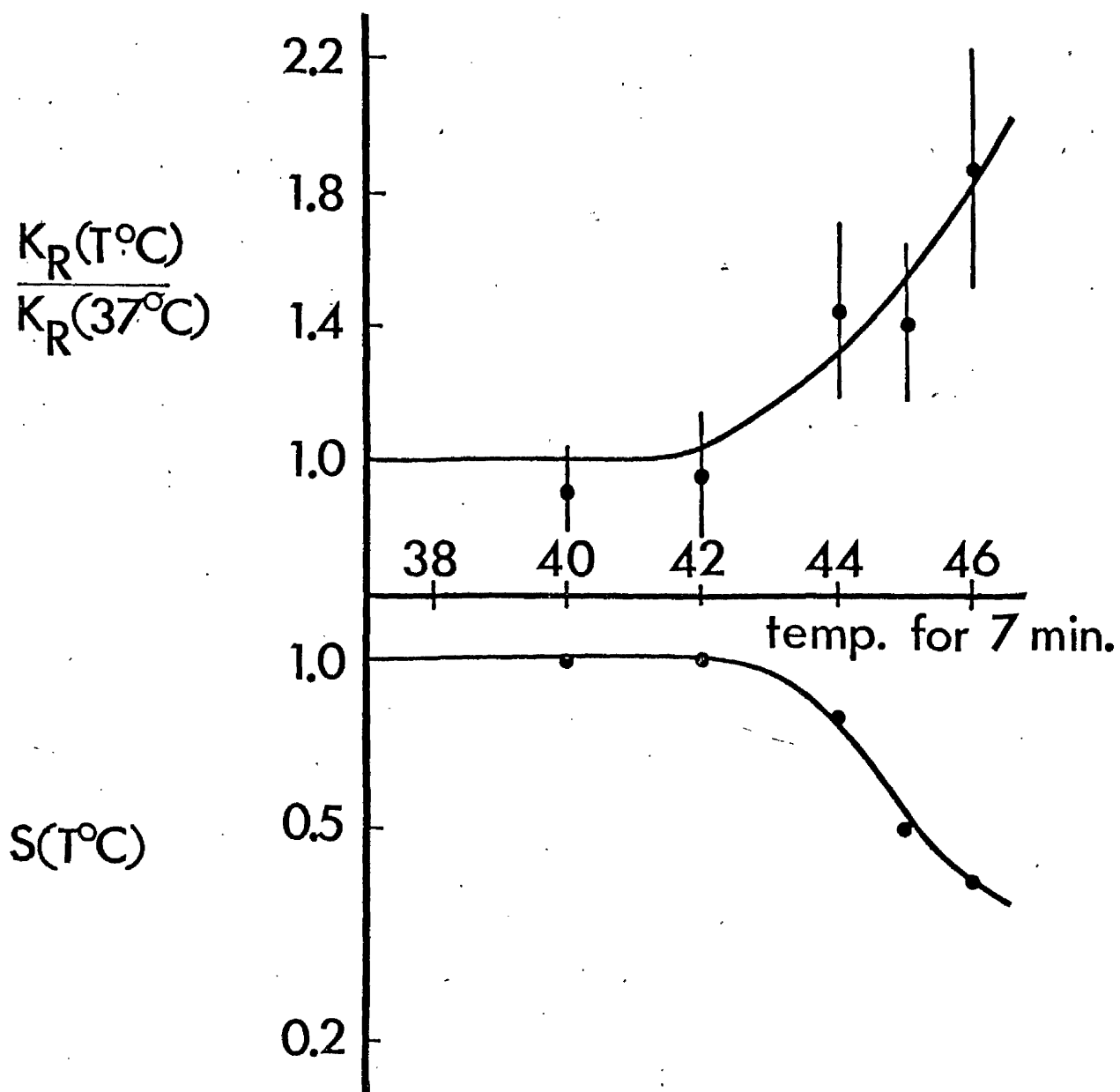


Fig. 3.10. Relative radiosensitization - $K_R(T^\circ)/K_R(37^\circ)$, and relative plating efficiency, $S(T^\circ)$, for irradiation during a seven minute exposure at a temperature T . Each point represents a separate experiment and the indicated errors are as described for figure 3.9.

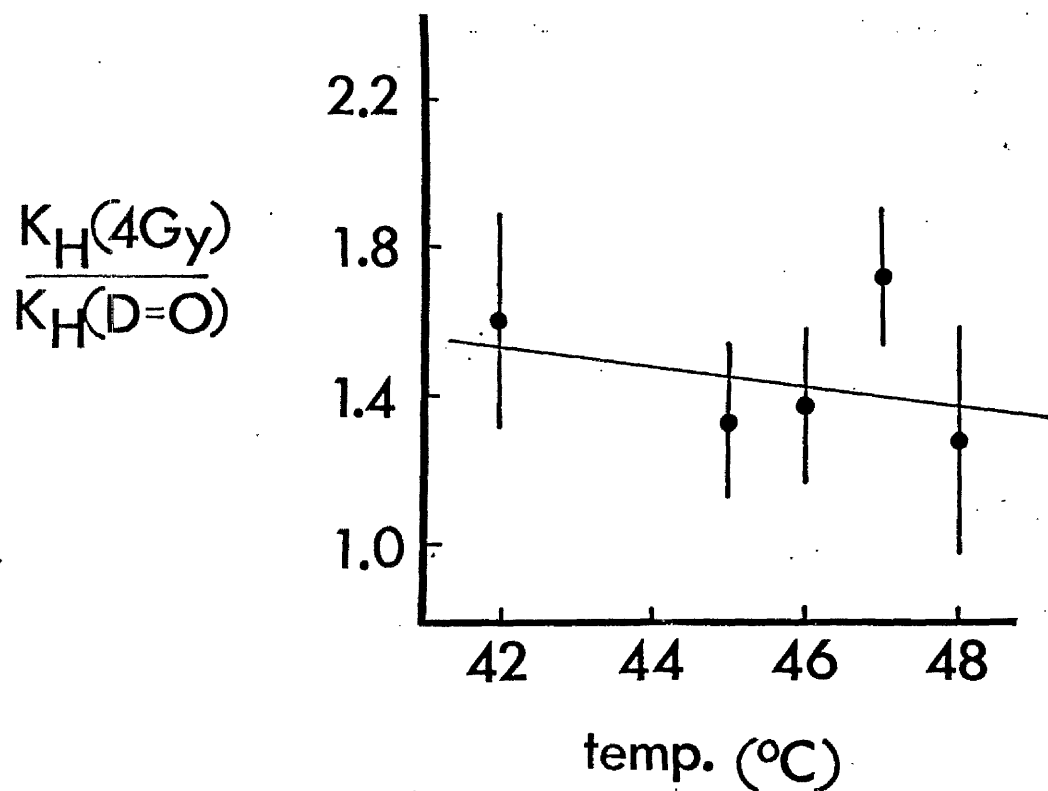


Fig. 3.11. Relative thermal-sensitization, $K_H(46Gy)/K_H(D=O)$, at a temperature, T , 30 minutes after a ^{60}Co radiation dose of 4 Gy at room temperature. Each point represents the results of a separate single experiment and the indicated errors are as described in figure 3.9.

As schematically illustrated in figure 3.8, irradiation started 5.25 minutes and stopped 0.25 minutes before the hyperthermic exposure was terminated by immersing the tubes in room temperature water.

The relative radiosensitivity and the corresponding relative plating efficiency are illustrated in figure 3.9. The results, similar to those reported by Robinson et.al. (1974), suggest a rise to a terminal value of radiosensitivity for a relatively small hyperthermia dose. The author however believes that this is not the case and is an illusory result of insufficient and/or inadequate data. In a later chapter, for a different situation, substantial data argue against such an exponential rise to a terminal value.

3.4.5. The Effect of Temperature on Sensitization of Radiation Response

One of the aspects of the effect of temperature on the interaction was explored by utilizing the treatment schedule of figure 3.8, in which the total time is fixed at 7 minutes and the hyperthermic temperature is varied from 40 to 46°C. The remaining procedure was as described in section 3.4.4. Figure 3.10 illustrates the relative radiosensitivities and relative

plating efficiencies as a function of temperature observed for this treatment. It is observed that radiosensitivity apparently increases for increasing temperature.

3.4.6. The Effect of Temperature on Sensitization of Hyperthermia Response

Another aspect of the effect of temperature was examined by irradiating cells suspended in Hams F10 in glass tubes (method A). Thirty minutes after a radiation dose of 4 Gy, the thermal sensitivity was assayed by immersing the glass tubes simultaneously in a waterbath, maintained at the experimental temperature, for graded periods of time. Figure 3.11 plots the relative thermal-sensitivity as a function of temperature. While the uncertainty is great, the data suggest that the sensitising effect of a radiation dose decreases with increasing temperature.

3.4.7 Discussion

The preliminary experiments described in the preceding section demonstrate or suggest that;

1. Hyperthermia increases the slope of the radiation survival curve.
2. Hyperthermia administered before radiation increases the extrapolation number of the radiation survival curve.

3. Radiation increases the slope of the hyperthermia survival curve.
4. Increasing hyperthermia doses result in increasing radiosensitization.
5. Increasing temperature results in an increase in radiosensitization by hyperthermia.
6. Increasing temperature results in a decrease in thermal-sensitization by radiation.

Both the fact that these are aspects of a single phenomenon, and the relationship between them are obscured by both the experimental and the experimenter's view point. The task of describing the interaction phenomenon from this viewpoint is analogous to the problem of the gemmologist, who must describe the geometry of a cut gem and is allowed to perceive only one facet at a time. It can be done, but the process is simplified by being allowed more than a one-sided view.

The very concept of "radiosensitization", omni-present in the literature, is a manifestation of this one sided viewpoint. For instance, one of the roles of oxygen in modifying the resulting free radical yield of radiation is commonly referred to as radiosensitization, but it is clear that in this role oxygen of itself does not alter the radiosensitivity of the cell, but rather interacts with radiation to

to provide a greater yield of damage events to which the cell responds with unchanged sensitivity. It is no more incorrect to say that radiation changes the oxygen-sensitivity of the cell.

It is not then the aspect of radiosensitization or thermal sensitization that is being investigated, but rather the interaction itself. By utilising a different, but not new, viewpoint and experimental technique that allows the realization of the interaction per se., the obscure relationships between the above phenomena are made clearer.

CHAPTER FOUR

THE SURVIVAL SURFACE AND THE MATRIX EXPERIMENT

4.1. Introduction

The experimental results described above show that, in the cell system studied, radiation and hyperthermia interact in their effects on the survival of the cells clonogenic ability. The interaction is manifested in increases in the slopes of the survival curves and, at least for radiation survival, increases in the extrapolation numbers. A minimal model is developed that would account for this behaviour. The subsequent expansion of this model to accommodate variable sensitising doses, reveals the hyperthermic sensitization of radiation response and the radiation sensitization of hyperthermia response to be two manifestations of a single phenomenon.

The interaction of the two stimuli can be expressed by mapping the response over a co-ordinate system, that consists of two orthogonal functions of the respective stimuli, generating a response surface. The determination of the response surface, while not conceptually difficult, presents problems in terms of time and manpower. With the possibility that the system response might change with time or changes in culture conditions, it is preferable to determine the surface over the shortest period of time possible and with the most nearly identical experimental conditions. An experimental technique that amply fulfills these requirements is described.

4.2 THEORY

4.2.1 A Minimal Model of Interaction

The fact that the radiation survival curves have shoulders at low doses can be interpreted as indicating that the cells have a limited ability to accumulate damage before it is expressed in lethality. Normally such accumulation is associated with a repair process which can be saturated by a sufficiently large demand and which restores the population of survivors to a condition similar to their initial one.

Although experimental evidence regarding the existence and time course of the saturable repair process is not presented in this chapter, the property of the cells accumulating or repairing damage, which is indicated by the shoulder, will be referred to for brevity as a saturable repair process.

Excluding any consideration of the detailed shape of the shoulder, it is assumed that portions of the survival curves of interest can be described by expressions of the form,

$$S = Me^{-KD}, \quad 4.1.$$

where S is the fractional survival, D is the dose, K is the slope of the survival curve, and M is the extrapolation number, a measure of the capacity of the saturable repair process.

It can be demonstrated that a change only in the effectiveness of a dose D, occasioned by a dose modifying agent, can cause an increase in slope without a change in extrapolation number. Such a change can be due to either an increased yield of radiation damage events or to an inhibition of an unsaturable repair process. The observation of an increase in slope alone cannot distinguish between the two mechanisms. However, if an increase in extrapolation number is also observed, then considerable further analysis is possible, and it is suggested that the following model is as simple as any which would adequately describe the phenomenon.

Let

D = absorbed dose
 G = number of damage events/unit dose
 R = number of damage events which can be repaired by a saturable process
 Z = inactivation constant expressed as lethal events/available damage events.

Then

$$-\ln S = Z(GD-R). \quad 4.2$$

If in equation 4.2, Z is unity, then an increase in slope is brought about by an increase in G. This would be produced by a sensitizing agent which acts purely as a dose modifier, one of the roles of oxygen being a common example.

If on the other hand, Z is less than unity, a constant proportion of available damage events never becomes lethal. That is, a non-saturating repair process acts on the damage events which have not been repaired by a saturable process. It can be seen from equation 4.2 that a sensitising agent which increases Z towards unity will increase the slope, ZG , and also increase the extrapolation number, e^{ZR} , R being unaffected by the agent.

Another way of approaching this is to consider the fates of all of the damage events which are included in this expansion of equation 4.2

$$-\ln S = ZGD [-1] + (1-Z)GD [0] + ZR [+1] + (1-Z)R [0] \quad 4.3$$

where the multiplier in square brackets reflects the effect each term has on cell survival. These terms can then be described as

- a) ZGD = Damage events which would be lethal if R were zero
- b) ZR = Damage events which would be lethal but are repaired by R
- c) $(1-Z)GD$ = Damage events which would not be lethal even if R were zero
- d) $(1-Z)R$ = Damage events which would not be lethal yet are repaired by R .

Thus R and the shoulder of the survival curve are aspects of a repair mechanism which is incapable of distinguishing damage events that are liable to be lethal (a) from non-lethal damage events (c). This repair of non-lethal damage events (d) does not affect cell survival and is therefore wasted effort.

If Z is increased by a sensitising agent, a smaller amount of R is wasted in process (d) in repairing non-lethal damage events, therefore more of R is available to repair damage which would otherwise be lethal causing the extrapolation number, e^{ZR} , to rise.

Equation 4.2 can be rewritten as

$$(-\ln S)/Z = GD - R \quad 4.4$$

While the effect of a change in G is simply to expand or contract the dose scale, causing the survival curve to rotate about the extrapolation number, the effect of a change in Z expands or contracts the $\ln S$ scale, causing the survival curve to rotate about the quasi-threshold dose, R/G . As an analogy to the term "dose modifier" applied to those agents which increase G , the term "expression modifier" might be appropriately applied to those agents which alter Z .

Although the survival curve of equation 4.2 rotates about the quasi-threshold dose, it is possible to elaborate the model so that the sensitized survival curve can rotate about any point without the necessity of invoking a dose modifying effect for the sensitizing agent in addition to its expression modifying effect. Let there be J different types of damage resulting from radiation and let

g_j = number of j th damage events/unit dose

r_j = number of j th damage events which can
be repaired by a saturable repair process

z_j = inactivation constant for j th damage events,
lethal events/ j th damage events

Then

$$-\ln S = \sum_j D z_j g_j - \sum_j z_j r_j. \quad 4.5$$

Equation 4.2 is a special case of equation 4.5 in which all the z_j terms are equal. Equation 4.5 describes sensitized survival curves which intersect the unperturbed curve at a dose D_{qI} , which we shall describe as the "interaction quasi-threshold dose".

$$D_{qI} = \Delta z_j r_j / \Delta z_j g_j \quad 4.6$$

The system presented above requires three parameters or three sets of parameters. $G + g_j$ quantitate the damage yield of the radiation events, R and r_j quantitate the saturable repair capability, and Z and z_j quantitate the non-saturable repair capability. The required temporal relationships between the three mechanisms is that G acts prior to R and R acts prior to Z .

A similar analysis of hyperthermia survival curves presenting $\ln S$ as a function of the time at an elevated temperature can be carried out.

The minimal model presented in equation 4.2 describes the characteristics of separate and distinct populations.

If Z has its unperturbed value then the survival is that of the unsensitized population. If the population has been sensitized and therefore changed, Z has a perturbed value, however the value of Z is determined outside the model of equation 4.2 and Z is only an implicit function of the sensitizing agent.

Before expanding the minimal interaction model into a model that explicitly describes the interaction, the topology of the interaction will be examined.

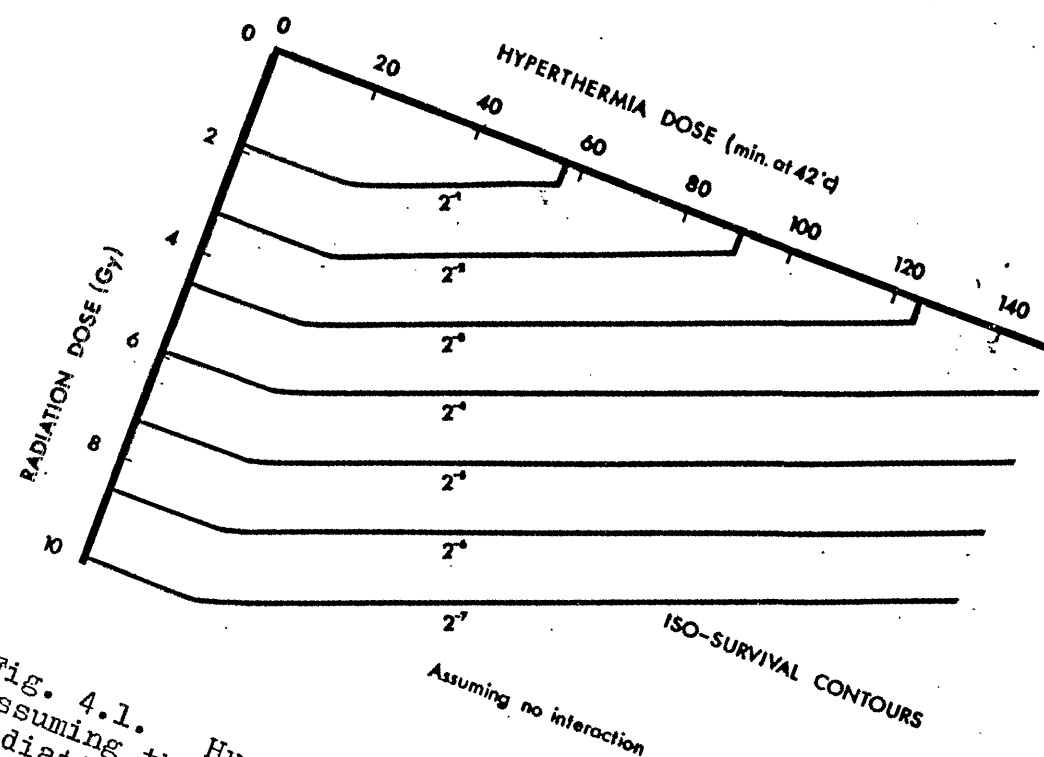


Fig. 4.1. Hypothetical iso-survival plot assuming that there is no interaction between radiation and hyperthermia.

4.2.2 The Survival Surface

Assume for the purpose of illustration that there is no interaction between hyperthermia and radiation. An iso-survival plot, as shown in figure 4.1, can be constructed. The contours on this plot represent equal survival levels each separated by a factor of 2, so that these contours represent survivals of $\frac{1}{2}, \frac{1}{4}, \frac{1}{8}$... respectively. In order to reduce the survival to $\frac{1}{8}$ we may give a radiation dose of 4.5Gy or 125 minutes at 42°C, or alternatively, 3.5Gy and 60 minutes at 42°C. That is, any combination of radiation dose along this contour will yield a survival of $\frac{1}{8}$.

This type of plot is similar to a relief map. Just as the separation of the contours on a relief map indicates the relative steepness of the terrain, so the separation of the contours on this plot indicates the relative steepness of the survival surface.

Along the hyperthermia axis, after a region of low sensitivity indicated by the wide spacing of the contours, the contours become closer and evenly spaced, indicating a steeper slope that is exponential. For increasing hyperthermia dose, since the lines are parallel, the slope of the survival surface in the direction of increasing radiation effect remains unchanged. That is, as was assumed, hyperthermia has not increased the slope of the radiation survival

SURVIVAL SURFACE $-\ln S(D,T)$

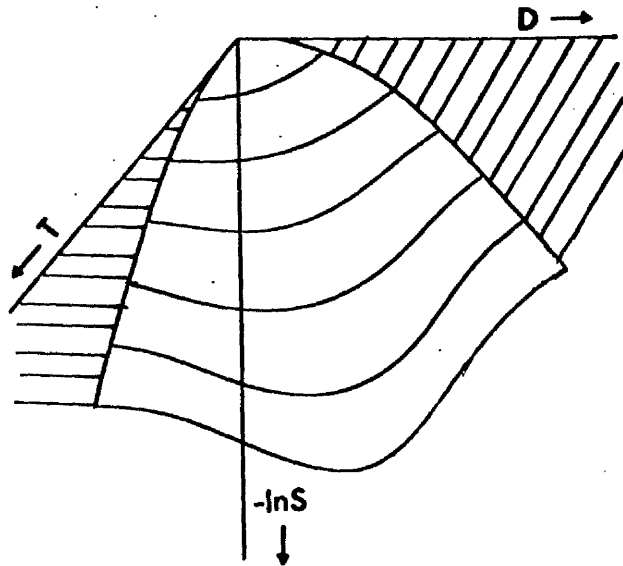


Fig. 4.2 Hypothetical survival surface. The radiation dose D , the hyperthermia dose T and $-\ln S$ form three mutually orthogonal axes. The straight parallel lines indicate the $D = 0$ plane and the $T = 0$ plane. The curved lines indicate the survival surface for combinations of D and T .

curve and conversely radiation has not affected the slope of the hyperthermia survival curve. It is evident, therefore, that if the interaction exists, the isosurvival contours cannot be straight parallel lines but must curve.

If we imagine the 3 dimensional survival surface corresponding to figure 4.1., we see that it exists in a space defined by radiation dose, D, hyperthermia dose, t, and the logarithm of the survival, $-\ln S$, as three mutually orthogonal axes and that it will be planar below those regions in figure 4.1 where the isosurvival contours are straight parallel lines. If however the contours curve as suggested, the surface will not be planar, but might appear as conceptualized in figure 4.2.

Since the surface is expected to be smooth and continuous, (i.e. there are no abrupt changes in survival or dose response for an infinitesimal change of t or D), the partial derivatives $\frac{\partial}{\partial t} \left(\frac{\partial \ln S}{\partial D} \right)$ and $\frac{\partial}{\partial D} \left(\frac{\partial \ln S}{\partial t} \right)$ will therefore be defined and continuous over a region away from $D = 0$ and $t = 0$. These are sufficient criteria for the partial derivatives being equal. That is

$$\frac{\partial}{\partial t} \left(\frac{\partial \ln S}{\partial D} \right) = \frac{\partial}{\partial D} \left(\frac{\partial \ln S}{\partial t} \right) \quad 4.7$$

Simply stated, this means that if for increasing hyperthermia doses the radiation survival curve is

increasingly sensitized, then the hyperthermia survival curve is increasingly sensitized for increasing radiation dose.

The intersection of the response surface in figure 4.2 with the $t = 0$ plane is the unperturbed radiation survival curve in the more usual two-dimensional representation. Similarly, the intersection with the $D = 0$ plane is the unperturbed hyperthermia survival curve. The minimal model of equation 4.2 describes the intersection of the survival surface with planes that are parallel to the $t = 0$ plane. The value of Z in the planes, an implicit function of the sensitizing dose in the minimal model, must be a continuous function of t that is explicit in the mathematical description of the survival surface. Therefore, if one can describe the surface, this will provide a complete description of the interaction.

4.2.3 First Order Interaction Model

The experimental evidence above has demonstrated that, at least over a limited range of doses, the perturbed and unperturbed radiation survival curves were approximately exponential. To this approximation, the slopes of the radiation survival curve are dependent on hyperthermia dose, but independent of radiation dose. This yields the differential equation

$$\frac{\partial \ln S}{\partial D} = f_1(t) \quad 4.8$$

Similarly, over at least a limited range of hyperthermia doses, the perturbed and unperturbed survival curves are approximately exponential. To this approximation, the slopes of the hyperthermia survival curves are dependent on radiation dose, but independent of hyperthermia dose, yielding

$$\frac{\partial \ln S}{\partial t} = f_2(D) \quad 4.9$$

Integration of both differentials yields two general solutions with a particular solution satisfying both equation 4.8 and 4.9. Specifically this is

$$-\ln S = C_1 D + C_2 t + C_3 Dt + C_4, \quad 4.10$$

while a distribution of the constant C_4 among the other three terms yields

$$-\ln S = D_1 K_R + t_1 K_H + D_2 t_2 K_I \quad 4.11$$

$$\begin{aligned}
\text{where } D_1 &= D - D_{q1} & \text{for } D > D_{q1} \\
&= 0 & \text{for } D \leq D_{q1} \\
t_1 &= t - t_{q1} & \text{for } t > t_{q1} \\
&= 0 & \text{for } t \leq t_{q1} \\
D_2 &= D - D_{q2} & \text{for } D > D_{q2} \\
&= 0 & \text{for } D \leq D_{q2} \\
t_2 &= t - t_{q2} & \text{for } t > t_{q2} \\
&= 0 & \text{for } t \leq t_{q2}
\end{aligned}$$

If t is 0 then both t_1 and t_2 are also 0 leaving only

$$-\ln S = (D - D_{q1}) K_R \quad 4.12$$

which is equivalent to equation 4.1 where K_R and D_{q1} are the radiosensitivity and the quasi-threshold dose for the control population. Similarly, K_H and t_{q1} are the thermal-sensitivity and quasi-threshold time, (hyperthermia dose), for the control population.

The terms of the minimal model for radiation can be derived.

$$ZG = K_R + (t - t_{q2})K_I \quad 4.13$$

$$ZR = D_{q1}K_R + D_{q2}(t - t_{q2})K_I \quad 4.14$$

Finally, using equation 4.5, D_{q2} and t_{q2} can be identified as the interaction quasi-threshold radiation dose and the interaction quasi-threshold hyperthermia dose respectively. In the context of equations 4.13 and 4.14 the expression, "interaction quasi-threshold dose," is appropriate, for this is the dose that is theoretically accumulated before interaction type damage events are evident.

4.3 Matrix Experiment

The matrix experiments were designed to overcome experimental instability and simultaneously maximise the amount of information obtained for the work expended. To obtain consistent survival data, it was desirable to collect the data for as many points as possible within the context of a single experiment. To maximise the useful amount of information that might be obtained without interpolation, each experiment was designed to yield survivals for a rectangular matrix of radiation and hyperthermia doses so that each row of the matrix would yield a radiation survival curve and each column would yield a hyperthermia survival curve.

4.3.1 Experimental Procedure

After trypsinizing, CHO cells in Hepes-buffered Hams F12 were plated into T30 flasks at three concentrations and allotted radiation and hyperthermia doses so as to produce a maximum of 500 clones per flask at any one concentration. Immediately after plating, the flasks were incubated at 37° for two hours and then cooled to room temperature. At this time cellular attachment to the plastic surface was virtually complete. The flasks were mounted in a rack and immersed in a 37° waterbath for 15 minutes, having been at room temperature for about 30 minutes.

The rack containing the flasks, heated to 37° , was quickly transferred to a waterbath maintained at 42°C .

At 15 minute intervals flasks were removed, 15 flasks at a time. These were cooled in room temperature water for 1 minute to terminate the heat exposure. Three minutes after removing the flasks, 12 of these flasks were irradiated simultaneously at 6 different dose rates, ranging from 2.8 to 1.4 Gy/min, leaving 3 flasks for the unirradiated controls. Twenty-four unheated flasks were irradiated at the same 6 dose rates but to a higher total dose. All flasks were maintained at room temperature during, and for 1 hour after irradiation or heating, before being incubated at 37° . After 6 days the flasks were stained and counted.

This technique provided survival data for 77 combinations of radiation and hyperthermia doses, 11 radiation survival curves and 7 hyperthermia survival curves.

4.3.2 Data Analysis

Data for separate experiments were averaged and normalized to unity survival at zero dose and zero time to obtain the survivals, $S(t,D)$. The parameters of the survival surface described by equation 4.11. were obtained by a non-linear iterative technique, "moving simplex", described in appendix III.

For each experiment, the radiation and hyperthermia survival curve parameters were obtained by the simplex method. Radiation survival normalized to unity at zero radiation dose was described by

$$\begin{aligned} -\ln \left[\frac{S(t,D)}{S(t,0)} \right] &= DK_R(t) - \ln M_R(t) \text{ for } D > \frac{\ln M_R(t)}{K_R(t)} \\ &= 1 \text{ for } D \leq \frac{\ln M_R(t)}{K_R(t)} \end{aligned} \quad 4.15$$

where

$S(t,D)$ = survival for hyperthermia dose,
t, and radiation dose, D
 M_R = extrapolation number
 K_R = slope of the survival curve.

Hyperthermia survival normalized to unity at zero hyperthermia dose was described by

$$\begin{aligned} -\ln \left[\frac{S(t,D)}{S(0,D)} \right] &= tK_H(D) - \ln M_H(D) \text{ for } t > \frac{\ln M_H(D)}{K_H(D)} \\ &= 1 \text{ for } t \leq \frac{\ln M_H(D)}{K_H(D)} \end{aligned} \quad 4.16$$

the
where M_H and K_H are/hyperthermia extrapolation number
and survival curve slope respectively.

For both the radiation and hyperthermia survival curves, all data points including those on the shoulder of the survival curve were used to derive the parameters of equation 4.15 and 4.16. This approach, approximately describing both the hyperthermia survivals due to the abruptness of the shoulder and the radiation survivals due to the high initial slope and the doses being larger than the quasi-threshold dose, eliminated any bias that might be introduced by an arbitrary datum rejection scheme.

Values of M_H , K_H , M_R and K_R were obtained for each experiment separately and the mean and standard error of the mean obtained.

An independent assessment of the interaction coefficient, K_I , was obtained by fitting the above parameters to equation 4.17 or 4.18

$$K_H(D) = \left\langle \frac{\partial K_H}{\partial D} \right\rangle D + \text{constant} \quad 4.17$$

$$K_R(t) = \left\langle \frac{\partial K_R}{\partial t} \right\rangle t + \text{constant} \quad 4.18$$

A conventional linear weighted least squares fit was used. The point corresponding to $t = 0$ or $D = 0$ was omitted from the fit to avoid biasing the fit through this point.

The residual variance on K_R and K_H , due mainly to inter-experiment variations in sensitivity, dominated the expected variance, predicted by repeated Monte Carlo simulations of the matrix experiments. The dominance of the residual variance resulted in a variance that was approximately proportional to a constant percentage of the square of the value of K_R or K_H . Accordingly, the weights for K_R and K_H in equation 4.17 and 4.18 were taken to be

$$w_i = n_i / y_i^2$$

where y_i is the value of K_R or K_H , n_i is the number of observations and w_i is the weight.

The best estimate of K_I was taken to be the weighted mean of $\langle \partial K_R / \partial t \rangle$ and $\langle \partial K_H / \partial D \rangle$, using the inverse variance of the parameters, $\langle \partial K_R / \partial t \rangle$ and $\langle \partial K_H / \partial D \rangle$, as weights. The error attached to K_I was the largest of the three— the standard error of the weighted mean, the standard error of $\langle \partial K_H / \partial D \rangle$, or the standard error of $\langle \partial K_R / \partial t \rangle$.

4.3.3 Experimental Results

Table 4.1 lists the parameters of equation 4.11 and the independent assessments of K_R , K_H , and K_I obtained as parameters of equations 4.15 to 4.18.

Table 4.1 Interaction parameters H-3min-Y.

PARAMETER	UNITS	x	EXP	SURFACE	UNBIASED
D_q	Gy		E-1	7.39	12.60+0.43
K_R	Gy ⁻¹		E-1	4.75	5.30+0.01
t_q	min		E+1	2.49	2.32+0.63
K_H	min ⁻¹		E-2	1.79	1.75+0.13
D_{qI}	Gy		E+0	1.39	2.13+0.44
t_{qI}	min		E+0	5.01	28.16+8.48
K_i	Gy ⁻¹ min ⁻¹		E-3	3.42	4.06+0.53
$\partial K_R / \partial t$	Gy ⁻¹ min ⁻¹		E-3	"	3.63+0.38
$\partial K_H / \partial D$	Gy ⁻¹ min ⁻¹		E-3	"	4.71+0.46

Note - SURFACE - parameters of equation 4.11.

UNBIASED - parameters of equations 4.15, 4.16, 4.17, 4.18.

Mean \pm Standard Error.

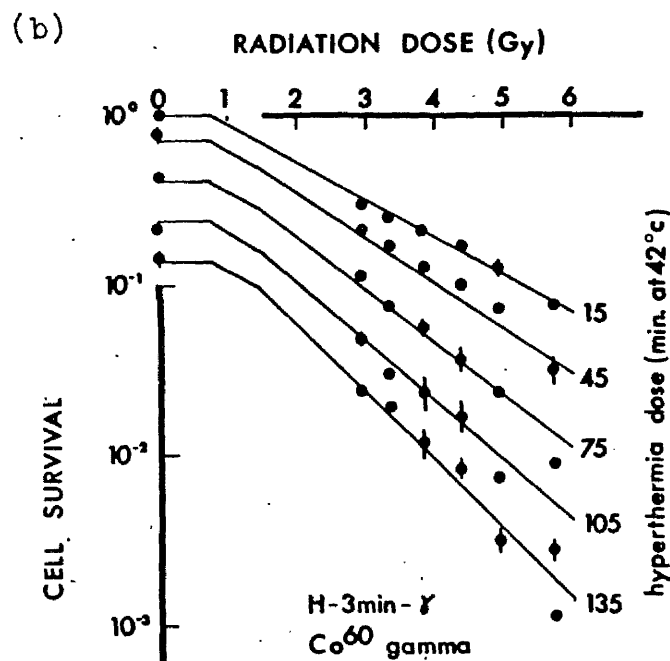
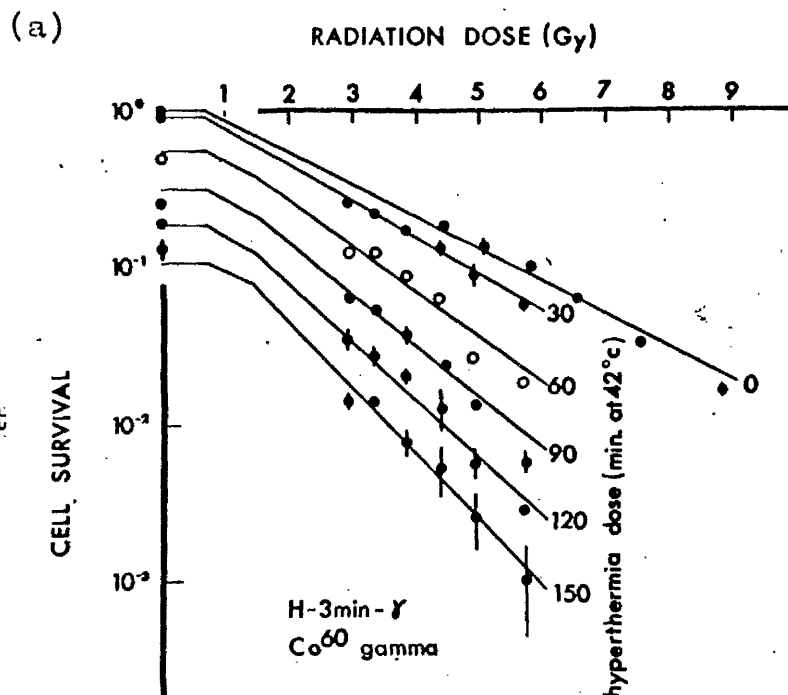
Figures 4.3a,b illustrate the observed survival data plotted as a function of radiation dose and labelled with the corresponding hyperthermia doses. Figures 4.3 c,d illustrate the same data plotted as a function of hyperthermia dose and labelled with the corresponding radiation dose. The solid lines in all four figures are the calculated survivals using equation 4.11 with the parameters listed in table 4.1.

Figure 4.4a illustrates the observed radiation survival curve parameters for equation 4.15. The slope of the value of K_R against hyperthermia dose is the interaction coefficient, $\partial K_R / \partial t$. A straight line through the values of K_R intersects the value of K_R corresponding to zero hyperthermia dose at the interaction quasi-threshold time, t_{qI} .

Figure 4.4b illustrates the observed hyperthermia survival curve parameters for equation 4.16. The value of the interaction coefficient, $\partial K_H / \partial D$, and the interaction quasi-threshold dose, D_{qI} , can be obtained as described above.

The iso-survival contours for this experimental configuration are presented in figure 4.5. These are obtained by solving equation 4.11 for the required radiation dose as a function of the hyperthermia dose

Figure 4.3.
Cell survival
for a hyperthermia
exposure at 42°C
followed three
minutes later
by a radiation
dose at room
temperature. The
data points represent
the mean and the
standard error of
two observations
except for open
circles which
represent a single
datum point. The
lines in all four
figures are the
survivals calculated
using equation 4.11.
(a,b) Survival as
a function of
radiation dose.



(c)

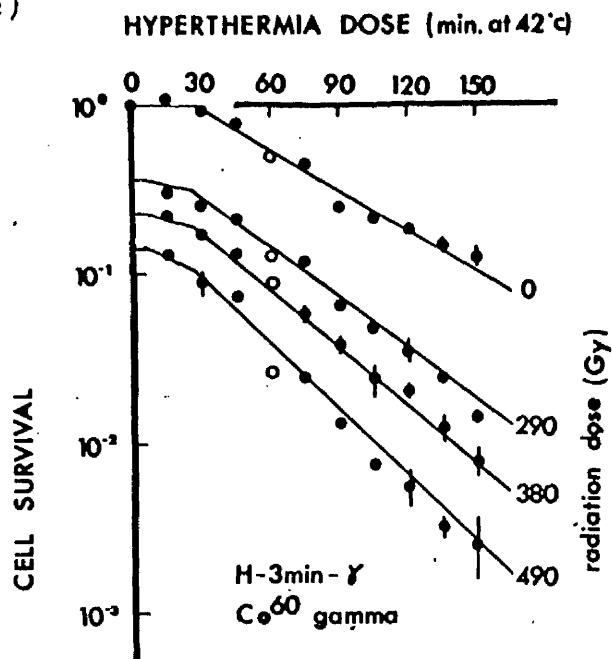


Figure 4.3. c,d
Survival as a
function of
hyperthermia
dose.

(d)

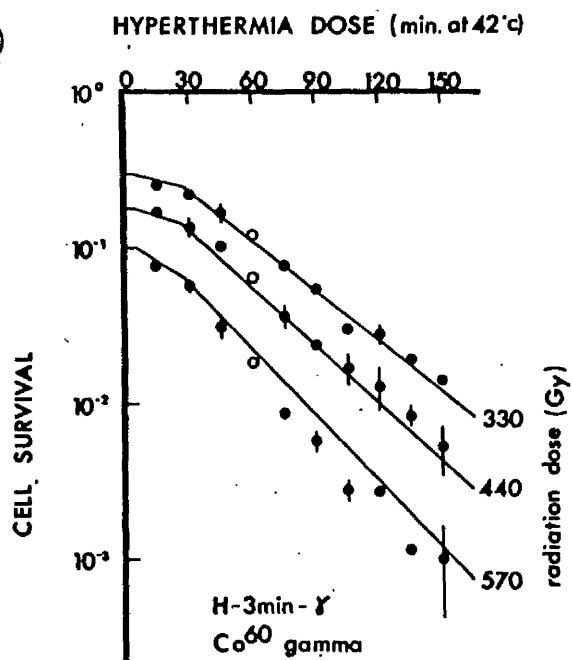


Fig. 4.4a
Extrapolation number, M_R , and radiosensitivity K_R , for the survival data of figure 4.3., as a function of hyperthermia dose. The data points represent the mean and standard error of two observations except for open circles which represent a single datum point. The lines represent the calculated values from equation 4.11.

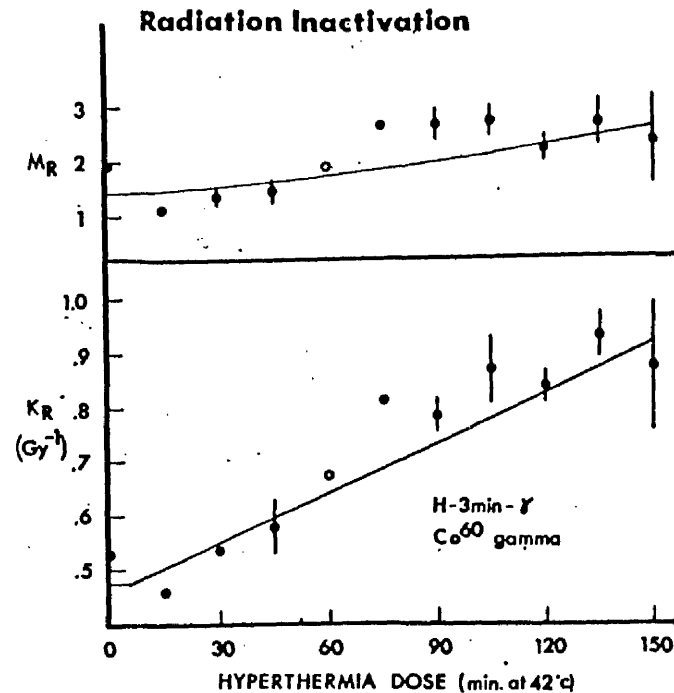
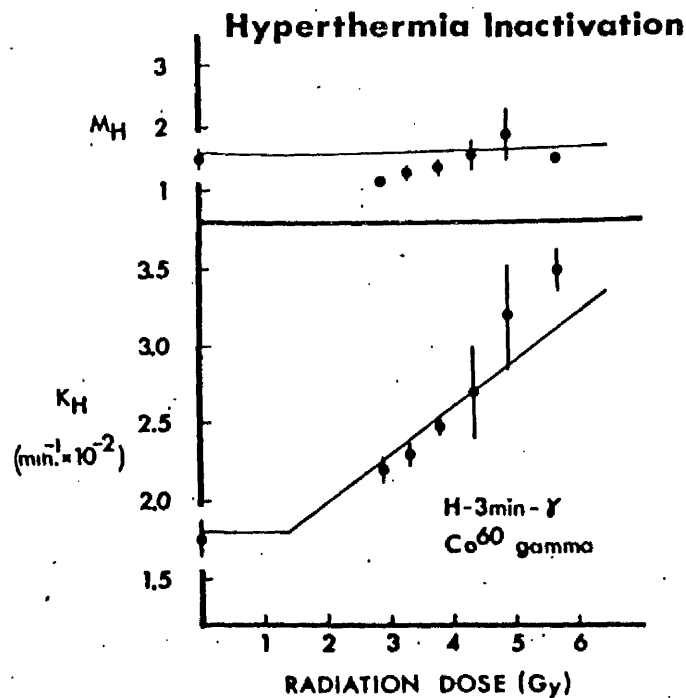


Fig. 4.4b
Extrapolation number M_H and thermal-sensitivity for the survival data of figure 4.3 as a function of radiation dose. lines and data points are as described in figure 4.4.



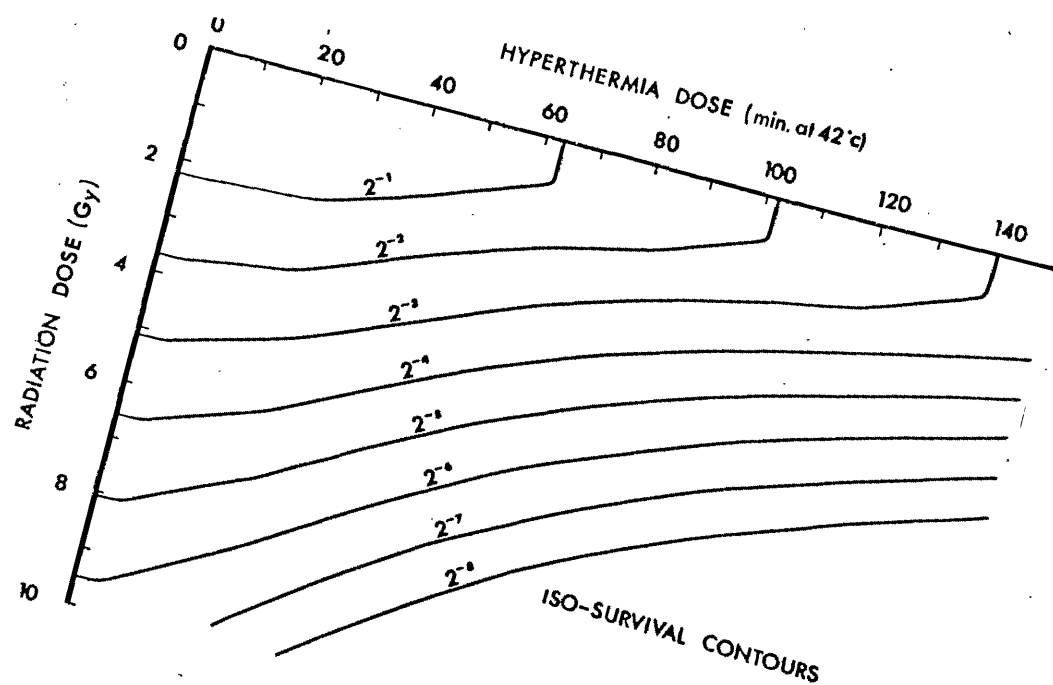


Figure 4.15 Iso-survival contours for survival data of figure 4.3 calculated from equation 4.11.

to obtain a given survival level. As suggested in section 4.2.2, the iso-survival contours exhibit a curvature.

4.3.4 Discussion

Examination of figures 4.3 and 4.4 reveals that the simple model of equation 4.11 provides only a qualitative description of the survival data. This perhaps, is to be expected, as equation 4.11, formulated to describe survival on the exponential portion of the survival curve, has been applied to survivals on the shoulder of the survival curve.

However, the survival model of equation 4.11 appears to adequately fit the shoulder of the hyperthermia survival curve due to the abruptness of the transition from the shoulder to the exponential slope. The radiation survival curves exhibit a large initial slope, accounting for the apparent agreement, at low doses, between the observed survivals and the first order response predicted by the survival model. In this connection, the values of radiosensitivity, in these and particularly in subsequent experiments, are slightly biased by the low radiation doses and might be referred to as local, rather than terminal, radiosensitivity values.

It is observed that the values for $\partial K_R / \partial t$ and $\partial K_H / \partial D$ do not exhibit the expected agreement, but

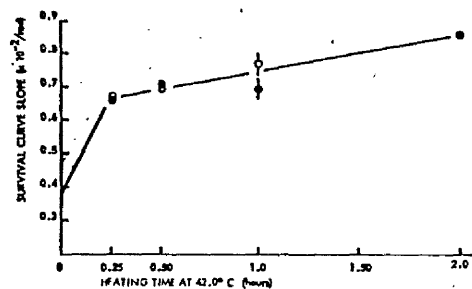


Fig. 4.6. Survival curve slopes for CHL cells as a function of time at 42°C. O after irradiation, ● before irradiation ⊕ before, during, and after irradiation. (from Robinson and Wizenberg 1974)

the mean of the two is, within experimental error, equal to the interaction coefficient, K_I , obtained for equation 4.11.

The model and the survival data are in partial agreement with the results of Robinson and Wizenberg (1974). They observed that subjecting CHL cells to 42° for variable times before, during, and after irradiation resulted in a steep initial rise in radiosensitivity, followed by a less steep increase for exposures of 15 minutes to 120 minutes at 42°C . Their data are illustrated in fig. 4.6. This pattern of sensitivity might be explained by at least two possible response mechanisms; an exponential rise to a terminal value of radiosensitivity or a biphasic rise in radiosensitivity.

It can be demonstrated that an exponential rise to a terminal value of radiosensitivity is necessarily associated with a perturbed hyperthermia response exhibiting a concave upward survival curve (note).

note

$$\partial S / \partial D = A_0 + A(1 - e^{-Bt})$$

Radiosensitivity is independent of radiation dose, rising exponentially with hyperthermia dose, t , to terminal value of $A_0 + A$.

differentiate w/r to t

$$\partial^2 S / \partial D \partial t = AB e^{-Bt}$$

integrate w/r to D

$$\partial S / \partial t = DAB e^{-Bt} + C$$

Thermal-sensitivity equals C for $D = 0$ and at large t for any radiation dose, D .

The hyperthermia survival curves in figure 3.7, which were qualitatively similar to other high dose hyperthermia survival curves, illustrate that for reasonably large hyperthermia doses, there is no indication of such an upward curvature of the survival curve. Thus it would appear that, for the experiments reported herein, such an interpretation is not supported by the experimental data.

While an exponential sensitivity response cannot be ruled out for Robinson's data, the apparently precise data suggest a biphasic interaction rather than an exponential form. The biphasic nature would be more clearly demonstrated if the authors had presented the associated hyperthermia survival curves, that were necessarily obtained to provide the data illustrated in figure 4.6. It is again possible to infer the shape of the perturbed hyperthermia survival curves. These curves necessarily exhibit a steep initial slope for the first 15 minutes followed by a less steep slope for hyperthermia doses greater than 15 minutes. Thus, in the case examined, there is probably not a simple interaction taking place, but in fact two interactions.

The linear interaction observed here is of importance in analysing results presented in a paper (Ben-Hur 1974) purporting to illustrate a large effect of radiation dose rate on the interaction of radiation and hyperthermia. It was reported that for low dose rates (.033 Gy/min), the radiosensitivity of Chinese hamster cells irradiated at 42°C was 6.3 times greater than the radiosensitivity at 37°C, whereas for high dose rates (3.6Gy/min), the radiosensitivity at 42°C was only 1.5 times as great as the radiosensitivity at 37°C. However, for the low dose rates, all of the cells were heated for three hours, while for the high dose rate, the cells were heated only during their radiation exposure, (i.e. the heating time was proportional to radiation dose and was a maximum of three minutes). While the low dose rate survival was indeed sensitized over four times as much as the high dose rate survival, those cells irradiated at the low dose rate had received 60 times the hyperthermia dose that the cells irradiated at the high dose rate had received. Thus it might seem that, contrary to the authors' suggestion, cells irradiated at a high dose rate are more susceptible to interaction than cells irradiated at a low dose rate.

4.3.5 Conclusion

The first order survival model has, as its virtue, a simplicity of expression rather than an accuracy of prediction. Four of the parameters are familiar to most readers. The remaining parameters are easily identifiable and conceptually similar to the parameters used to describe the unperturbed radiation survival curve. More elaborate mathematical expressions might fit the data better, but unless the additional parameters could be given significance and meaning, elaboration would not contribute to a better understanding.

The first order model is thus only a vehicle for the expression of the surface and the matrix experiment is no more than the technique by which the surface is determined. It is the surface itself, the interplay of radiation and hyperthermia response, that is the essence of this investigation.

CHAPTER FIVE

THE EFFECT OF RADIATION QUALITY

5.1 Introduction

The experiments described in the previous chapter demonstrate that cell survival after a combined hyperthermia and radiation insult could be approximately described by a three component model. The normal radiation component and the normal hyperthermia component describe the response when only radiation or hyperthermia is applied. When both are applied, a third component, the interaction component operates.

The interaction component exhibits a roughly first order dependence on both radiation and hyperthermia dose. The interaction can be thought of as two mechanisms, one dependent on radiation dose only and one dependent on hyperthermia dose only. In this and the next chapter these hypothetical mechanisms are separately investigated by a perturbation of the two interaction damage processes.

Many agents affect the radiation response of living organisms and it might be expected that these would affect the radiation mediated interaction. However many of the agents that affect the radiation response also affect the hyperthermia response, thus leading to problems of interpretation and preventing a separation of radiation and hyperthermia interaction effects.

Thus a change of the physical characteristics of the radiation was suggested as a perturbation. A change of radiation dose rate was rejected as a variable because of the large dependence on biological state. Accordingly the effects of a variation of radiation quality were investigated.

5.2.1 Experimental Procedure

The following experiments required Method C. CHO cells were trypsinized and suspended at a concentration of 1.25×10^5 cells/ml in seven plastic T30 flasks. Allowing one flask for a radiation control, the flasks were irradiated with graded doses of X, γ , or neutron radiation. Each of the resulting seven populations was plated into replicate T30 flasks at a concentration to yield 500 clones/plate if they were not further treated. One hundred minutes after the cells had been irradiated, heat treatment was started by immersing the flasks, except for the hyperthermia controls from each of the seven populations, in a waterbath at 42°C. Samples from each population were removed simultaneously, at 15 minute intervals, and after one hour at room temperature were incubated at 37° for six days, stained and counted.

Four flasks were allotted to each unheated point, three flasks to the heated, but not irradiated points, and two flasks to each remaining point. The number of clones per plate decreased for increasing hyperthermia dose. The resulting

loss of statistical certainty about the observed survival was allowed for by using a least chi-square fit for the expected and observed total number of clones per point. The X and γ irradiations were sequential, irradiating the high dose point first and the low dose point last. The six irradiations required a time interval of 15 minutes for X and 20 minutes for γ . This additional time is not included in the 100 minute interval which is the time from the last irradiation to the start of heating. The neutron irradiations were simultaneous over a period of 25 minutes at variable dose rates. The irradiation conditions were;

X - 250kVp, 15 ma, 1.8 mm Cu HVT, 1.35 Gy/min

γ - ^{60}Co , 0.96 Gy/min

n - $^3\text{H(d,n)}$, 14.7 MeV, .15 - .03 Gy/min

5.2.2 Results

The experimental procedure described above yields a hyperthermia survival curve for each radiation dose and a radiation survival curve for each hyperthermia dose. That is, typically, 63 data points per experiment yield 7 hyperthermia

Table 5.1 Interaction parameters (eqn. 4.11) radiation-100min-H

Parameter	Unit	Exp.	$^{60}\text{Co } \gamma$	250kVp x	14.7MeV n
K_R	Gy^{-1}	E-1	5.15	5.01	8.95
K_H	min^{-1}	E-2	2.04	2.46	2.68
K_I	$\text{Gy}^{-1}\text{min}^{-1}$	E-3	4.77	5.48	7.69
D_q	Gy	E-1	5.42	3.09	-0.13
t_q	min	E+1	2.25	2.00	2.52
D_{qI}	Gy	E-1	4.66	4.03	1.36
t_{qI}	min	E+1	1.44	0.54	1.18
K_I/K_R	min^{-1}	E-3	9.26	10.9	8.59
K_I/K_R	Gy^{-1}	E-1	2.34	2.23	2.87

(Temperature) (41.90°) (41.86°) (41.86°)

Table 5.2 Interaction parameters (independent) radiation-100min-H

Parameter	Unit	Exp.	$^{60}\text{Co } \gamma$	250kVp x	14.7MeV n
K_R	Gy^{-1}	E-1	5.03 ± 0.14	5.15 ± 0.018	9.06 ± 0.02
K_H	min^{-1}	E-2	2.04 ± 0.11	2.19 ± 0.09	2.72 ± 0.27
$\Delta K_R / \Delta t$	$\text{Gy}^{-1}\text{min}^{-1}$	E-3	5.08 ± 0.31	4.78 ± 0.46	7.13 ± 0.90
$\Delta K_H / \Delta D$	$\text{Gy}^{-1}\text{min}^{-1}$	E-3	4.64 ± 0.45	5.03 ± 0.61	8.60 ± 1.14
K_I	$\text{Gy}^{-1}\text{min}^{-1}$	E-3	4.94 ± 0.45	4.87 ± 0.61	7.70 ± 1.14
K_I/K_R	min^{-1}	E-3	9.82 ± 0.92	9.45 ± 1.18	8.50 ± 1.25
K_I/K_H	Gy^{-1}	E-1	2.42 ± 0.26	2.22 ± 0.29	2.83 ± 0.51

survival curves perturbed by 6 radiation doses and 9 radiation survival curves perturbed by 8 hyperthermia doses.

Data for 3 experiments for neutrons and γ radiation and 4 experiments for x-radiation were analysed as described in section 4.3.2. The parameters of the first order interaction model, equation 4.11, are listed in table 5.1. The independent assessment of the interaction coefficient yields values of $\partial K_R / \partial t$ and $\partial K_H / \partial D$ that are, within experimental error, equal for each of the three radiation qualities. These values with the independent assessment of the unperturbed radiation and hyperthermia survival curve slopes are listed in table 5.2 and are found to be in fair agreement with the parameters derived by fitting all of the data points to equation 4.11.

Figures 5.1 a,b illustrate the ^{60}Co survival data plotted as a function of radiation dose and labelled with the corresponding hyperthermia dose. Figures 5.1 c,d illustrate the same set of data plotted as a function of hyperthermia dose and labelled with the corresponding radiation dose.

The solid lines in all four diagrams are those obtained using equation 4.11 with the parameters in table 5.1.

Figures 5.2 a,b,c,d illustrate the 250 kVp x-ray data as described for ^{60}Co . Figures 5.3 a,b,c illustrate the neutron data again as described for ^{60}Co .

Figures 5.4 a,b,c illustrate the extrapolation numbers and slopes of the radiation survival curve for γ , X, and neutron radiation as a function of hyperthermia dose. Figure 5.4d illustrates the relative radiation survival curve slopes as a function of hyperthermia dose.

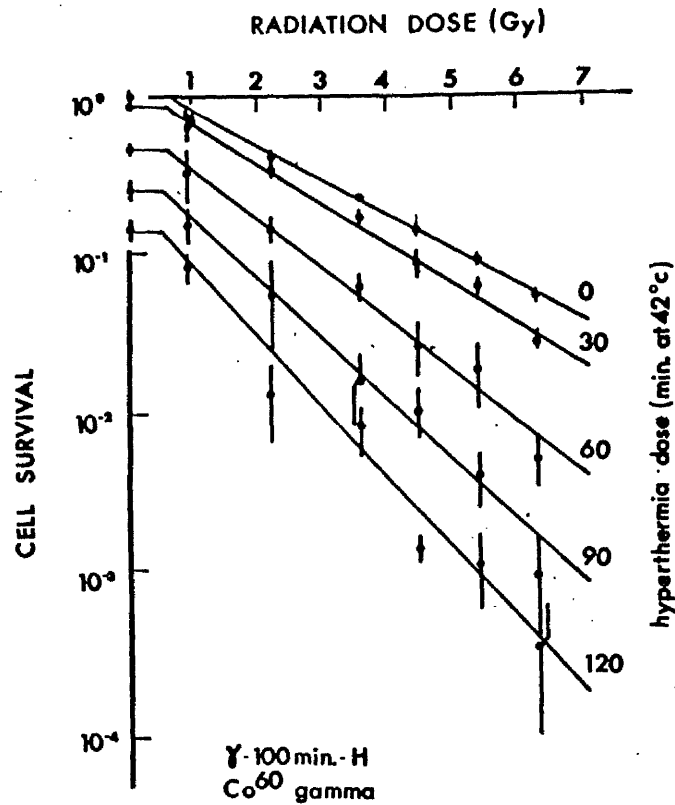
Figures 5.5 a,b,c illustrate the extrapolation numbers and slopes of the hyperthermia survival curves as a function of radiation dose. The solid lines in both figures 5.4 and 5.5 are the values obtained from equation 4.11 using the appropriate parameters from table 5.1.

Figures 5.6 a,b,c illustrate the survival surface, for each radiation quality, in the form of iso-survival plots, described in section 4.2.2.

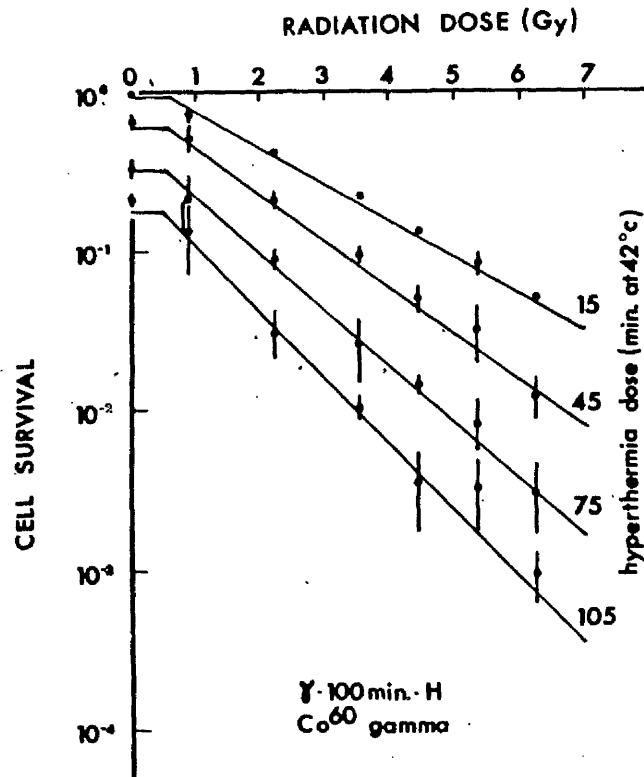
(a)

Figure 5.1. Cell survival for a ^{60}Co radiation dose at room temperature followed 100 minutes later by a hyperthermic exposure at 42° . Data points represent the mean and standard error of three observations. The lines are the survival calculated from equation 4.11 utilising the appropriate parameters in table 5.1.

- (a,b) Survival as a function of radiation dose.
(c,d) Survival as a function of hyperthermia dose.



(b)



(c)

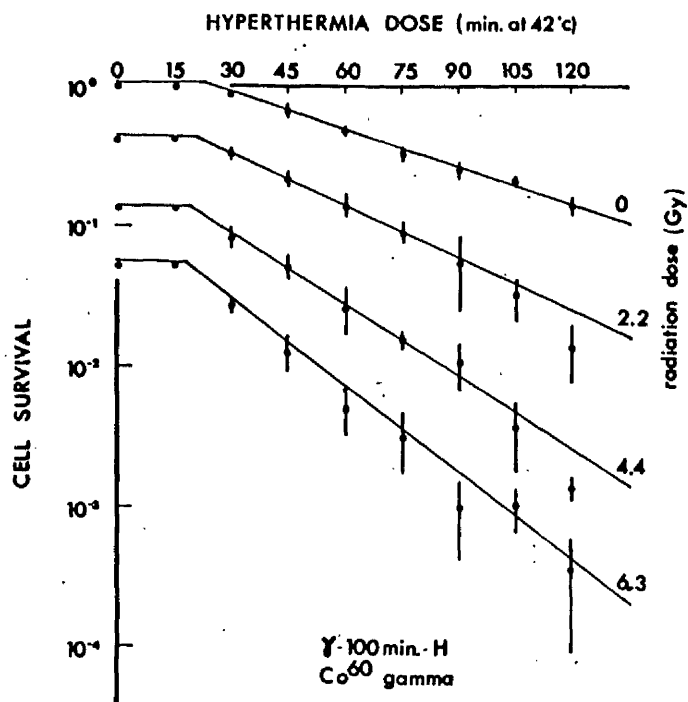


Figure 5.1. c,d

(d)

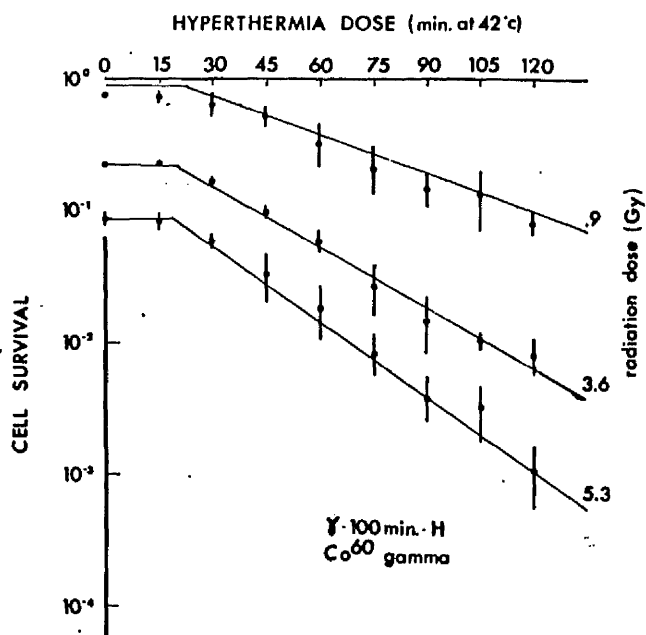
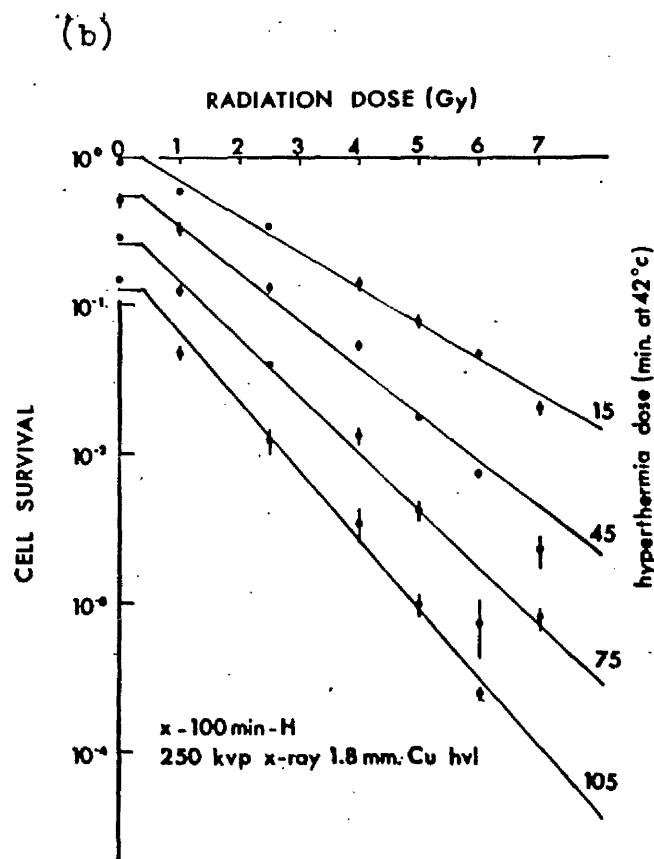
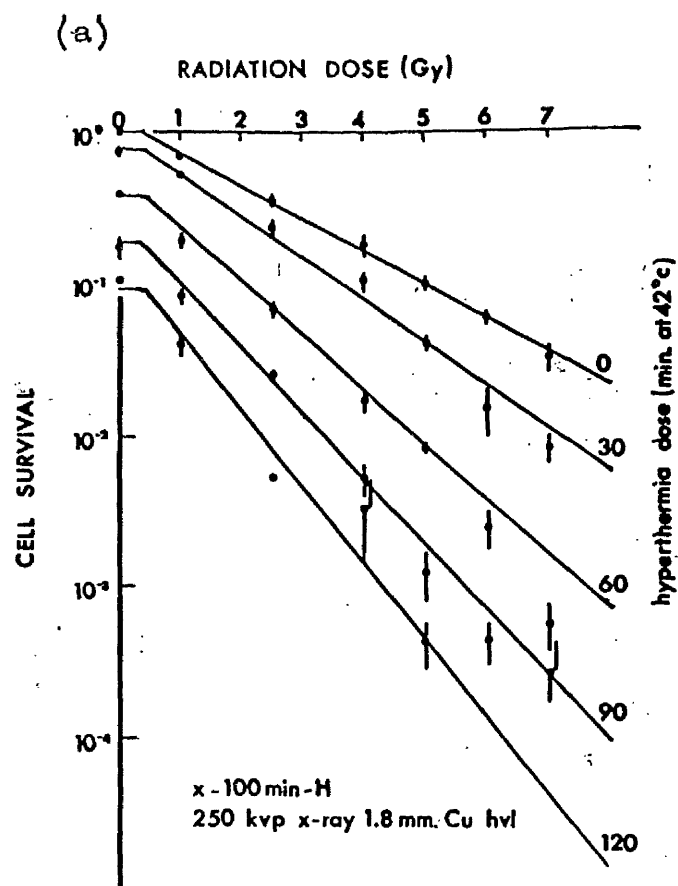


Figure 5.2. As described in figure 5.1 except 250kVp x-rays and four experiments.



(c)

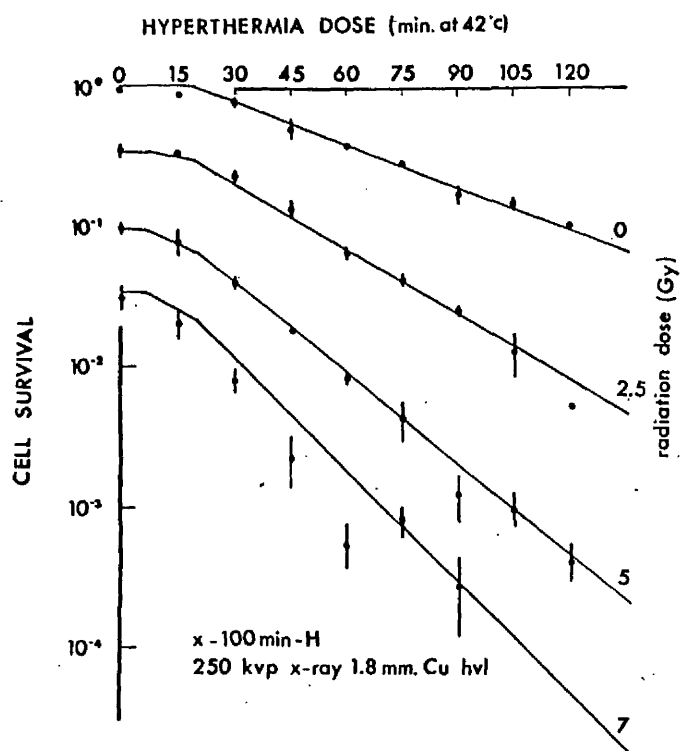
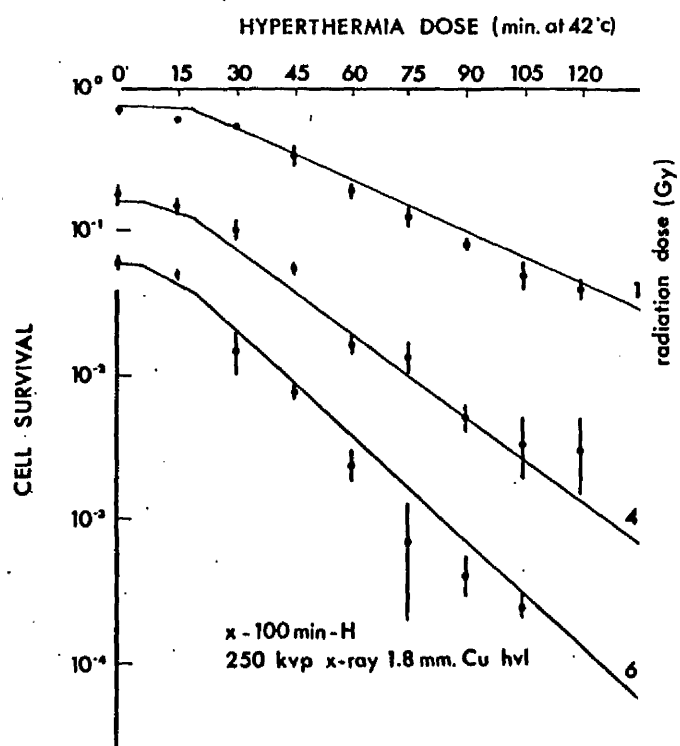


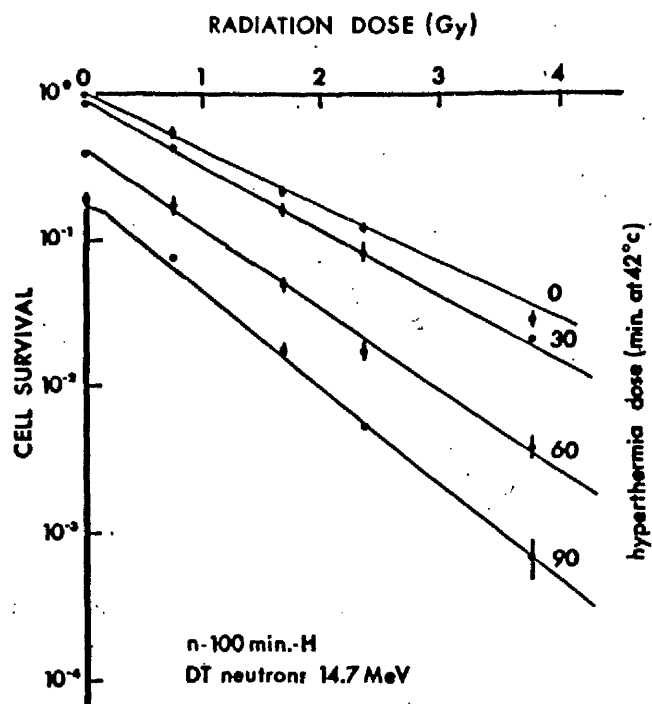
Figure 5.2. c,d

(d)

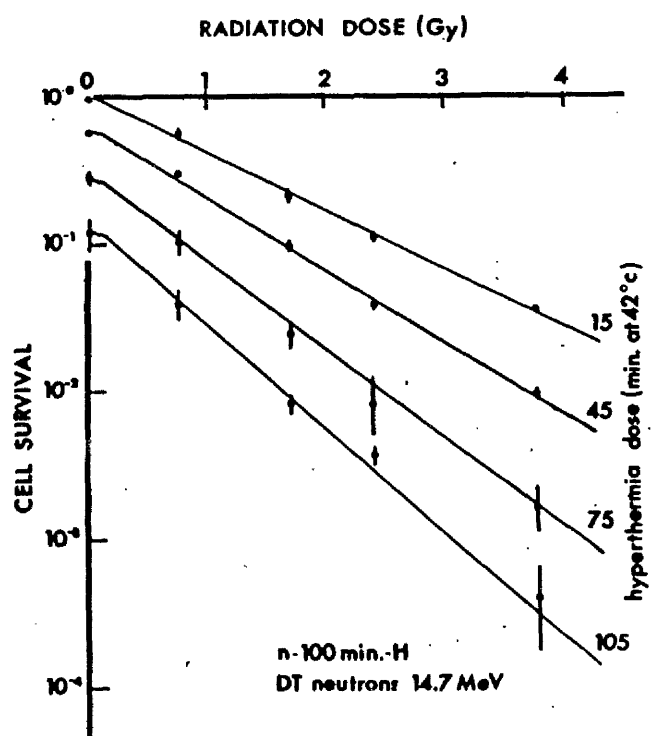


(a)

Figure 5.3. As described in figure 5.1 except 14.7 MeV neutrons.



(b)



(c)

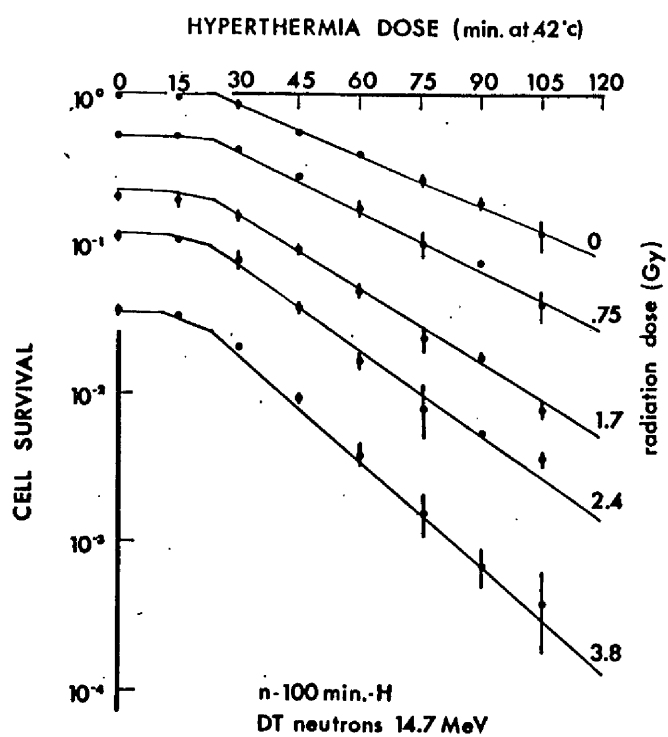
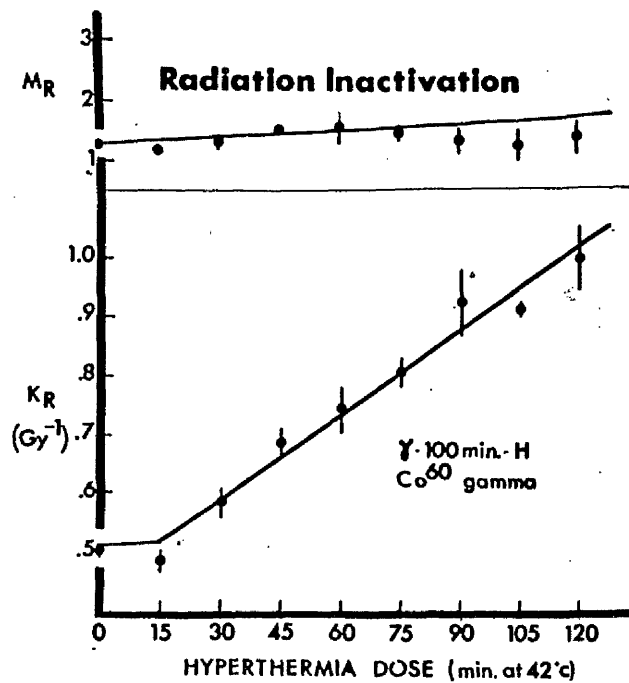


Figure 5.3. c

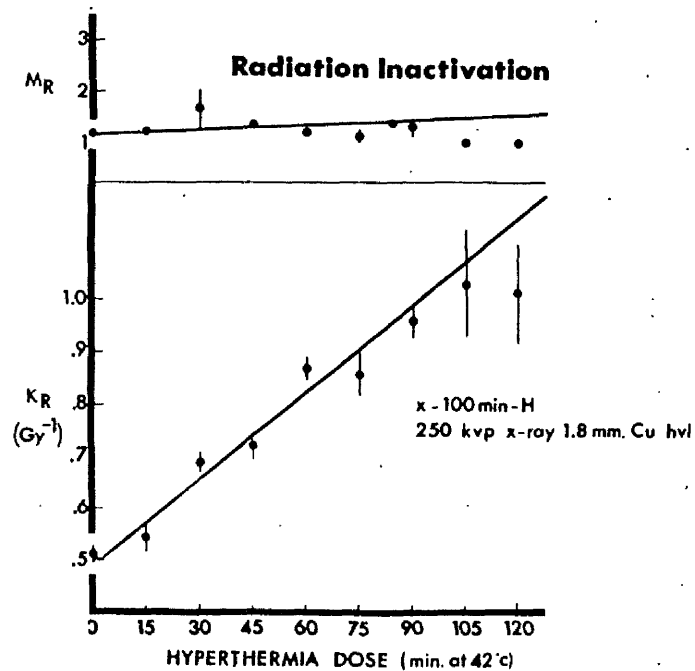
(a)

Figure 5.4. Radiation survival curve parameters, M_R and K_R for a radiation dose at room temperature followed 100 minutes later by the indicated exposure time at 42°C. The data points represent the mean of three or four observations. The lines are the values calculated from equation 4.11.

- (a) ^{60}Co gamma
- (b) 250kVp x-ray
- (c) 14.7 MeV neutron
- (d) relative radiosensitivity



(b)



(c)

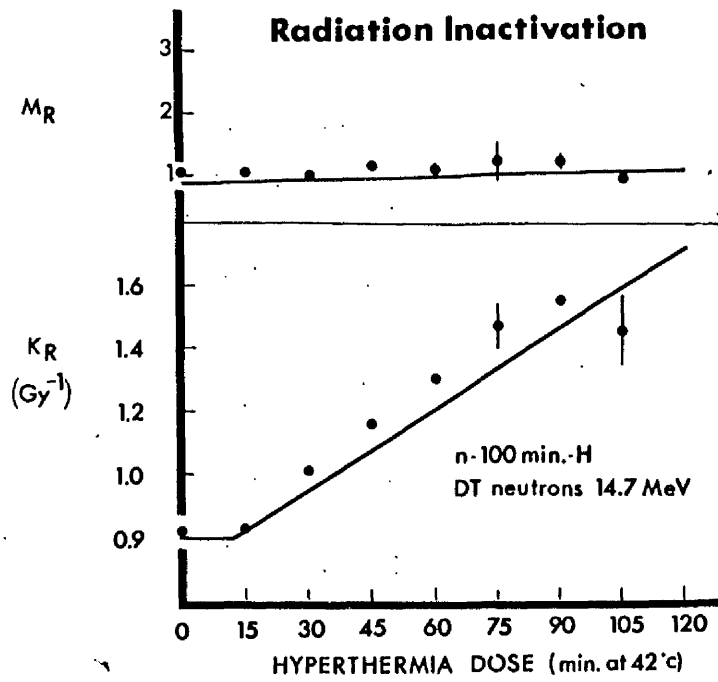
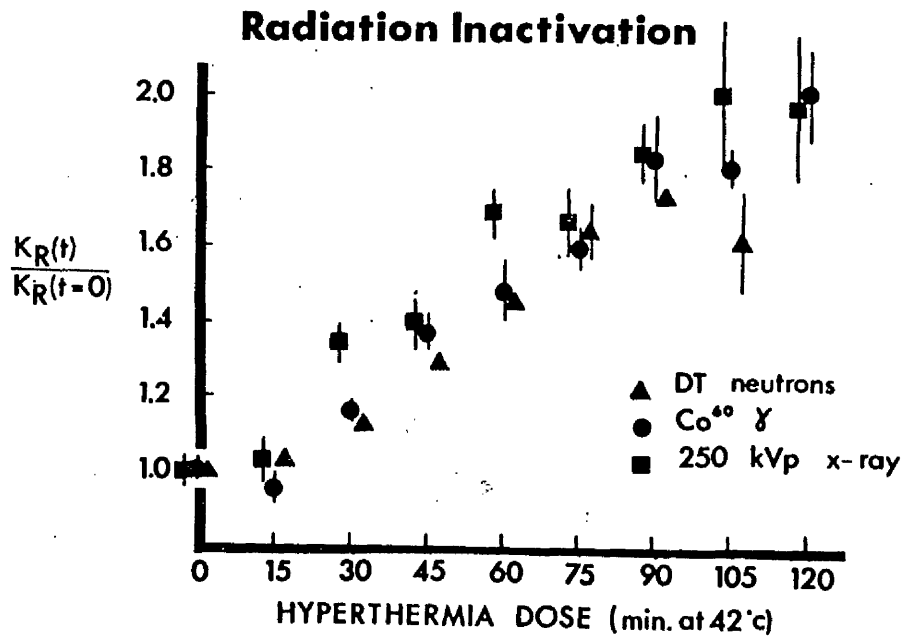


Figure 5.4. c,d

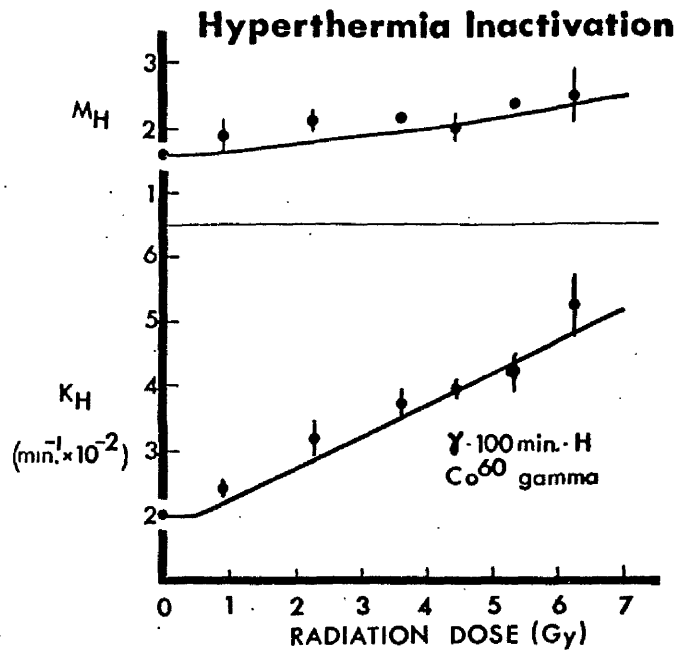
(d)



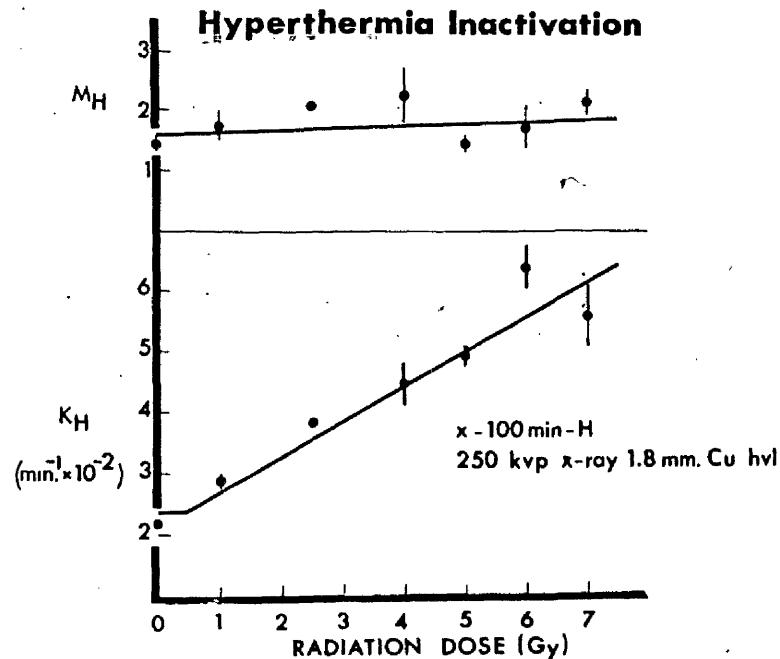
(a)

Figure 5.5.
Hyperthermia
survival curve
parameters, M_H
and K_H 100 minutes
after the indicated
radiation dose at
room temperature.
The data points
represent the mean
and standard error
of three or four
observations. The
lines are the values
calculated from
equation 4.11.

- (a) ^{60}Co gamma
- (b) 250kVp x-ray
- (c) 14.7 MeV neutron
- (d) relative thermal
sensitivity.



(b)



(c)

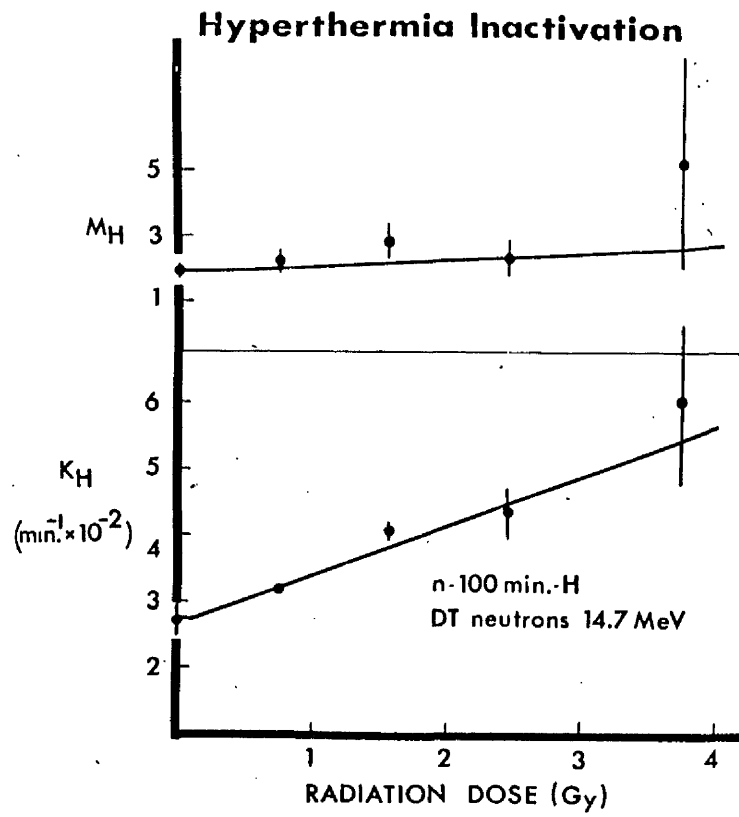
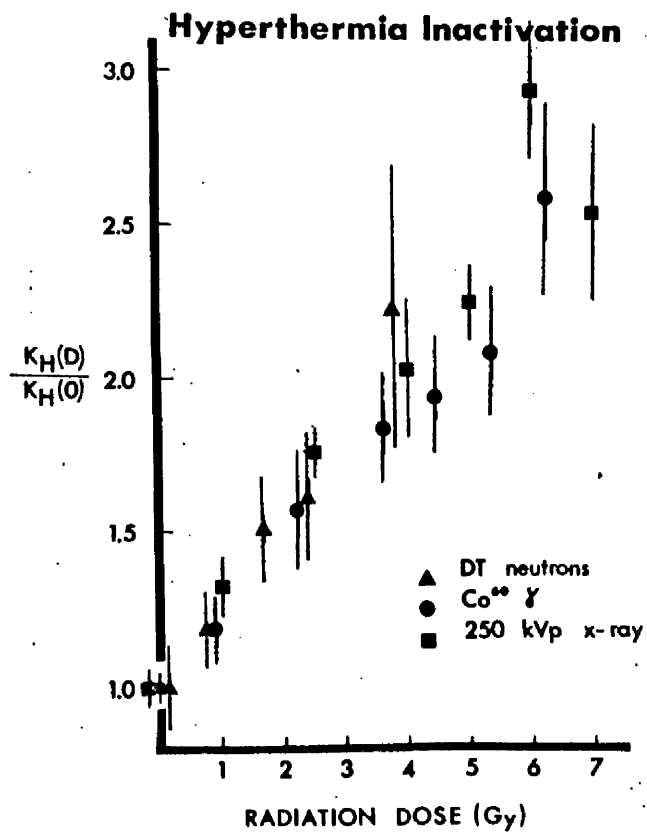


Figure 5.5. c,d

(d)



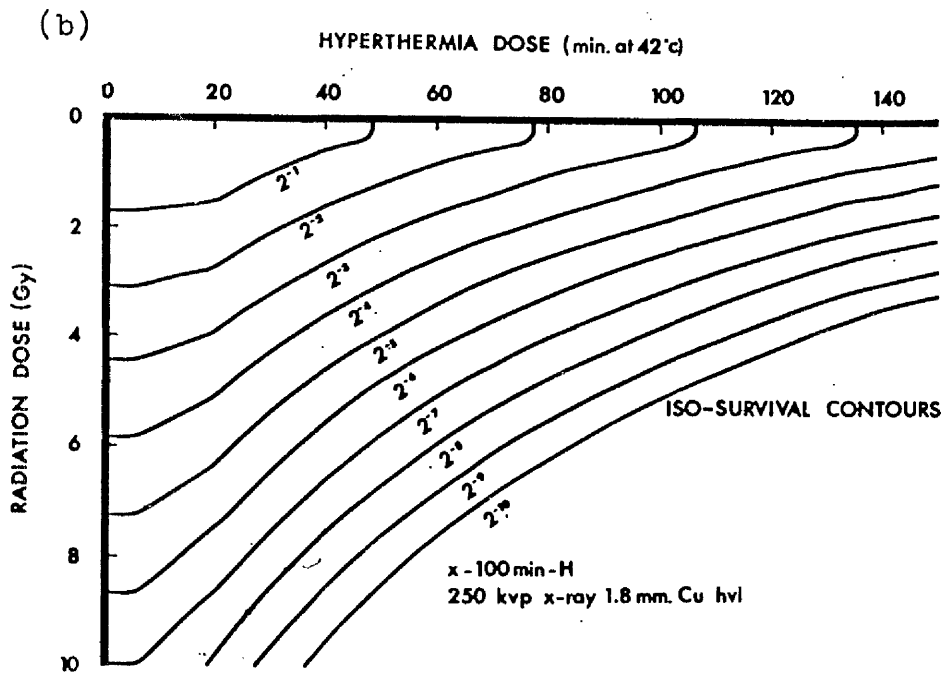
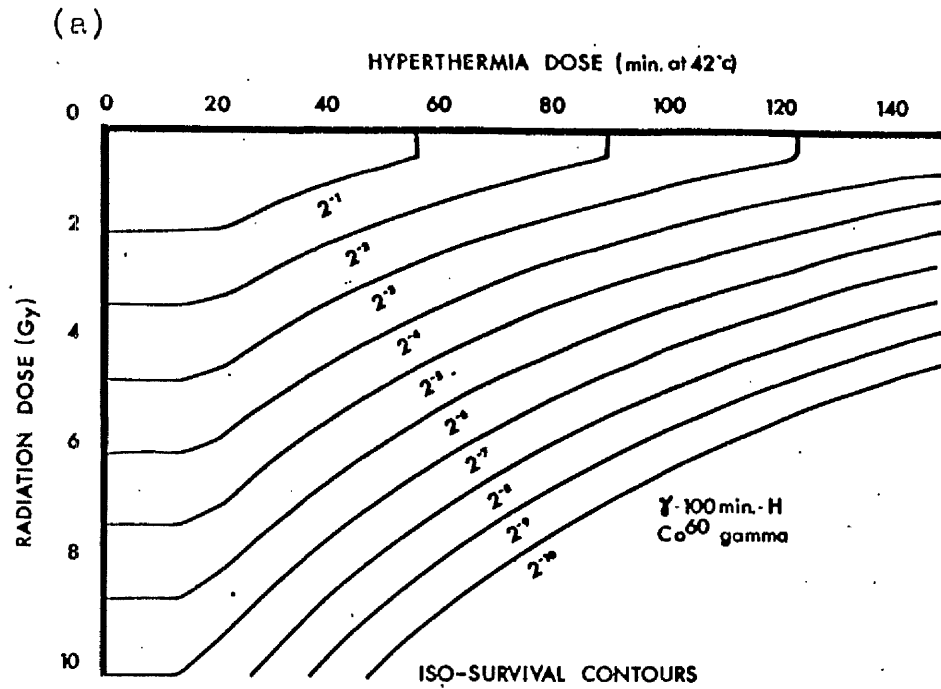


Figure 5.6. Iso-survival plots derived from equation 4.11 using the parameters in table 5.1. (a) ⁶⁰Co gamma, (b) 250kVp x-ray, (c) 14.7 MeV neutron.

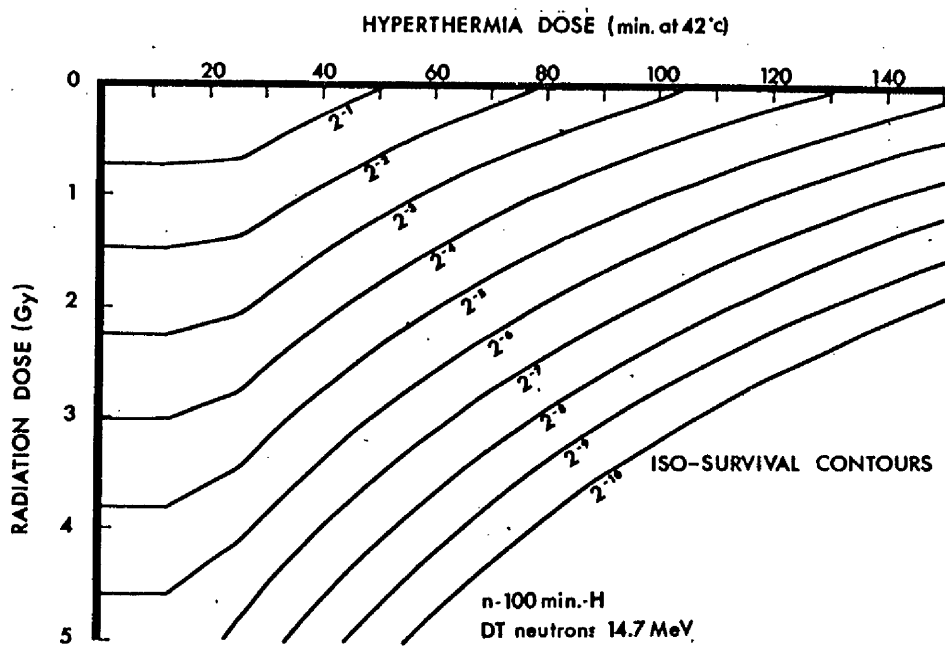


Figure 5.6. c

5.3 Discussion

5.3.1 Comparison of Analytical Methods

Comparison of the parameters, K_R and K_H obtained for equation 4.11 with those obtained independently reveals no significant differences. The values of $\partial K_R / \partial t$ and $\partial K_H / \partial D$ are not significantly different for any one of the radiation qualities and the weighted mean, K_I , is not significantly different from the value obtained for the survival surface, equation 4.11. Thus it is seen that for these three data sets either method might be used.

It is, however, worth emphasising that the degree of fit for the surface equation, for these data sets and all others presented in this thesis, is poor. The best data set, that for the neutron interaction, exhibits 2.75 units of χ -square/degree of freedom, all other data sets being substantially poorer. While some data sets suggest that the poor degree of fit arises from random deviations, there is some evidence for a systematic deviation from the simple survival surface equation. Therefore, while the parameters of the survival surface may be used for purposes of illustration, no argument presented in this chapter or subsequent chapters depends explicitly on the survival surface equation.

5.3.2 Comparison of Radiation Qualities

The values of K_R , K_H , and K_I obtained for ^{60}Co γ and 250 kVp x-rays reveal no statistically significant variations. The neutron data, in addition to the increased radiosensitivity K_R , exhibit significantly larger values of the interaction coefficient, K_I , than those for the low LET radiation. It is observed that there is an unexplained variation in thermal-sensitivity, however the coefficient of relative sensitization of thermal response, K_I/K_H , is still marginally higher for neutrons while the coefficient of relative radiation sensitization, K_I/K_R , is marginally lower. K_I/K_R is the rate of relative sensitization of radiation response per unit hyperthermia dose. Similarly K_I/K_H is the rate of relative thermal sensitization of hyperthermia response per unit radiation dose. Thus, it is observed that hyperthermia sensitizes neutron effects relatively less than low LET radiation effects, however neutrons are more effective than low LET radiation at sensitising hyperthermia response. This large interaction observed with neutrons was surprising and is worth examining in greater detail.

5.3.3 The Effects of Dose Rate

Before comparing the neutron interaction data with the ^{60}Co data it is necessary to discuss the difference in dose rate between the two experiments. With this same cell line in CO_2 -buffered Hams F10, Railton (1975) observed that in split dose experiments the maximum recovery was not significantly affected by a change of neutron dose rate from 0.10 to 0.60 Gy/min. Therefore, extremely little repair can have taken place during the lower dose irradiation.

If the ^{60}Co dose rate had been lowered, one would have expected that the normal radiation survival curve slope, K_R , would decrease due to a concurrent repair of radiation damage. It has been demonstrated that the damage due to a radiation dose responsible for interaction is capable of being repaired, as evidenced by the gradual disappearance of the interaction with separation of the hyperthermia and radiation doses (Gerwyck et.al. 1975). Accordingly, at low dose rates a concurrent repair of the sensitizing damage may take place resulting in decreased values of the interaction coefficient.

Ben-Hur et.al. (1974) have suggested the inverse effect, that is, as the dose rate decreases, the interaction increases.

In the previous chapter, it is suggested that their argument is fallacious. Secondly, his report deals with an entirely different situation, namely the inhibition of repair of sublethal damage due to irradiation at elevated temperatures, whereas, in the case we are examining, any marginal repair of sublethal damage should be complete before hyperthermic exposure begins.

It is concluded that the values of K_I and K_R obtained for ^{60}Co radiation may be applied to the low LET component of the neutron data at least as a limiting upper value.

5.3.4 A Theory of High LET Radiation Action in Relation to Interaction.

A theory of cell inactivation proposed by Katz et.al. (1971) postulates that cell survival can be described as a composite survival function due to two modes of inactivation, ion-kill and gamma-kill. The ion-kill mode is caused by initial ionization and excitation due to primary particles and recoil protons. Survivors of the ion-kill mode are, according to theory, unaffected and only exhibit the damage due to the gamma-kill component of the radiation.

The ion-kill mode is characterized by an exponential survival curve, cautiously described by the authors as arising from a saturated multi-hit mechanism. The gamma-kill mode is characterized by a shouldered survival curve indicating an accumulation of damage before a lethal event is registered.

A previous analysis of ^{60}Co γ and 14 MeV neutron data on the same cell line, carried out at this Institute (Railton et.al 1975; Katz and Sharma 1974) indicated that about 25% of the total dose was expended in ion-kill. If it is assumed that the interaction is due to the gamma-kill component only, and that the gamma-kill component is similar to that observed for 1 MeV photons, the interaction coefficient, K_I , should be equal to or less than $0.75 \times .00494 \text{ Gy}^{-1} \text{ min}^{-1} = .00371 \text{ Gy}^{-1} \text{ min}^{-1}$, whereas the observed coefficient is nearly twice this value. This would mean that the gamma-kill mode due to neutrons is nearly twice as effective in producing interaction type damage as gamma rays themselves. This sensitization therefore cannot be due to a purely gamma type radiation effect at the estimated fraction of ion-kill. While the weight of the argument

decreases with decreasing ion-kill component, the increased interaction is still significant at a hypothetical level of 100% gamma-kill.

There exist two possibilities

1. The fraction of the dose expended in ion-kill changes with increasing hyperthermia dose.
2. The ion-kill component takes part in the interaction.

If the sensitizing effect of hyperthermia were to progressively shift damage from the gamma-kill mode to the ion-kill mode, this could partially explain the observation. However, it is difficult to maintain the concept of the initial spatial distribution of energy as the basis for distinguishing the types of radiation damage, if the categorization is to be controlled by the hyperthermia dose, particularly when the hyperthermia exposure occurs after the radiation exposure.

Finally, it is concluded that if no reasonable value of the ion-kill fraction will allow the sensitization observed, a concurrent interaction with the ion-kill component must take place. The only mechanism that can be envisaged for sensitization of the ion-kill component would be, that, in addition to the actual killing events, a

a substantial and proportional number of surviving cells are being damaged in a way which can be lethalized by hyperthermia, but which cannot interact with the low LET component of radiation.

This behaviour, if it is real, suggests that the interaction event "targets", which must be "holes" for killing events, are not located in small highly vulnerable bodies within the cell. It is imagined that the interaction coefficient should increase with LET up to a LET at which the increased radiochemical yield of interaction events is balanced by the decreased probability of threading the "killing holes".

. CHAPTER SIX

THE EFFECT OF TEMPERATURE

6.1. Introduction

In the previous chapter, the radiation mediated mechanism of interaction was probed by a perturbing agent that did not directly affect the hyperthermia mediated interaction mechanism. To probe the hyperthermic mechanism it was necessary to use a perturbation that would be without effect on the radiation mechanism.

Radiation events exhibit an extremely low coefficient of temperature both for direct and indirect effects. Further by applying the high temperature separately, this small effect is removed. Thus a change of temperature is the obvious perturbation for this mechanism.

This approach allows a thermodynamic analysis which implicates protein denaturation as a cause of hyperthermic killing. A similar analysis of the thermodynamic properties of the interaction is made. The examination suggests at least two possible mechanisms of interaction in which the denaturation of proteins may take part.

6.2.1 Experimental Procedure

The matrix experiment described in section 5.2.1 was repeated at nominal temperatures of 42°, 43°, 44°, and 45°C, reducing the time intervals roughly by a factor of 2 for each degree rise in temperature. The data were analysed as described in section 4.3.2 providing the hyperthermia inactivation rates, K_H , as functions of radiation dose and the radiosensitivities, K_R , as functions of the hyperthermia dose. The slopes $\Delta K_R / \Delta t$ and $\Delta K_H / \Delta D$ of the sensitivity curves were obtained as before. These parameters are referred to in table 6.1 as the unbiased parameters.

Assuming the interaction quasi-threshold dose to be zero, the parameters of the surface model, equation 6.1, were obtained for each experiment separately.

$$-\ln S = D_1 K_R + t_1 K_H + D K_I \quad 6.1$$

$$\begin{aligned} \text{where } D_1 &= D - D_q \text{ for } D > D_q \\ &= 0 \quad \text{for } D \leq D_q \end{aligned}$$

$$\begin{aligned} t_1 &= t - t_q \text{ for } t > t_q \\ &= 0 \quad \text{for } t \leq t_q \end{aligned}$$

for each experiment separately. Equation 6.1 attributes a common hyperthermia and a common radiation extrapolation number to the survival curves for each row and column of the matrix. The procedure of

allowing the interaction quasi-threshold doses to be zero was adopted to reduce the number of parameters of the first order model. This was further justified by the lack of a significant first order correlation of extrapolation number with sensitizing dose.

The parameters of equations 6.2 and 6.3 were determined by a combined iterative search for the best common extrapolation numbers M_R and M_H and a linear least squares determination of the corresponding slopes, K_H and K_R .

$$- \ln S = DK_R(t) - \ln M_R \quad \text{for } D > 0 \quad 6.2$$

$$- \ln S = tK_H(D) - \ln M_H \quad \text{for } t > 0 \quad 6.3$$

The slopes $\partial K_R / \partial t$ and $\partial K_H / \partial D$ of the sensitivity curves were obtained as described earlier, but include the zero dose points in the fit, unlike those for the unbiased fits. The parameters of the surface model and for the independent assessment of radio-sensitivity, thermal-sensitivity, and interaction are listed in table 6.1.

Table 6.1 Interaction parameters X-100min-H

EXPT	PARAMETER	UNITS	*	EXP	UNBIASED	DOSE MOD.	SURFACE
42°C	K_R	Gy^{-1}		E-1	5.39±0.28	5.35±0.19	5.02±0.24
(41.86°)	D_q	Gy		E-1	5.56±3.45	5.05±0.78	4.61±1.14
5 expts.	K_H	min^{-1}		E-2	2.20±0.73	2.14±0.16	2.22±0.13
	t_q	min		E+1	2.24±0.58	1.86±0.20	2.05±0.15
	K_I	$Gy^{-1}min^{-1}$		E-3	4.64±0.37	4.87±0.42	4.57±0.09
	$\Delta K_R/\Delta t$	$Gy^{-1}min^{-1}$		E-3	4.28±0.37	5.00±0.33	
	$\Delta K_H/\Delta D$	$Gy^{-1}min^{-1}$		E-3	5.02±0.37	4.66±0.42	
43°C	K_R	Gy^{-1}		E-1	5.03±0.04	5.46±0.07	5.21±0.07
(42.88°)	D_q	Gy		E-1	5.67±0.97	9.50±2.18	7.53±0.17
2 expts.	K_H	min^{-1}		E-2	6.12±0.52	6.06±0.35	6.43±0.41
	t_q	min		E+1	3.02±1.16	0.92±0.27	1.06±0.16
	K_I	$Gy^{-1}min^{-1}$		E-3	9.29±3.35	8.39±1.07	6.95±0.42
	$\Delta K_R/\Delta t$	$Gy^{-1}min^{-1}$		E-3	5.88±1.44	8.24±0.85	
	$\Delta K_H/\Delta D$	$Gy^{-1}min^{-1}$		E-3	12.58±1.41	8.63±1.07	
44°C	K_R	Gy^{-1}		E-1	5.55±0.18	5.61±0.21	5.65±0.13
(43.87°)	D_q	Gy		E-1	4.73±4.09	5.22±4.15	4.80±3.20
2 expts.	K_H	min^{-1}		E-2	15.60±0.46	14.70±0.73	14.90±0.80
	t_q	min		E+1	1.01±0.13	0.93±0.15	0.93±0.12
	K_I	$Gy^{-1}min^{-1}$		E-3	12.09±4.54	14.51±1.61	12.20±0.60
	$\Delta K_R/\Delta t$	$Gy^{-1}min^{-1}$		E-3	17.57±4.54	15.21±1.61	
	$\Delta K_H/\Delta D$	$Gy^{-1}min^{-1}$		E-3	10.61±2.57*	14.17±1.13	
45°C	K_R	Gy^{-1}		E-1	6.09±0.18	6.07±0.26	5.83±0.25
(44.77°)	D_q	Gy		E-1	8.42±1.93	8.15±2.34	6.48±1.65
3 expts.	K_H	min^{-1}		E-2	26.10±7.70	25.80±2.39	27.30±3.10
	t_q	min		E+1	0.56±0.08	0.54±0.07	0.55±0.03
	K_I	$Gy^{-1}min^{-1}$		E-3	22.17±4.92	17.15±1.93	16.10±1.70
	$\Delta K_R/\Delta t$	$Gy^{-1}min^{-1}$		E-3	21.95±2.48	21.93±1.93	
	$\Delta K_H/\Delta D$	$Gy^{-1}min^{-1}$		E-3	23.03±4.92	14.77±1.36	

Note - UNBIASED - parameters of equations 4.15, 4.16, 4.17, 4.18

DOSE MOD - " " " 6.2, 6.3, 4.17, 4.18

SURFACE - " " equation 4.11

Mean ± Standard Error

* $\Delta K_H/\Delta D$ (44°) unbiased parameter determination does not include 7.0 Gy point.

6.2.2 Experimental results

Figures 6.1 - 6.4 illustrate the interaction survival data plotted as a function of hyperthermia dose and labelled with the corresponding radiation dose. The lines drawn through the data points are the calculated survivals using equation 6.1 with the parameters listed in the third column of table 6.1.

Figure 6.5 illustrates the values of the radiation survival curve slopes, calculated using a common extrapolation number within each experiment. It is observed, as anticipated, that as the temperature increases, the rate of sensitization of radiation response increases, as indicated by the divergence of the experimental points at different temperatures. Figures 6.6 a,b illustrate the thermal inactivation rates at different temperatures, plotted as a function of radiation dose. As the radiation dose increases, the logarithms of the thermal-sensitivities for different temperatures converge. This indicates that, for a given radiation dose, the relative thermal sensitivity decreases for increasing temperature.

The hyperthermia inactivation rates for each radiation dose were used to calculate the activation

Figure 6.1. Cell survival due to a 250 kVp x-ray dose at room temperature followed 100 minutes later by a hyperthermic exposure at 42°. The data points represent the mean and standard error of five observations. The lines are the survivals calculated from equation 6.1 using the parameters in table 6.1.

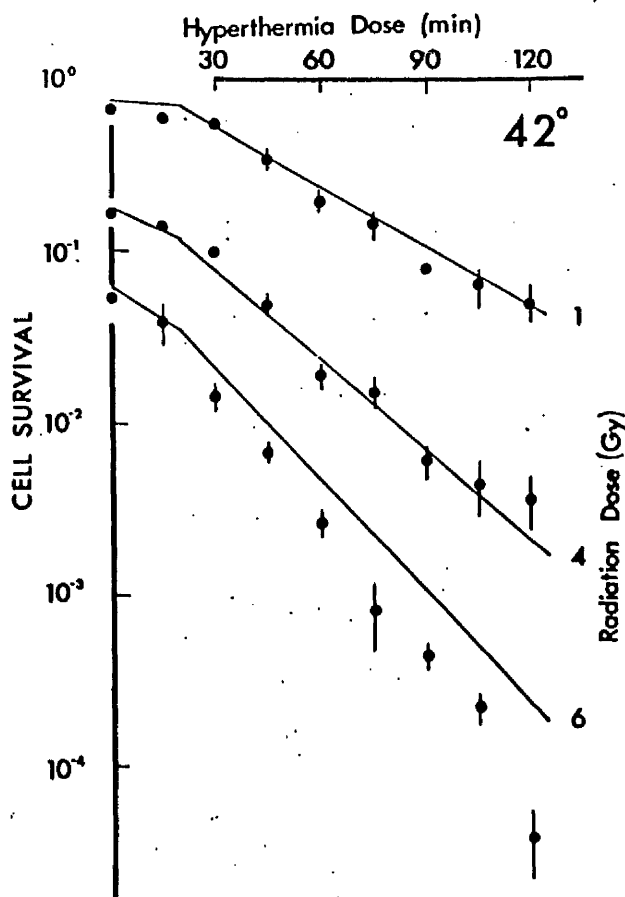
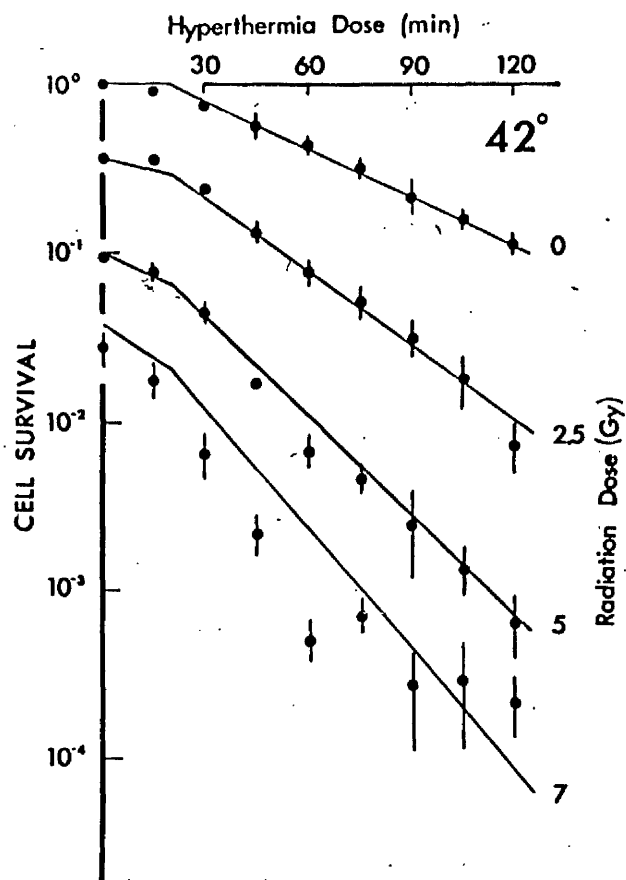


Figure 6.2. As described for figure 6.1 except hyperthermic temperature of 43° . Data points represent two observations.

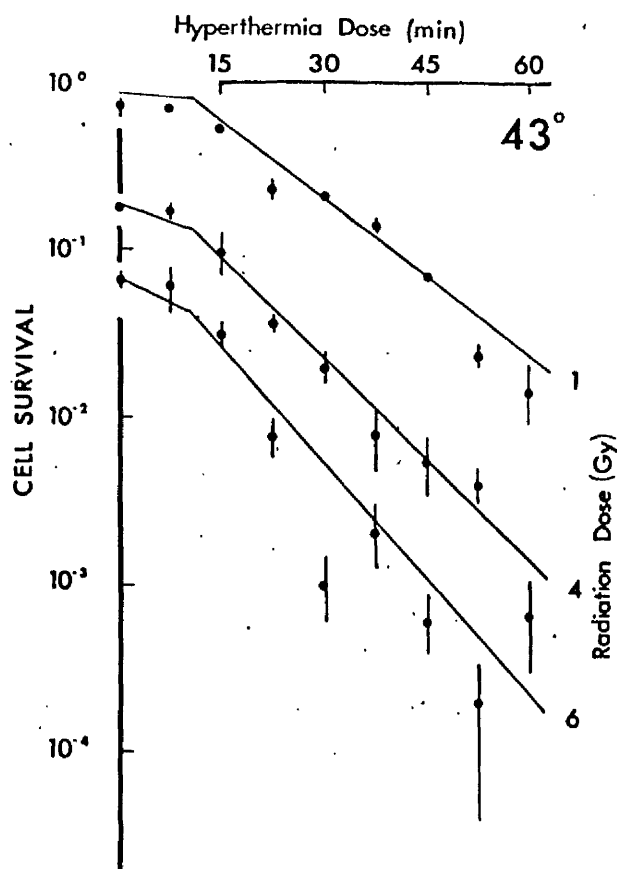
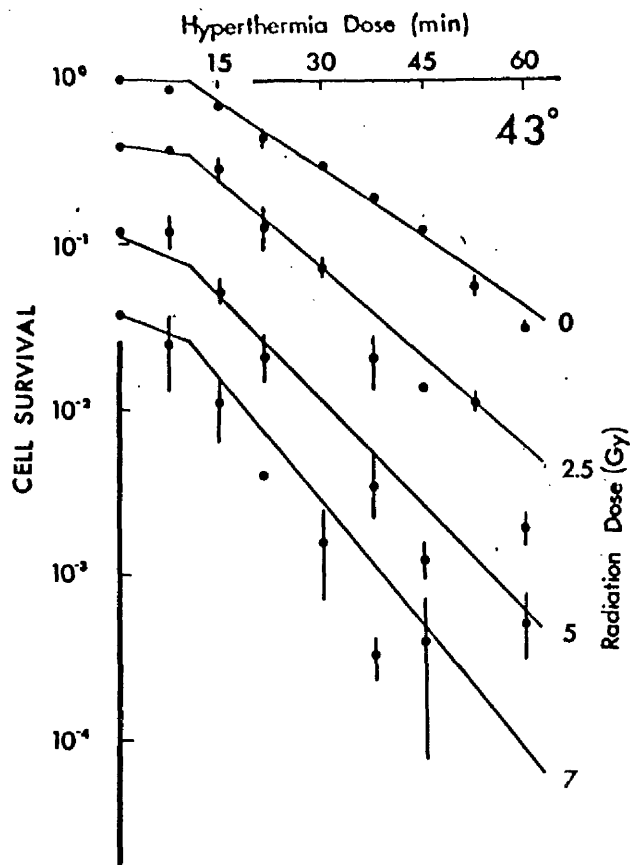


Figure 6.3. As described for figure 6.1., except hyperthermic temperature of 44° . Data points represent two observations.

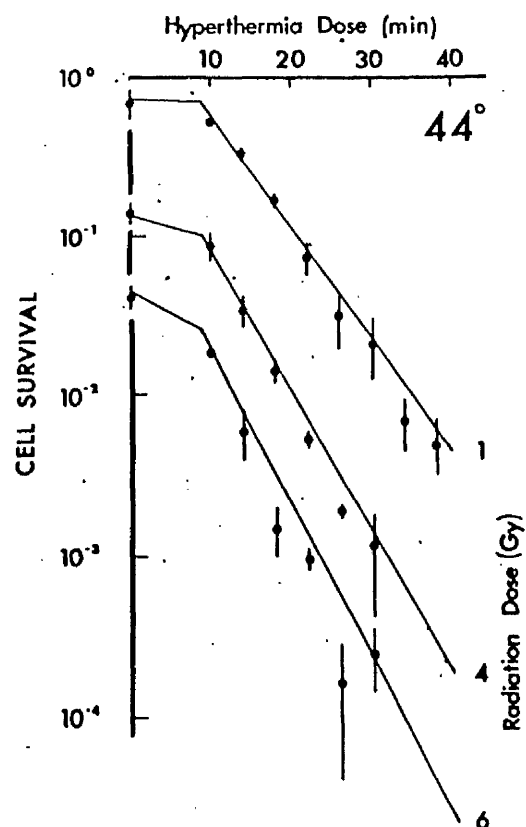
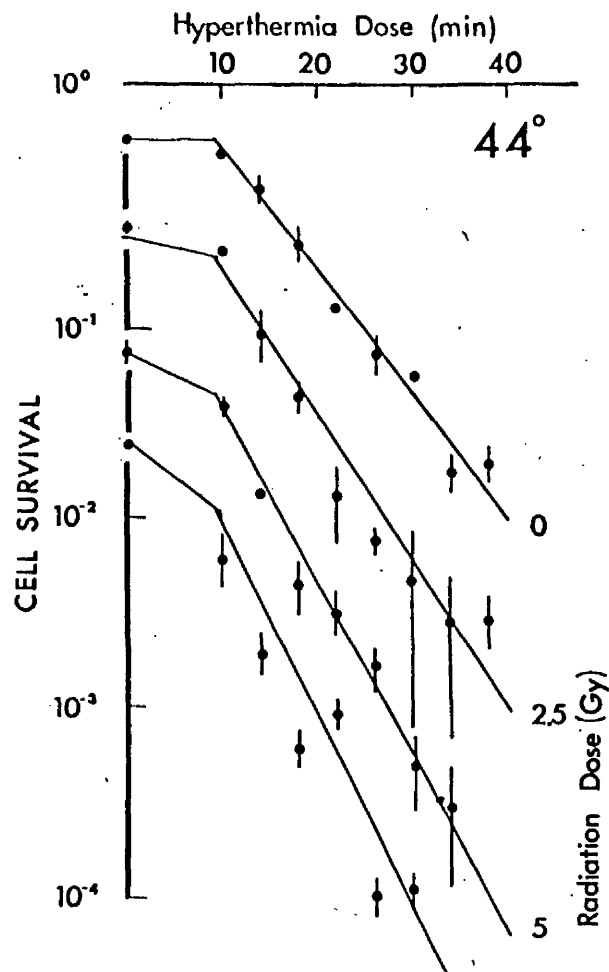
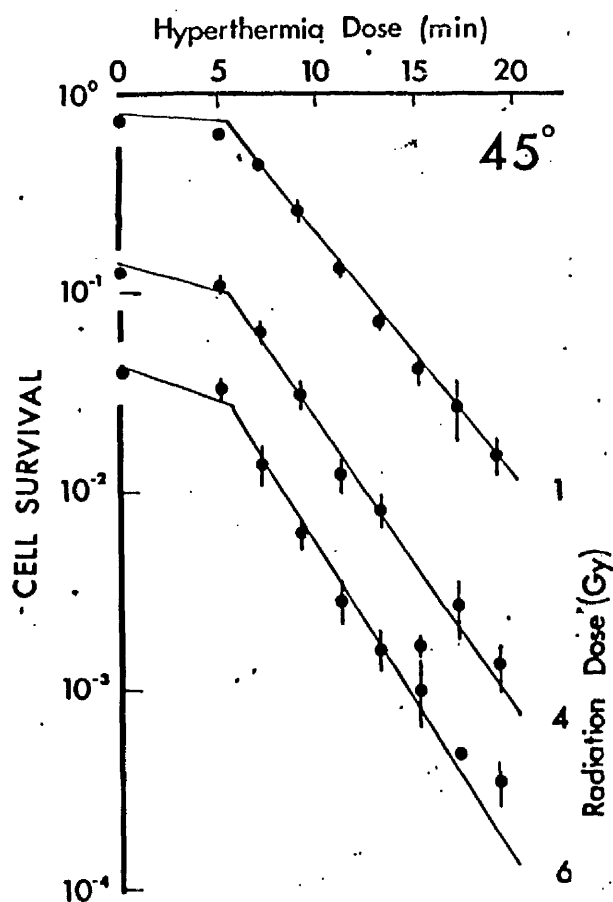
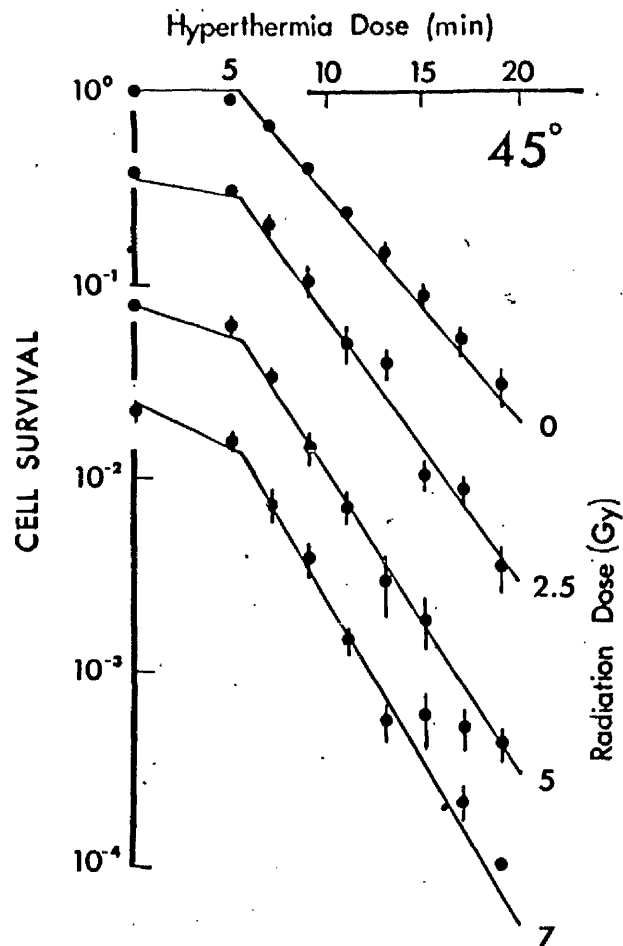


Figure 6.4.
As described for
figure 6.1 except
hyperthermic
temperature of 45° .
Data points represent
three observations.



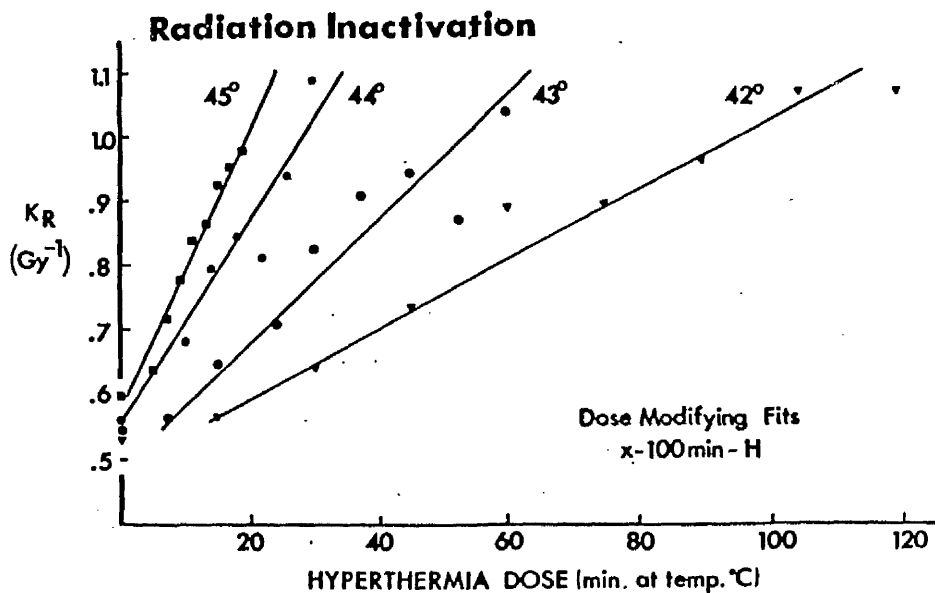
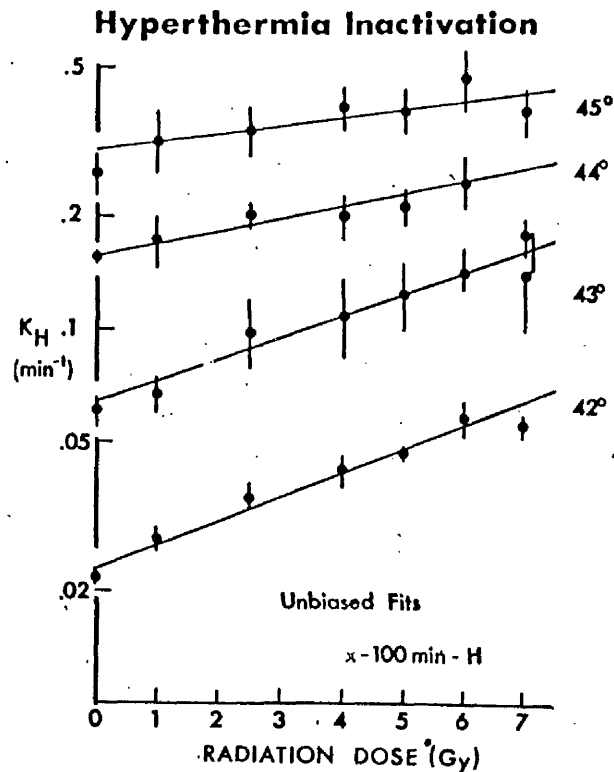


Figure 6.5. Radiosensitivity, K_R , to 250 kVp x-rays at room temperature followed 100 minutes later by a hyperthermia exposure at the indicated temperature and duration. K_R was calculated assuming a common radiation extrapolation number for each experiment. Data points represent the mean of the number of experiments indicated in figures 6.1 to 6.4. Standard errors are not indicated.

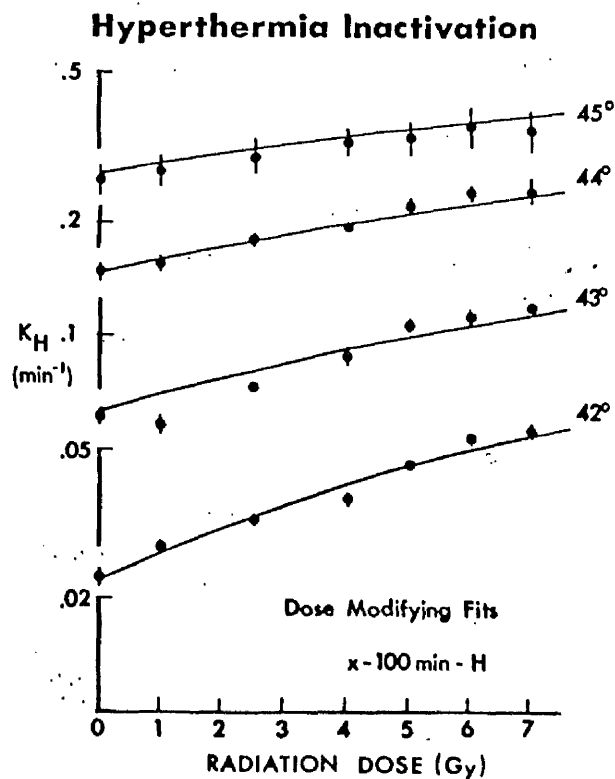
(a)

Figure 6.6.
Thermal-
sensitivity, K_H ,
100 minutes after
a 250 kVp x-ray
dose at room
temperature.
The data points
represent the
mean and
standard error for
the number of
observations
indicated in
figures 6.1 to
6.4.

- (a) Unbiased fits
Lines are
drawn by eye.
- (b) Common
extrapolation
number fits.
Lines are
the thermal-
sensitivities
calculated
from equation
6.1 using the
parameters in
table 6.1.



(b)



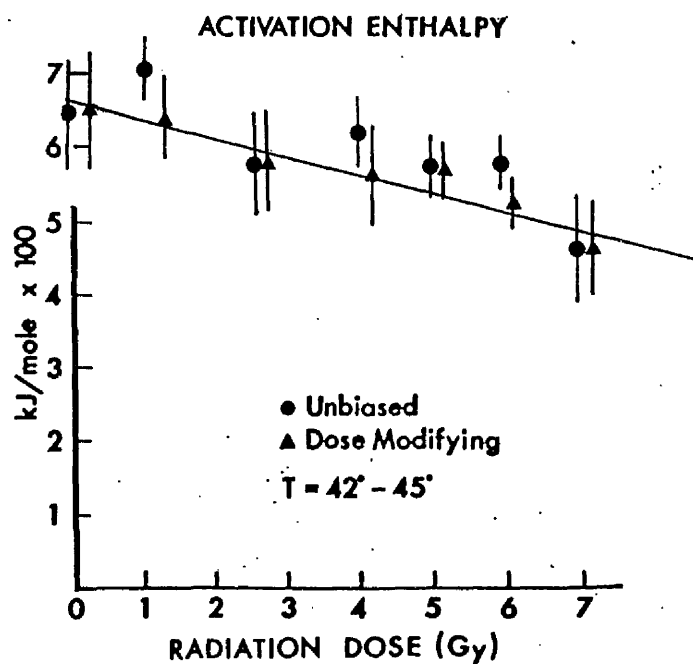


Figure 6.7. Activation enthalpy for hyperthermia inactivation 100 minutes after a 250 kVp x-ray dose at room temperature. Data points represent the mean and the standard error of fit.

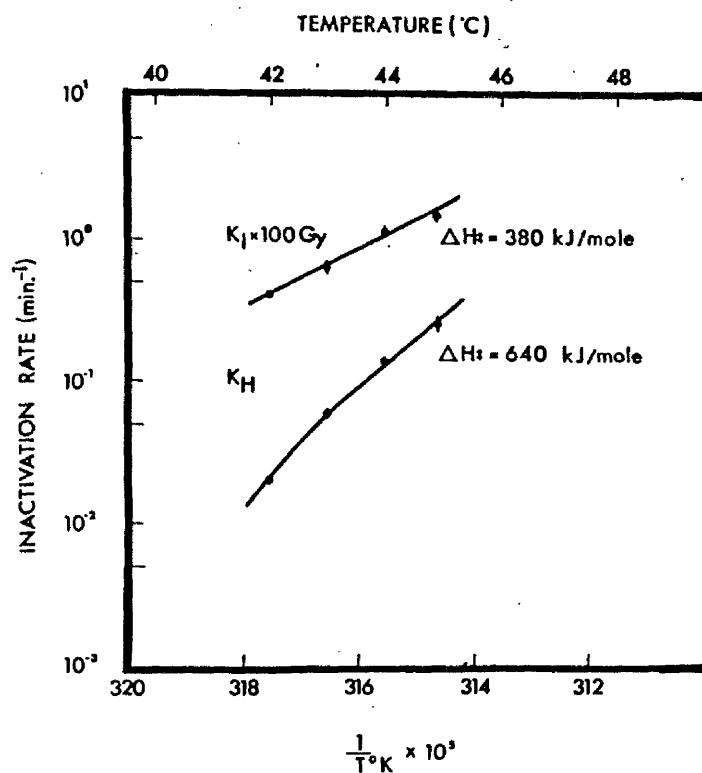


Figure 6.8. Arrhenius plot of the temperature dependent parameters of equation 6.1. K_H , thermal sensitivity, $K_I \times 100 \text{ Gy}$, interaction coefficient scaled by multiplying by 100 Gy. Data points represent the mean and standard error of the mean for the number of observations listed in table 6.1.

enthalpies, illustrated in figure 6.7. While the difference in enthalpy values is only marginally significant, the trend towards a reduction in activation enthalpy for increasing radiation dose is evident.

The increase in relative radiation sensitivity for a given hyperthermia exposure time and the decrease in relative hyperthermic sensitization for a given radiation dose are compatible with the increasing prominence of a component of cell killing which possesses a significantly smaller activation enthalpy than the hyperthermia killing component. That this can be considered to be the situation is illustrated by the Arrhenius plots of the unperturbed hyperthermia inactivation rates, K_H , and the interaction coefficient, K_I in figure 6.8.

Table 6.2 lists the activation enthalpies for the unperturbed hyperthermia inactivation rates, K_H , and the interaction coefficients, K_I , calculated from the three sets of parameters. It is observed that the calculated values for the three sets of parameters are significantly lower than the activation enthalpy for hyperthermic killing.

Table 6.2 Activation enthalpies for the temperature dependent interaction parameters.

PARAMETER	ACTIVATION ENTHALPY (kJ/mole)		
	SURFACE	DOSE MOD.	UNBIASED
K_H	660 \pm 60	650 \pm 70	650 \pm 70
K_I	380 \pm 50	320 \pm 70	450 \pm 70
$\partial K_R / \partial t$		350 \pm 60	480 \pm 30
$\partial K_H / \partial D$		330 \pm 60	370 \pm 190

6.2.3 Limitations of the Experimental Data

The control values of K_R obtained for the 45°C experiments exhibit an unexplained variation compared to the experiments at the other temperatures, although experiments at 44°C and 42°C were done before, between, and after experiments at 45°C. This variation has not been compensated for. The Arrhenius plots of the independent assessments of K_I do not all exhibit the same degree of linearity as that illustrated in figure 6.8. The activation enthalpies have, nevertheless, been computed and reflect only the average temperature sensitivity of the interaction.

6.2.4. Discussion

A comparison of the normal hyperthermia, K_H , and radiation, K_R , component parameters obtained by the three analytical methods reveals only marginally significant variations. A comparison of the interaction coefficient, K_I , obtained by the three methods, however, reveals marked variations in a few of the estimates. Using the best common radiation and common hyperthermia extrapolation number for each experiment resulted in a reduction of the standard errors in three of the four data sets,

as illustrated in figures 6.6a,b. Fitting common extrapolation numbers and utilizing the zero dose points in the independent assessment of K_I , which simulates the constraints of equation 6.1, resulted in better agreement between the values of $\Delta K_R/\Delta t$, $\Delta K_H/\Delta D$, and of K_I . These observations suggest that the technique was appropriate, although the principal observation, of reduced activation enthalpies for K_H for increasing radiation doses, does not depend on this technique.

While the three techniques do not yield precisely the same activation enthalpy for K_I , the differences between the values for K_I and K_H are significant for each technique. There are at least two possible interpretations of this finding. Firstly, an increase in temperature may alter the proportion of available hyperthermia SLD and ISD, or secondly, hyperthermia induced ISD may result from a mechanism distinct from that producing SLD.

Examining the first possibility, if hyperthermia were to exhibit an effect parallel to the radiation dose rate phenomenon, then there would be an unsaturated repair of hyperthermia SLD, that would be progressively inhibited as the temperature increases

Thus, for a given survival level the ratio of lethalized to non-saturably repaired (by-passed) SLD would decrease for increasing temperature, corresponding to increasing "dose" rates. If this damage is capable of acting as ISD, despite being prevented from acting as SLD, the observed phenomenon could be explained.

As a simple example of how this scheme might operate, imagine that a prior radiation dose inhibits the unsaturated repair of SLD. SLD that was repaired in the unirradiated controls, and therefore non-lethal, would be available to damage the irradiated cells and thus would appear as hyperthermia ISD. The corresponding radiation ISD for the interaction is the damage to the repair mechanism for hyperthermia SLD, which in the absence of hyperthermia damage is non-lethal.

It might be assumed that the extent of the hyperthermia "dose" rate phenomenon could be assessed by the deviation of the thermal sensitivities at low temperatures from the straight line portion of the Arrhenius plot, figure 3.3. If this were the situation, the relative amounts of non-saturably repaired SLD and lethalized SLD would remain constant over the

the straight line portion of the plot from 43° to 47°C. The activation enthalpy for the formation of the non-saturably repaired SLD must necessarily be the same as for the lethalized SLD, since only their respective fates are assumed to be different. Therefore, the activation enthalpy for K_I must equal K_H .

Since it is observed that the activation enthalpy for K_I is significantly less than the value of 640kJ/mole observed for the data in fig. 3.3, the second possibility of a different mechanism is suggested.

It has been observed, in this and the preceding chapters, that the interaction is associated with a decrease in survival due to the required hyperthermia dose alone. Others (Ben-Hur et.al 1972, 1974, 1975; Robinson and Wizenberg 1974) have reported an interaction due to sublethal doses of hyperthermia. These observations suggest that the mechanisms of hyperthermic killing and interacting are not coupled, but rather represent distinct mechanisms further supporting the second hypothesis.

That a complex intermolecular organization is not required for the observations is well illustrated

by the results of Sanner, Kovacs-Proszt and Vas (1972). They observed that a vegetable enzyme, pectin methyl esterase, was more heat labile after a radiation dose and that the degree of thermal sensitization decreased for increasing temperature. The thermal sensitivity was characterized by an unperturbed activation enthalpy of 410 kJ/mole that decreased linearly with radiation dose to 290 kJ/mole, for a radiation dose that reduced the enzymatic activity to 40%.

This behaviour, similar to that observed for CHO cells reported herein, occurs in a biological system in which a complex repair mechanism probably does not exist. While a "transfer of bypassed SLD to ISD" mechanism cannot be ruled out, this observation is suggestive of a dual action mechanism.

The data presented are not sufficient to decide between the possibilities presented. Further it will be demonstrated that there is at least one more possible interpretation of these results. This requires an examination of the thermodynamics of hyperthermia inactivation and interaction.

6.3 Thermodynamics of Thermal Sterilization

6.3.1 Theory of Absolute Reaction Rates

The Arrhenius equation, presented earlier, is often associated with the simple kinetic theory of molecular reactions. This postulates that for a molecule to react it must possess sufficient energy, the activation energy, to initiate the reaction. If the molecules are uncharged monatomic particles the distribution of energy among the particles is described by the Maxwell-Boltzman distribution. Integration of this distribution over energies greater than the activation energy yields the relative reaction rate in the form of the Arrhenius equation. Since the simple kinetic theory has, as a basis, the energy distribution for particles with energy distributed about 3 degrees of freedom, the application of the theory to biological macromolecules possessing many times this number of energy terms seems, at first, dubious.

The theory of absolute reaction rates, first postulated by Eyring (1935) and applied by Stearn (1949) and Johnson, Eyring and Polissar (1957) to biological processes, allows further analysis.

The Eyring formulation stresses the importance of the "free energy" of activation rather than the energy of activation.

Consider a potential energy surface. Initially the reactants will be in quantized states at or near the bottom of a potential well. Transitions from this well are described by statistical mechanics. The most probable transition, the one that will dominate the kinetics of the reaction, is from the ground state of the potential well to the ground state of an energy configuration, referred to as the "activated complex". Since any minor deviation from the most probable transition results in a larger change of energy, the potential energy surface possesses a saddle point corresponding to the activated complex.

The activated complex is, then, represented by an energy configuration that is stable in all but one degree of freedom. Thus, a system composed of particles possessing many degrees of freedom can be simply treated as a system in which there is a single degree of freedom for each particle.

Regardless of the reaction type, the specific rate of decomposition into reaction products is dependent only on temperature and is equal to kT/h ,

where k is the Boltzman constant, h is the Planck constant, and T is the absolute temperature.

Assuming that the activated complex is in virtual equilibrium with the reactants and that the probability of the forward transition is unity, the rate of reaction is

$$k = (\kappa T/h) K^\ddagger \quad 6.4$$

where K^\ddagger is the equilibrium constant.

Let ΔF^\ddagger , ΔH^\ddagger , and ΔS^\ddagger represent the changes in free energy, enthalpy, and entropy when the activated complex is formed. Using the van't Hoff equation,

$$\Delta F^\ddagger = \Delta H^\ddagger - T \Delta S^\ddagger = -RT \ln K^\ddagger, \quad 6.5$$

to rewrite equation 6.4, yields

$$k = (\kappa T/h) \exp \left(-\Delta H^\ddagger / RT + \Delta S^\ddagger / R \right) \quad 6.6$$

Assuming that ΔS^\ddagger is independent of temperature, taking logarithms, and differentiating equation 6.6 with respect to temperature, yields the Arrhenius equation

$$k = A e^{-(\Delta H^\ddagger + RT)/RT} \quad 6.7$$

where $\Delta H^\ddagger + RT$ is the activation energy. Thus, a simultaneous solution of equations 6.6 and 6.7 allows the determination of ΔH^\ddagger , ΔS^\ddagger , and ΔF^\ddagger without a knowledge of the equilibrium constant, K^\ddagger .

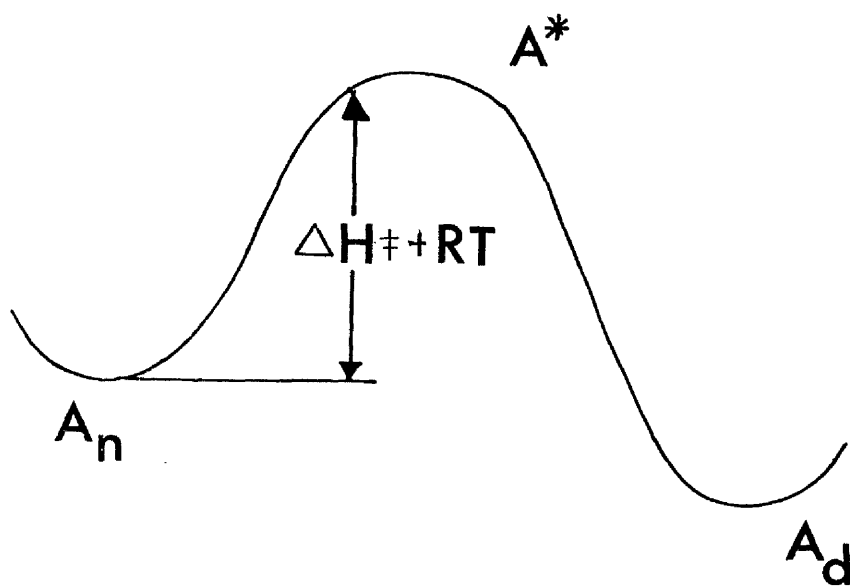
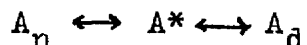


Figure 6.9. Schematic representation of the mechanism of protein denaturation.

6.3.2 A Model for Protein Denaturation

It is instructive to examine the thermodynamic variables as they apply to a reaction of interest, viz. the thermal denaturation of protein. Consider the monomolecular reaction



where A_n and A_d represent the native and denatured form of A, and A^* represents the activated complex.

In the native state, A exists in a potential energy well depicted in figure 6.9. To become activated, the molecule must acquire an amount of energy, $\Delta H^\ddagger + RT$, the activation energy. Once activated, the molecule is unstable, and must either proceed down the other side of the energy hill and become denatured or fall back down the left side and return to its original state.

The energy absorbed on activation often changes the configuration of the native molecule. If this change in configuration results in a decrease in the conformation of the molecule, energy is lost in the form of an entropy increase. The difference between the activation enthalpy and the energy associated with the increase in entropy is the free energy that is available to do work.

Most large proteins, in addition to the primary ordering and secondary orientation of the amino acids, exhibit a tertiary organization consisting of convolutions of the primary protein strands. This configuration is thought to be maintained by many disulphide, sulphhydryl, and hydrogen bridges.

Upon warming, the heat content of the molecule increases due to the absorption of energy, resulting in an increase in length of the low energy bonds maintaining the tertiary structure. These weak bonds will occasionally break, but will tend to rejoin as they are held in close proximity by the remaining unbroken bonds.

Occasionally, however, a single molecule acquires sufficient internal energy to break 20 or 30 such bonds simultaneously. This state, the activated complex, exists only momentarily, when the remaining bonds, stretched to their limit, are broken and the molecule unfolds violently. The probability of such a molecule randomly acquiring the energy to re-fold in the same way is extremely small and the reaction is essentially irreversible.

This model of protein denaturation is supported by the simultaneous observations of the high temperature

coefficients of expansion for proteins, the increase in viscosity for denatured proteins, and the detection of exposed sulphhydryl, disulphide, and phenol groups that are undetectable in the native protein.

In summary, to become activated, a molecule must increase its internal energy by ΔH^\ddagger . This is acquired by random fluctuations in the internal energy, due primarily to collisions with other molecules. In the activation process, a number of low energy bonds are broken, resulting in a loss of order and an increase of entropy, ΔS^\ddagger , entropy increasing for decreasing order. The difference between the heat ΔH^\ddagger , absorbed and the energy, $T\Delta S^\ddagger$, released due to the entropy increase is the change in free energy, ΔF^\ddagger , available to do work. It is worth emphasising that this reflects only the activation process and not the complete reaction, which, in the model of protein denaturation described, would exhibit enormous entropy increases.

Since energy must be supplied to activate the molecule, the reaction is endothermic, however this energy is compensated by the increase in entropy, resulting in negative values of ΔF^\ddagger (i.e. net energy release) and therefore the reaction is exergonic, occurring naturally even at environmental temperatures, albeit at a reduced rate.

Table 6.3 Thermodynamic parameters for Sindbis virus inactivation by heat. (from Barnes et. al. 1969)

Catalyst	Conc. mM	ΔH^\ddagger $\frac{\text{kJ}}{\text{mole}}$	ΔS^\ddagger $\frac{\text{J}}{\text{mole}^\circ}$	$\Delta F^\ddagger(50^\circ)$ $\frac{\text{kJ}}{\text{mole}}$	$k(50^\circ)$ sec^{-1}
Na_2HPO_4	.3	109	52.3	92.1	8.69E-3
	.5	130	111	94.1	4.13E-3
	.68	163	216	93.2	5.77E-3
	.84	205	339	95.5	2.45E-3
MgSO_4	.23	134	139	89.1	2.65E-2
	.34	159	213	90.2	1.76E-2
	.50	180	269	93.1	5.99E-2
	.63	205	352	91.3	1.17E-2

6.3.3 Compensation Phenomena

Barnes, Gordon, and Vogel (1969) examined the thermal sterilization of Sindbis virus in the presence of various concentrations of Na_2HPO_4 and Mg SO_4 . They observed that, as indicated in table 6.3, despite a considerable variation in ΔH^\ddagger and ΔS^\ddagger , the free energy of inactivation, ΔF^\ddagger , remained essentially constant. Such behaviour, referred to as entropy - enthalpy compensation, is observed in many physico-chemical systems and is thought to indicate a common mechanism in each situation. A similar compensation phenomenon is observed for thermal denaturation of proteins. The effect of pH is, perhaps, the most studied. A naïve explanation of this phenomenon is that, at low values of pH, many of the low energy bonds are disrupted resulting in an equilibrium configuration of the native state, characterized by an energy that is intermediate between the native state, at the pH corresponding to optimum stability, and the activated complex. If it is assumed that the activated complex is independent of pH, then the activation enthalpy decreases due to the reduced number of bonds that have to be broken, but there is a concurrent decrease in the entropy change since the entropy of the native state has

Table 6.4 Thermodynamic parameters for protein denaturation by heat. (from Stearn 1949)

Protein	Temp °C	ΔH^\ddagger $\frac{\text{kJ}}{\text{mole}}$	ΔS^\ddagger $\frac{\text{J}}{\text{mole}^\circ}$	$\Delta F^\ddagger(50^\circ)$ $\frac{\text{kJ}}{\text{mole}}$	$k(50^\circ)$ sec^{-1}
Insulin	80	149	100	117	8.2E-7
Trypsin	50	167	187	108	2.3E-5
Emulsin	60	188	273	100	4.6E-4
Solanain	60	257	456	109	1.6E-5
Hemoglobin	60.5	316	640	110	1.1E-5
Leucosin	55	353	774	103	1.5E-4
Invertase	50	462	1100	107	3.4E-5
Vibriolysin	50	536	1360	95	3.0E-3
Egg Albumen	65	553	1320	125	4.2E-8
Tetanolysin	50	722	1920	102	2.2E-4
Hemolysin	50	829	2250	103	1.5E-4

Table 6.5a Thermodynamic parameters for mammalian cell inactivation by heat.

Cell	Temp	ΔH^\ddagger $\frac{\text{kJ}}{\text{mole}}$	ΔS^\ddagger $\frac{\text{J}}{\text{mole}^\circ}$	$\Delta F^\ddagger(50^\circ)$ $\frac{\text{kJ}}{\text{mole}}$	$k(50^\circ)$ sec^{-1}	Ref
CHO	43-48	640	1720	83.7	2.0E-1	1
CHO	43 $\frac{1}{2}$ -46 $\frac{1}{2}$	590	1570	82.9	2.7E-1	2
CH	35-46	774	2130	86.0	8.4E-2	3
CHL*	42-44	678	1840	83.7	2.0E-1	4
PK *	44-48	507	1290	90.3	1.7E-2	5
PK *	45-48	404	967	91.7	1.0E-2	6

* - non-linear Arrhenius plot (i.e. $d\Delta E^\ddagger/dT \neq 0$)

1. Chapter 3
2. Westra, and Dewey (1971)
3. Johnson and Pavelec (1972)
4. Robinson and Wizenberg (1974)
5. Harris (1967)
6. Same data as no. 5, except reduced temperature range

increased due to the disruption of the internal bonds. Thus the decreased entropy change offsets the decreased enthalpy change, resulting in only marginal changes of free energy. In terms of this naive approach, the existence of the compensation phenomenon suggests that the activated complex is independent of the perturbing forces.

The criteria, for the demonstration of a genuine compensation phenomena are widely disputed (Exner 1964; Barnes, Vogel, and Gordon 1969; Lumry and Rajender 1970), but the most frequently encountered (and the least exacting) is that the data satisfy the relation in equation 6.8

$$A = \Delta H^\ddagger + B \Delta S^\ddagger, \quad 6.8$$

where A and B are constants. Reference to equation 6.5 indicates that B has the dimensions of temperature and is referred to as the "compensation" or "iso-kinetic temperature". This is an appropriate term since the reaction in question theoretically proceeds at the same rate at this temperature, independently of the perturbing agent. Similarly A is the free energy of activation at the iso-kinetic temperature.

Table 6.4 presents inactivation parameters for protein denaturation taken from Stearn (1949).

Figure 6.10a
Iso-kinetic plot for
protein inactivation by
heat. The regression
line is described by
 $H = 326 S + 98.5$. (from
Johnson, et. al. 1954;
July 1965)

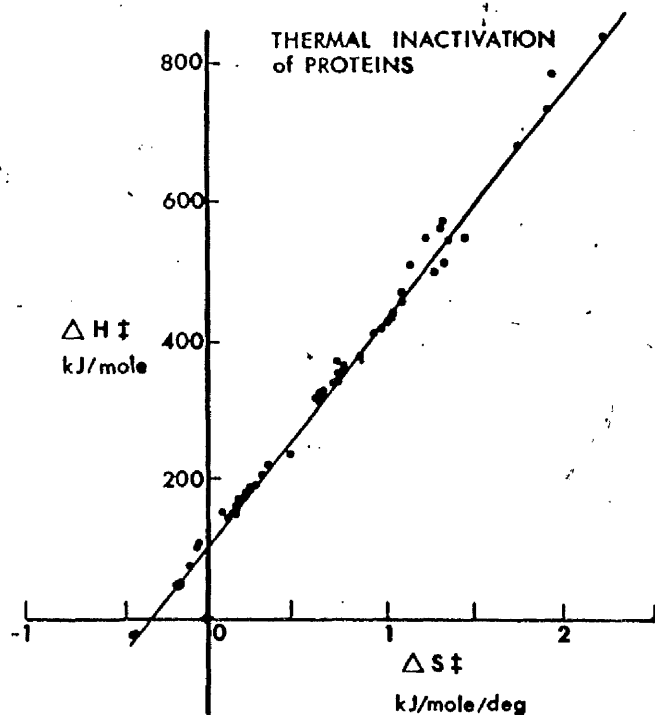
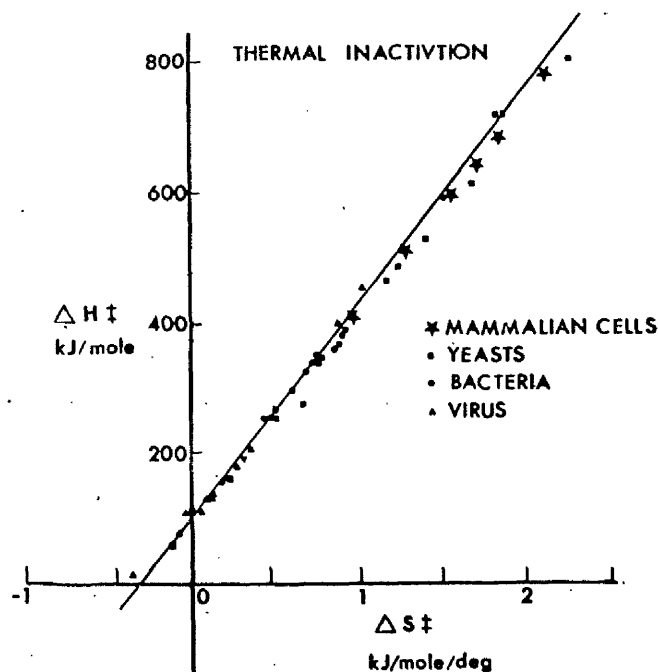


Figure 6.10b
Iso-kinetic plot for
living organism
inactivation by heat.
The regression line is
that for protein
inactivation. (from
Rosenberg, et. al. 1971;
Johnson and Pavelec
1972; Robinson and
Wizenberg 1974; Harris
1967; Westra and Dewey
1971)



Observe that in contrast to the large range of ΔH^\ddagger and ΔS^\ddagger values, the free energy of activation ΔF^\ddagger remains essentially constant. Rosenberg, Kemeny, and Switzer (1971) analysed thermal inactivation data for protein and single celled organisms - virus, yeast, and bacteria and presented similar values of A and B as evidence for protein denaturation being a principal mechanism in cellular inactivation. Iso-kinetic plots of the thermodynamic variables for protein and single celled organisms are illustrated in figs. 6.6 a, b. The solid line in both cases is the regression line for proteins. It is observed that the living organism plot reveals approximately the same slope as that for proteins, but in most cases the values for living organisms fall below the regression line for proteins.

The insensitivity of this type of plot is illustrated in table 6.5, in which the thermodynamic variables for mammalian cells are tabulated. In the last two columns the extrapolated free energy and reaction rate at 50°C are tabulated. While it is observed that the points corresponding to the mammalian cells fall just below the regression line for proteins, the mean value of ΔF^\ddagger at 50°C for mammalian cells is 20% lower than the mean value for the proteins listed in table 6.4. This difference in ΔF^\ddagger corresponds to a factor

of 2000 for the increased inactivation rate of mammalian cells.

Evans and Bowler (1973) analysed the thermodynamic parameters of thermal inactivation of various multicellular organisms. The iso-kinetic plot of these data exhibited a marginally reduced iso-kinetic temperature compared to that for proteins, and a few unusually high values of ΔH^\ddagger and ΔS^\ddagger well in excess of those observed for any protein investigated to date. These data, and indeed the data presented by Rosenberg for *Drosophila melanogaster*, have been omitted from this analysis, as possibly inappropriate due to the complex survival kinetics of a multicellular organism.

Evans and Bowler (1973) also suggest if entropy-enthalpy occurs in vivo, that the proteins with the least value of ΔH^\ddagger will be most rapidly denatured at temperatures less than the iso-kinetic temperature. If this were the case, then the most thermally susceptible proteins would be relatively non-essential to cell survival. However, Airas (1972) found that Pantothenate hydrolase exhibited an activation enthalpy of 220kJ/mole in vitro, compared to an activation enthalpy of 540kJ/mole in whole cells of *Pseudomonas Fluorescens*. The metabolites - succinate, glyoxylate, and oxylate added to the enzyme in vitro resulted in values of 550 to 630 kJ/mole. Thus, it may occur that proteins are compensated in vivo, resulting in a narrow range of ΔH^\ddagger values corresponding to that observed for thermal sterilization.

6.3.4. The Effect of Water on Conformation Reactions

The denaturing solvent has already been attributed a role in the compensation phenomenon. While thermal vibration and electrostatic repulsion are primarily responsible for breaking the low energy bonds, polar solvents such as water reduce the already marginal stability of the hydrogen bridges and bind lightly to hydrogen atoms replacing internal hydrogen bridges with water.

If the protein is dehydrated the hydrogen bridges are more stable and tend to rejoin if temporarily broken, so that a high activation enthalpy might be expected. However, this is not the case. While the proteins are very heat resistant when dry, the observed activation enthalpy is quite low and the activation entropy is zero or negative. This is thought to be the result of a change in mechanism. In the absence of water, the hydrogen bridges can be easily re-formed when broken since they have not become hydrated. The result is that the molecule does not experience an unfolding upon activation so that the activation entropy is low. Since it is the large entropy increase that makes the unfolding reaction possible in wet protein, this mechanism, while probably possessing the indicated high activation enthalpy, is not spontaneous.

A possible explanation of the observed low activation energy and zero entropy is that rather than being due to a conformational change, the denaturation is caused by the breakage of a single or a few strong covalent bonds at or near the active site. Since the activation for this breakage of a single bond requires no disordering of the molecule, the change in activation energy would be zero.

The thermodynamic parameters for thermal inactivation of Emulsin and Lipase and T1 and Φ X 174 virus are given in table 6.5b. The protein and the virus exhibit parallel changes in the thermodynamic variables in the wet or dry state, the most prominent change being to zero or negative entropy values.

Table 6.5b Thermodynamic parameters for protein and virus inactivation by heat. (from Johnson et.al. 1954, Trujillo and Dugan 1972)

	Wet				Dry			
	ΔH^*	ΔS^*	$\Delta F^*(50^\circ)$	$k(50^\circ)$	ΔH^*	ΔS^*	$\Delta F^*(50^\circ)$	$k(50^\circ)$
	$\frac{\text{kJ}}{\text{mole}}$	$\frac{\text{J}}{\text{mole}^\circ}$	$\frac{\text{kJ}}{\text{mole}}$	sec^{-1}	$\frac{\text{kJ}}{\text{mole}}$	$\frac{\text{J}}{\text{mole}^\circ}$	$\frac{\text{kJ}}{\text{mole}}$	sec^{-1}
PROTEINS								
Emulsin	188	273	-99.7	5.13E-4	107	-32.9	-117.6	6.5E-7
Lipase					101	-54.4	-118.6	4.5E-7
VIRUS								
T1	397	871	-115.7	1.32E-6	117	0	-117	8.2E-7
Φ X174					112	-26.4	-120.5	2.2E-7

The data for dry denaturation for both virus and protein fall on (and have been included in) the respective iso-kinetic plots of figure 6.6. This may seem contrary to either the supposition of a common denaturing mechanism proposed in section 6.3.3 or the proposed scheme of dry denaturation, but probably reflect the insensitivity of the iso-kinetic plot.

6.3.5 The Effect of Pressure on Conformation Reactions

Equation 6.6 is an abbreviated form of the more complete relation of equation 6.9 which takes account of pressure and volume changes.

$$k = \frac{kT}{h} \exp\left(-\Delta H^\ddagger / RT + \Delta S^\ddagger / R - P \Delta V^\ddagger / RT \right) \quad 6.9$$

where P is the pressure and ΔV^\ddagger is the change in molar volume for activation. At atmospheric pressures, and assuming ΔV^\ddagger is 100 ml/mole, the pressure term is only 1.1×10^{-4} times as large as the enthalpy-entropy term, justifying its usual omission from biological applications.

An increase in pressure usually decreases the rate of a reaction involving large volume increases. Very large pressures have been found to have an inhibitory effect on the thermal inactivation of some, but not all, proteins, bacterial cells, bacterial spores, and viruses. (Johnson et.al. 1954)

6.3.6 Summary of the Evidence for the Implication
of Protein Denaturation in the Thermal
Inactivation of Living Organisms.

For mammalian cells, the primary piece of evidence for a conformation type of reaction is the extremely high activation enthalpy, non-conformational reactions exhibiting activation enthalpies significantly less than 200 kJ/mole. The value of activation enthalpy of 640 kJ/mole, reported here, which is not atypical of other mammalian cell lines, may be compared to the values for thermal induced - depurination of DNA of 120 kJ/mole (Greer and Zamenhof 1962), loss of transforming ability of DNA of 140 kJ/mole (Ginoza and Zimm 1961), and loss of infectivity of RNA of 80 kJ/mole (Ginoza 1958).

The large entropy increase for activation was observed to partially compensate the change in activation enthalpy for individual proteins and at least one virus. Further, various proteins and various single celled organisms exhibited entropy-enthalpy compensation displaying roughly the same iso-kinetic temperature. However the inactivation rates for living organisms, particularly mammalian cells, were significantly lower than those for protein denaturation. The analogy to respective

radiosensitivities is apparent, but not satisfying.

Finally the parallel effects, on protein and living organism inactivation, of moisture content and pressure suggest a common mechanism, that is not exhibited in most other physico-chemical reactions.

While the targets for thermal inactivation and the reaction kinetics are not manifest, it is concluded that protein denaturation is the most probable mechanism for thermal inactivation of mammalian cells and other living organisms and that in the absence of evidence to the contrary it will be assumed that protein denaturation is the cause of the observed thermal inactivation of CHO cells.

6.4 The Thermodynamics of Hyperthermia and Ionizing Radiation Interaction

6.4.1 Comparison of the Observed Thermodynamic Parameters

In the previous section, it was demonstrated that it was possible to evaluate ΔF^\ddagger , ΔH^\ddagger , and ΔS^\ddagger for the thermal inactivation of CHO cells and other living organisms. The separation of the interacting system into three components, the temperature-independent radiation component and the temperature-dependent hyperthermia and interaction components, allows the assessment of a value of ΔH^\ddagger for the interaction component. Since the interaction component is an explicit function of the radiation dose, it cannot be treated as a pure rate term. Therefore, it is incorrect to attach activation entropy or free energy to the term. However the activation enthalpy of the interaction coefficient K_I is high enough to possibly implicate a protein denaturation as being involved in the interaction between hyperthermia and radiation.

Data for mammalian cells that would allow a direct comparison of the observed temperature coefficient have not been published. However by making a few, quite possibly unwarranted assumptions,

it is possible to extract values that are proportional to K_I from data sets provided by Robinson and Wizenberg (1974) and Ben-Hur et.al. (1974).

If the hyperthermia exposure is a constant time at different temperatures, it might be assumed that the interaction coefficient is proportional to the increase in radio-sensitivity at the hyperthermic temperature compared to 37° or 20°C. Thus $K_I(T^\circ) = K(T^\circ) - K(37^\circ)$, where $K(T^\circ)$ is the observed radiosensitivity at a temperature T.

Applying this analysis to Robinson's data for CHL cells, heated for 2 hours, before, during, and after radiation over the temperature range of 40° to 42°C yields an activation enthalpy for interaction of about 320 kJ/mole, compared to approximately 680 kJ/mole for hyperthermic killing over temperatures from 42° to 44°C. These values, although derived from sparse data are in good agreement with the observed activation enthalpies for CHO cells.

In contrast, Ben-Hur's data, obtained at a low dose rate (.03Gy/min), which is the only set amenable to this analysis due to the technique used, yields an activation enthalpy for interaction in excess of 1MJ/mole for temperatures from 40° to 42°C. This high

Table 6.6 Thermodynamic parameters for virus inactivation by heat. (from Trujillo and Dugan 1972)

Virus	Φ X174	T_1	T_1	N.D.V.	T_4
Radiation	^{60}Co	x-ray	x-ray	^{60}Co	^{60}Co
Dose Rate krad/hr	1500	25	25	291	30.6
Conditions	Dry	Dry	Wet	Wet	Wet
$k_H \Delta S^\ddagger$ J/mole $^\circ$	-26.5	0	871	93.8	1028
ΔH^\ddagger kJ/mole	112	117	400	129	450
$k_I \Delta H^\ddagger$ kJ/mole	26.8	73.1	252	222	265

value is, however, probably due to two actions, the normal interaction and a progressive suppression of concurrent repair of SLD, which at this dose rate alters the radiosensitivity observed.

More extensive data exist for the interaction that has been observed for micro-organisms. Trujillo and Dugan (1972) examined the interaction between hyperthermia and radiation for T4 virus and other data for viruses in the literature. They used equation 6.10 to describe survival due to an exposure of duration, t , to a radiation flux at an elevated temperature.

$$-\ln S = (K_R + K_H + K_I) t \quad 6.10$$

The thermodynamic parameters for inactivation of 4 viruses are listed in table 6.6.

It is observed that the activation enthalpies for interaction for the three wet viruses are similar and all distinctly different from the corresponding hyperthermia component enthalpies. Perhaps more important however, is the fact that the activation enthalpy for both hyperthermia "killing" and interaction is decreased for irradiation under dry conditions. For T1 virus, the decrease in ΔH^\ddagger almost exactly parallels that for hyperthermia inactivation

(i.e the ratio of wet and dry ΔH^\ddagger 's for killing and interaction are nearly equal). This suggests that the same type of mechanism may be acting for both hyperthermic killing and interaction.

Equation 6.10 is superficially similar to equation 4.11. To apply equation 4.11 to the same situation of irradiation for a fixed period of time at an elevated temperature results in equation 6.11, in which the various quasi-threshold doses have been omitted.

$$-\ln S = (K_R + K_H + K_I K_1/K_2 - K_I K_1/K_2 e^{-K_2 t})t$$

6.11.

where K_1 = rate of formation of ISD

K_2 = rate of disappearance of ISD

K_I = number of lethal events/unit ISD

K_R = number of radiation lethal events/unit time

and all the other factors are as described previously.

If K_2 is very large equation 6.11 is approximately equal to equation 6.10. The extreme disparity between this value of K_2 and the small value of K_2 required for separated interactions in mammalian cells suggests that mechanisms of interaction in viruses and mammalian cells are possibly not the same.

Wood (1954) analysed the temperature dependence of yeast radiosensitivity. Survival was again given

as a function of exposure time to a radiation flux at an elevated temperature. Unlike Trujillo's data, which exhibited only marginal discrepancies from a first order exponential survival, for both radiation and hyperthermia, the yeast data exhibited a curvature of the survival curve at high temperatures and a persistence of interaction for separated heating and radiation, that suggests a low rate of decay of the ISD during and after radiation. The observed activation enthalpies for hyperthermic killing and interaction were 690 kJ/mole and 355 kJ/mole respectively, in good agreement with the observations for mammalian cells.

6.4.2 Interaction as a Compensation Phenomenon

If a physico-chemical process exhibited a true enthalpy-entropy compensation effect, a perturbing agent that lowered the activation enthalpy would increase the rate of the process at any temperature below the iso-kinetic temperature. As the temperature increased, the relative increase in rate would decrease.

With a single exception, all of the above interactions for protein, viruses, yeasts, and mammalian cells exhibited an activation enthalpy for interaction that was significantly less than that for hyperthermic inactivation. The result is that the relative increase in thermal sensitivity due to the radiation dose will decrease for increasing temperature. Thus the interaction between radiation and hyperthermia might be considered to exhibit a compensation effect. That is, radiation might alter the molecular configuration to allow a thermal denaturation to occur with reduced enthalpy and entropy changes.

Table 6.7 lists the thermodynamic parameters for the thermal inactivation data of the previously described experiment.

Table 6.7 Thermodynamic parameters for heat inactivation of CHO cells, 100 minutes after a radiation dose(250 kVp x-rays).

RADIATION DOSE (Gy)	ΔH^\ddagger kJ/mole	ΔS^\ddagger J/mole $^\circ$	ΔF^\ddagger kJ/mole	$k(46.2^\circ)$ $\times 10^{-2} \text{sec}^{-1}$
0	648	1746	90.4	1.08
1	642	1729	90.2	1.16
2.5	584	1548	90.3	1.13
4	567	1495	89.9	1.30
5	577	1527	89.7	1.41
6	533	1389	89.7	1.39
7	471	1194	90.3	1.13

Note - Dose Modifying Data from table 6.1.

These exhibit a parallel decrease of entropy with enthalpy, which if plotted in an iso-kinetic plot, (not illustrated), reveals an unrealistic precision of compensation. This apparent precision of compensation is due to the fact, first that ΔS^\ddagger is not an independent quantity but is derived as a function of ΔH^\ddagger , and second, that the observation temperatures are very close to the indicated iso-kinetic temperature of 46.2°C .

Utilising a different criterion of compensation (Exner, 1964) it is observed that the dose modifying data of figure 6.6 exhibit a more precise compensation than the unbiased data. While this may be attributable to a smoothing of the data, it may equally well be that the assumption of a compensation process is equivalent to the assumption of a dose modifying nature of the interaction.

The fact that the data satisfy a more exacting criteria of compensation is of little consequence due to the very small range of temperatures over which the observations were made. Despite the lack of data, it is instructive to examine the hypothetical response of a compensated interaction.

If radiation were to affect every susceptible hyperthermia target to the same degree, as perhaps

by a solvent effect, the interaction would decrease with increasing temperature until, at the iso-kinetic temperature the interaction would vanish. Above this temperature the interaction would be antagonistic (i.e. radiation would act as a protective agent for hyperthermia effects).

If radiation were to affect only a subpopulation of the susceptible hyperthermia targets, perhaps by direct effects on the individual targets, then the interaction would approach zero asymptotically as the temperature increased. This asymptotic approach would be due to the increasing dominance of the hyperthermia effects on the unaltered targets.

Thus a compensation phenomenon could explain the results of this chapter. The implication would be that, unlike the deposition of radiation ISD which must be independent of hyperthermia dose (i.e. dependent only on the absorption of energy prior to the hyperthermia insult), radiation would affect the rate of deposition of hyperthermia SLD. Thus while hyperthermia appeared to act as an expression modifying agent for radiosensitivity, radiation would be acting as a (hyperthermia) dose modifying agent for thermal-sensitivity.

It is important to note that the simple explanation of compensation effects presented in section 6.3.3 would not account for the observed interaction for radiation applied after hyperthermia. Therefore if compensation is responsible for the observed results, there must be a second mechanism that affects the interaction when the stimuli are reversed. It seems more plausible, however, that the compensation effect observed is, rather than the cause of the interaction, merely the artifactual result of a less obvious mechanism which is operational independently of the order of radiation and hyperthermia insults.

6.4.3 Conclusion

The significance of the activation enthalpy for K_I and the mechanism by which interaction occurs is not clear. The difference in the activation enthalpy for K_I and K_H suggests that the interaction either involves a hyperthermia ISD that is distinct in type from hyperthermia SLD or is similar, but arises from a distinct mechanism.

The first situation would require that radiation ISD interacted with hyperthermia ISD resulting in a lethallization of damage that is invariably present. Thus radiation (and hyperthermia) would be acting as an "expression modifying agent". The second situation would require that radiation ISD modified the damage mechanism producing hyperthermia SLD, thereby providing a greater yield of SLD. Thus radiation would be acting as a "dose modifying agent" for hyperthermia. These data and the experiment design are not adequate to choose between them.

In the previous section, the similarities between cell and protein inactivation by heat suggested that protein denaturation played a part in the cellular inactivation.

The activation enthalpies of the interaction coefficient for some wet viruses, yeast, and mammalian cells are in excess of the values observed for chemical reactions other than those involving a large conformational change of the reactants. For viruses, the observed activation enthalpies display a variation with moisture content that is typical of protein denaturation. The changes,

brought about by a prior radiation dose, in the activation enthalpy and entropy of thermal inactivation are similar for both CHO cells and a protein in solution. Thus, it is suggested that protein denaturation involving large conformational changes in molecular structure is involved in the interaction of hyperthermia and radiation effects on living organisms.

CHAPTER SEVEN

CONCLUSION

7.1 Introduction

The various aspects of the interaction revealed by the preliminary experiments viz.

1. that hyperthermia increases the slope of the radiation survival curve,
2. that radiation increases the slope of the hyperthermia survival curve,
3. that increasing hyperthermia doses result in increasing radiosensitization,
4. that hyperthermia administered before radiation increases the extrapolation number of the radiation survival curve,
5. that increasing temperature results in an increase in radiosensitization by hyperthermia,
6. that increasing temperature results in a decrease in thermal-sensitization by radiation,

are resolved as the non-conflicting results of equation 7.1,

$$-\ln S(t, T, D) = D' K_R + t' K_H(T) + D'' t' K_I(T), \quad 7.1$$

where t = hyperthermia dose
 T = temperature
 D = radiation dose
 K_R = radiosensitivity
 K_H = thermal-sensitivity
 K_I = interaction coefficient

and

$$\Delta K_H / \Delta T > \Delta K_I / \Delta T$$

The interaction term, being a function of both radiation dose and hyperthermia dose, accounts for the first three observations. The accumulation of radiation ISD ($D \rightarrow D''$) accounts for the fourth observation.

The fifth observation is explained by the temperature sensitivity of interaction being non zero, while the sixth observation is a result of the temperature coefficient of interaction being less than the normal hyperthermia component. Thus this simple approach has placed this at first confusing array of observations into perspective.

This investigation, while having given insight to some aspects of the interaction, has raised questions about the distinction of targets for cell killing and interaction and about the role of high LET radiation events in cell killing and damage. A final experiment with relevance to the latter question is described. Conclusions are made and further research suggested.

7.2 A Final Experiment

It was anticipated that it would be possible to repeat the experiments described in chapter five, collecting data simultaneously for the neutron-hyperthermia and gamma-hyperthermia surfaces. This would eliminate the experiment to experiment instability, that lends a certain dubiety to the conclusions reached in chapter five. Unfortunately, this was not to be the case, as a suitable neutron generator was not available for the remainder of this period of investigation.

In addition, the validity of the comparison depended heavily on the supposition that the interaction between radiation and hyperthermia decreased for decreasing dose rate, contrary to one set of published results (Ben-Hur et.al. 1974). To confirm this aspect, another investigator, at my suggestion and to my design, performed the following experiment.

7.2.1 Experiment Design

CHO cells, suspended in Hams F12 at a concentration of 1.25×10^5 cells/ml in three plastic T30 flasks, were either untreated or given

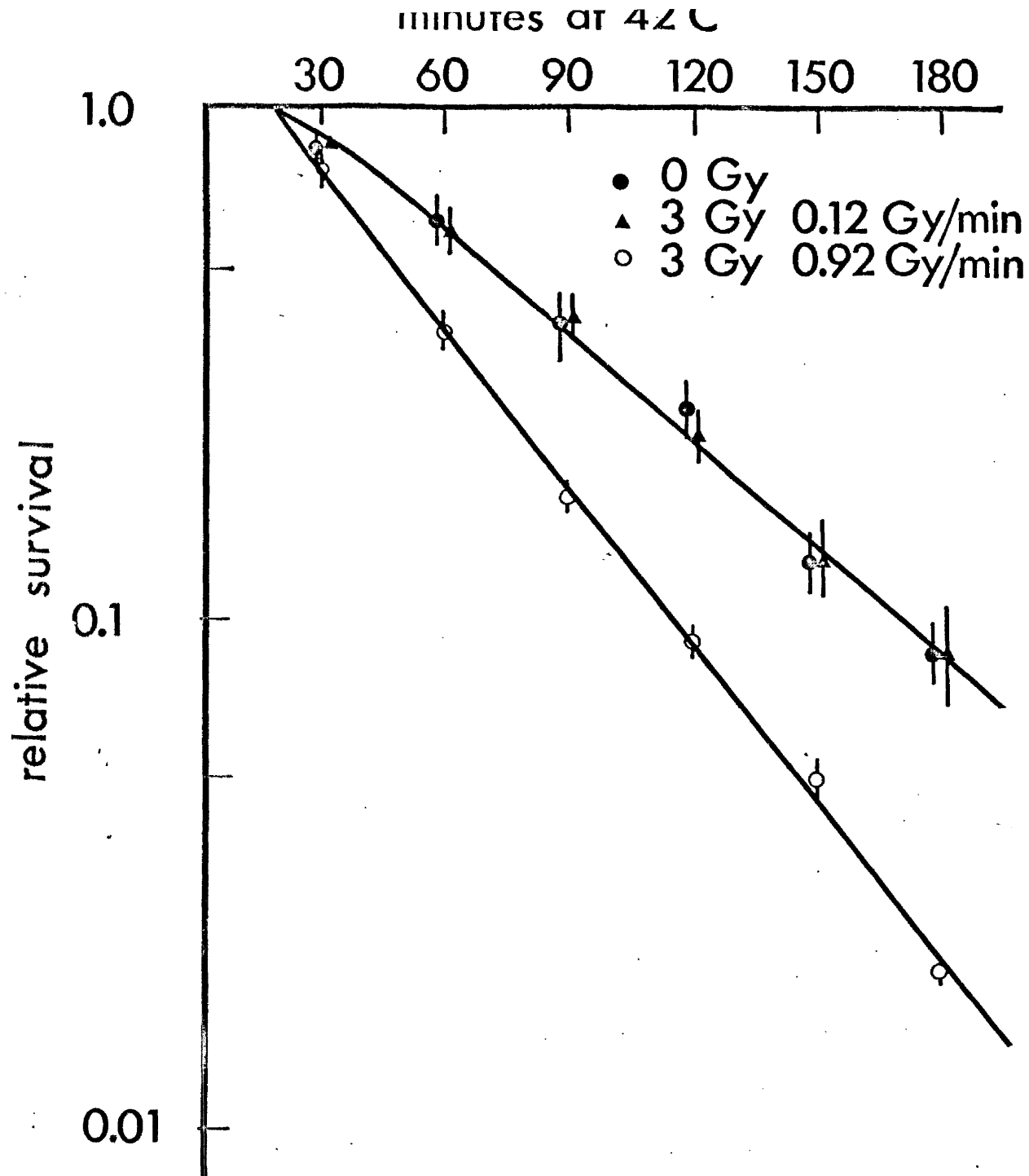


Figure 7.1. CHO cell survival, normalized to unity at zero hyperthermia dose, sensitized by a γ radiation dose at the indicated dose rate, 100 minutes prior to heating. Data points represent the mean and standard error of three experiments.

3.0 Gy of radiation at a dose rate of 0.12 Gy/min (4 m SCD) or 0.92 Gy/min (46 cm SCD). One flask was irradiated at the low dose rate, followed immediately after by the irradiation of the second flask at the high dose rate. The total time interval between the completion of the two irradiations was six minutes.

The cells were diluted and plated into replicate T30 flasks at concentrations of 500, 750, 1000 cells/flask depending on the radiation treatment. One hundred minutes after the high dose rate irradiation was completed, these flasks were heated to 42°C (41.96°C). Samples from each radiation population were removed at 30 minute intervals. After one hour at room temperature, the plates were incubated at 37°C for six days, stained, and counted.

7.2.2 Results

Table 7.1 lists the mean plating efficiencies and parameters M_H and K_H of three experiments. The survival curves, normalized to unity at zero hyperthermia dose, are illustrated in figure 7.1.

Table 7.1.

Dose Rate	Plating Efficiency	M_H	$K_H (\times 10^{-2} \text{ min}^{-1})$
0	.950 \pm .029	1.62 \pm .30	1.60 \pm .14
.12Gy/min	.795 \pm .033	1.47 \pm .12	1.54 \pm .11
.92Gy/min	.526 \pm .076	1.54 \pm .15	2.35 \pm .07

It is interesting to note the plating efficiency of 95% obtained with a different subclone from the same parent stock, but otherwise apparently unchanged materials or procedures. The slope of the unperturbed survival curve is lower than that observed for the neutron and gamma interaction experiments, but not outwith the range of the observed thermal sensitivities at 42°C.

7.2.3 Discussion

The results of this experiment are twofold. Firstly, the results yield fundamental insight into the nature of ISD. Secondly, the results lend credence to the suggestion of a high LET interaction.

The observation of increased extrapolation numbers for sensitized radiation survival (section 3.4.1) suggests a cellular capability of accumulating ISD. The relaxation experiments (section 3.4.2) demonstrate a cellular ability to repair ISD. Finally the above experiment demonstrates that at a low dose rate there is a concurrent repair of radiation ISD during irradiation. This repair appears to be complete, compared to the lesser degree of repair observed for radiation SLD suggesting a further dissimilarity between radiation ISD and SLD.

The results of this experiment verify the suggested change of interaction coefficient with radiation dose rate. Since the experiment simulates the low LET radiation characteristics for both the gamma-hyperthermia and the neutron-hyperthermia experiments of chapter five, the suggested upper limit of the interaction coefficient of the neutron-hyperthermia interaction K_I (neutron) = $0.75 \times K_I$ (gamma) seems over cautious. Further if the gamma-kill component of neutron irradiation was similar to that of ^{60}Co at a comparable dose rate, it may be concluded on the basis of these experiments that virtually none of the interaction need be attributed to the low LET component and therefore nearly all of the interaction can be attributed to the high LET component of neutron radiation.

As a qualification to the above, it should be observed that if the ion-kill component of the neutron effects reduces the capacity for the repair of ISD contributed by the low LET component, the observations could be explained, but not without fundamental alteration to the Katz theory.

7.3 Conclusions

7.3.1 Firm Conclusions

1. The interaction between radiation and hyperthermia depends explicitly on the radiation and hyperthermia dose in an approximately linear fashion.
2. The interaction occurs when radiation and hyperthermia are given simultaneously or separated.
3. Under certain circumstances, the interaction exhibits a relaxation for increasing time intervals between the radiation and hyperthermia dose.
4. CHO cells are capable of an essentially total repair of radiation ISD during low dose rate irradiation.
5. A variation of the magnitude of interaction occurs with a variation of radiation quality.
6. The interaction component for hyperthermia following x-rays is less temperature sensitive than the normal hyperthermia inactivation component.

7.3.2 Supported Conclusions

1. Hyperthermia inactivation is associated with protein denaturation.
2. Radiation and hyperthermia interaction is associated with protein denaturation.
3. At least a part of the radiation ISD is of a different nature from radiation SLD.

4. Some of the high LET radiation events are capable of depositing ISD without killing the cell.
- (or) 5. High LET radiation events interfere with the concurrent repair of low dose low LET events.
6. Since the Katz theory cannot account for either 5 or 6, it is fundamentally inadequate and requires review.
7. The interaction between radiation and hyperthermia exists for reasons other than a complementary cell age sensitivity distribution (Appendix III).

7.4 Future Developments

7.4.1 High LET interaction

The experiments investigating neutron- hyperthermia interaction would be less ambiguous if an assessment of low LET interaction could be made simultaneously. It is therefore tentatively planned to repeat the matrix experiment of chapter five, by simultaneously collecting data for three neutron doses and three ^{60}Co gamma ray doses at a comparable dose rate. This procedure will eliminate the inter-experiment variability that prevents an unequivocal statement.

7.4.2 Temperature Sensitivity of Interaction

The interpretation of the experiments of chapter six, might be clarified by repeating these experiments reversing the order of application of the two stimuli. This would eliminate the possibility of a direct radiation effect on the hyperthermia inactivation reaction and rule out an enthalpy-entropy compensation phenomenon as the factor responsible for the interaction.

7.4.3 Interaction Relaxation

This aspect of the interaction was only briefly touched upon in this investigation and then primarily as an assessment of experimental stability. The comparison of the rates of repair of SLD and ISD would provide additional insight into their natures. If hyperthermia SLD and ISD are the results of irreversible protein denaturation, repair might be expected to occur as a result of a synthetic process. Thus the repair of hyperthermia ISD and SLD should exhibit a strong temperature dependence unlike that observed for radiation. The phenomenon of induced thermotolerance (which was not observed for this cell line) might be investigated in relation to interaction. If the decreased thermal sensitivity was not associated

with a decreased interaction, this would suggest that hyperthermia ISD and SLD mechanisms were not coupled.

7.4.4 The Oxygen Effect

Experimentally deriving the oxic and anoxic survival surfaces would allow an assessment of the oxygen effect for each component separately. Thus the relative importance of direct and indirect radiation effects on the interaction could be assessed. If, in addition, the oxic and anoxic high LET interaction surface could be determined, considerable further analysis would be possible.

7.5 The Application of the Component Approach In Vivo Situation

The component approach to radiation-hyperthermia interaction is straightforward due to the existence of only two states of the outcome, however, for the critical situations of tumour control in vivo, additional factors and additional possible outcomes modify the simple situation described in vitro. Indeed it is these additional factors that will

ultimately guide the therapist towards a particular combination of treatments.

However, it is felt that there might be a few model systems for which the component approach may be utilized and provide useful information for the application of interaction therapy to more complex in vivo systems.

Assume that for an in vivo system, the end point in question may be reached by either radiation or hyperthermia alone. For simplicity, assume that this is a tumour control system. It has been demonstrated that cell survival for two different configurations of the combination of hyperthermia and radiation can be represented approximately by

$$-\ln S = D'K_R + t'K_H + D't'K_I \quad . \quad 7.2$$

This equation can be solved for a dose D to yield a particular survival level as a function of the associated hyperthermia dose resulting in the iso-survival plots shown earlier. It might be expected that a plot of TCD_{50} as a function of the associated hyperthermia dose should have the same general shape as one of the iso-survival contours. Thus it would be possible to infer the relative magnitude of the interaction.

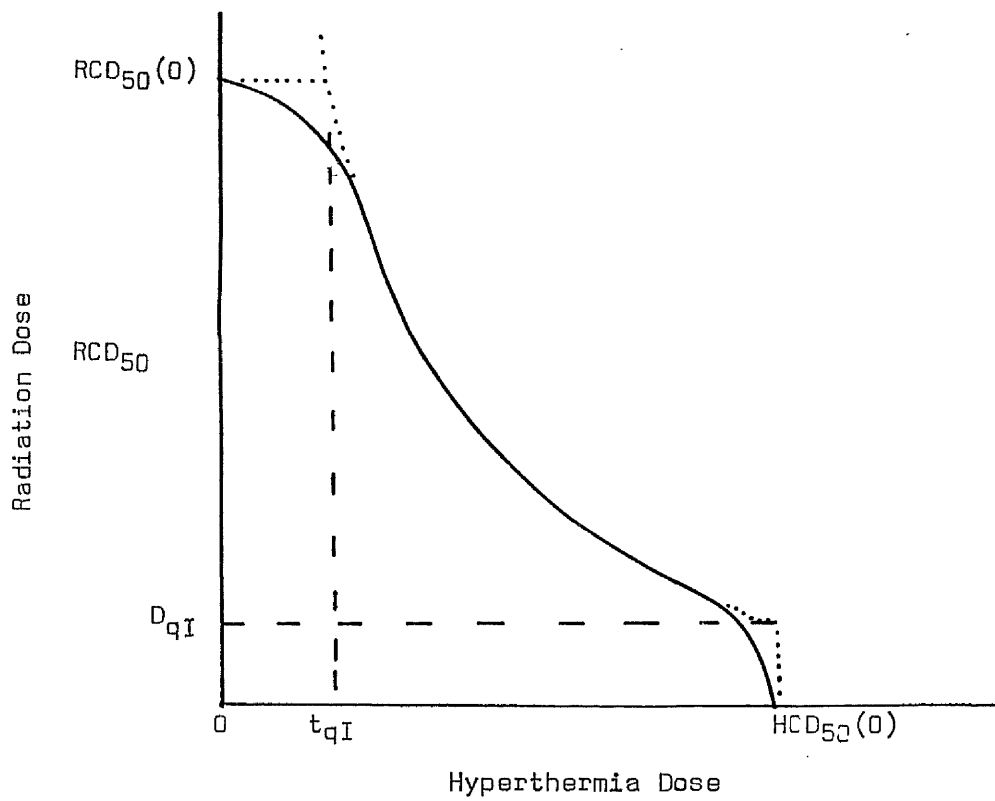


Figure 7.2. Hypothetical iso-response curve for in vivo test system.

Ignoring the quasi-threshold doses in equation 4.11, this can be solved to yield

$$D = \frac{\text{constant} - t\alpha}{1 - t\beta} \quad 7.3$$

or,

$$\text{RCD}_{50}(t) = \frac{\text{RCD}_{50}(0) - t\alpha}{1 - t\beta} \quad 7.4$$

where $\text{RCD}_{50}(t)$ is the 50% control radiation dose observed in conjunction with a hyperthermia dose, t , and $\text{RCD}_{50}(0)$ is the unperturbed $\text{RCD}_{50} = \text{TCD}_{50}$.

The parameter, α , yields the equivalent radio-sensitivity for the hyperthermia treatment,

$$\alpha = \text{RCD}_{50}(0)/\text{HCD}_{50}(0), \quad 7.5$$

where $\text{HCD}_{50}(0)$ is the unperturbed hyperthermia 50% control dose.

In this simple case in which the quasi-threshold doses have been ignored, β is equal to K_I/K_R and α is equal to K_H/K_R . Evaluation of α and β at various temperatures would allow an in-vivo assessment of the temperature dependence of hyperthermia and interaction effects.

One can only speculate as to what the quasi-threshold doses for the normal components of radiation and hyperthermia are and these would have to be neglected. However the interaction quasi-threshold doses are measurable and crucially important to the

determination of β . A typical $RCD_{50}(t)$ curve might be expected to appear as in figure 7.2. Observe that the curve for small hyperthermia dose t , is first negatively curved and then positively curved. The extrapolate of the positively curved portion at the $RCD_{50}(0)$ value yields the hyperthermia interaction quasi-threshold dose, t_{qI} . D_{qI} may be similarly determined. Equation 7.4 then applies in the transformed co-ordinate system ($t \rightarrow t - t_{qI}$, $D \rightarrow D - D_{qI}$) indicated by the dashed lines in figure 7.2.

Equation 7.3 is independent of the test effect and therefore could be used to determine α and β for any number of situations, malignant or normal, provided these fulfilled the basic requirement of yielding the end point for both treatments separately. Despite the fact that this approach is limited to those experimental systems which do not require the combined treatment in the first place (i.e. curable by either treatment alone), this technique will yield vital information, that might be applied clinically to design combination therapy which would be capable of dealing with radio-resistant and thermal-resistant neoplasms.

The questions to be answered that could be determined by this approach are -

1. Do hyperthermia and radiation interact in vivo?
2. Does fractionated hyperthermia radiation treatment yield an enhanced (reduced) interaction?
3. What are the effects of tumour nutrition, pH, and oxygen tension on the interaction?
4. Is there an optimum combination of radiation and hyperthermia dose in terms of immediate or long term side effects?
5. What is the variability from tumour to tumour and system to system in thermal-sensitivity and interaction?

APPENDICES

I 1 The Effects of Hyperthermia at the
Subcellular Level

I 1.1 The Effects of Hyperthermia on
Cellular Respiration

Respiratory activity essential for the ultimate formation of high energy phosphate bonds has received much attention particularly with regard to a differential sensitivity of normal and neoplastic cells. The hypothesis of a differential respiratory requirement of normal and neoplastic cells, as proposed in the Warburg theory of oncogenesis, is today in some doubt (Pitot, 1966). However, there is an abundance of reports citing a differential effect of hyperthermia on normal and neoplastic cells with regard to respiratory activity.

Westermarck (1927), using Warburg manometry, measured the respiratory response to hyperthermia in tumours and normal tissues of the rat. The rates of aerobic and anaerobic glycolysis of the Flexnor-Joblings carcinoma and Jensens sarcoma decreased after exposure to temperatures of 45.5°C to 49°C. The decrease in rate was evident after a 30 minute exposure and was completely inhibited after 85 minutes at 45.5°C. In contrast, the oxygen consumption remained constant until anaerobic glycolysis had been depressed to negligible levels. Tissues from normal liver and spleen exhibited a similar constancy of respiration and indeed maintained the respiration for longer exposures before being depressed.

Johnson (1940) reported a decrease, but not complete inhibition, of anaerobic glycolysis in slices of Jensen sarcoma and Walker 256 carcinoma of rats, over the temperature range from 42.5°C to 47°C.

Burger and Fuhrman (1964 a, b), investigating the response to thermal injury in different normal tissues of the rat, observed that the rate of oxygen consumption fell off smoothly as a function of time at the elevated temperature, over the range of 40° to 47.5°C.

Dickson and Shah (1972), investigating a cell line derived from a chemically induced Adenocarcinoma of the breast in rats, observed that respiration decreased for exposures at temperatures over 40°C. Anaerobic glycolysis was only affected after long periods of heating. They noted that only in cells, heated long enough (6 hours 42°C) to prevent the growth of tumours, were respiration and anaerobic glycolysis irreversibly depressed.

Muckle (1971, 1973) and Dickson (1972) together investigated the effects of hyperthermia of normal tissues and the VX-2 carcinoma of the rabbit. Measuring the respiration both during and after heating, they observed that oxygen consumption increased at temperatures up to 40°C. At 42°C, the oxygen uptake was significantly depressed in the VX-2 cells, but not in samples from skin, lymph node, or lung of the rabbits. Cells derived from lymph node metastases exhibited an initial depression of respiratory rate, but whereas the tumour oxygen uptake fell off after four hours, the metastatic cells continued to respire at the same reduced rate.

The effects of an in vivo application of hyperthermia on respiration rate were assayed by heating the VX-2 tumour in a waterbath maintained at 46°C. The entire hind limb, in which the tumour was implanted, was immersed and the intra-tumour

temperature was maintained at 42°C for 1 hour on three consecutive days. Slices and cell suspensions of the tumour were then assayed for respiratory activity at 37°, revealing a decrease in oxygen uptake which persisted for four weeks.

Cavaliere (1967) and Mondovi (1969), together with others, observed the rates of oxygen consumption and anaerobic glycolysis of several tissues, during and after hyperthermia. They experimented with the addition of .015M glucose + .013M succinate, which will be referred to as the presence of substrates in the discussion.

A human melanoma, in the presence of added substrates, exhibited a slight inhibition of oxygen uptake during exposure at 43°.

An Erlich ascites tumour, propagated in Swiss mice, exhibited a depression of respiration during exposure at 44°C in the absence of substrates, but with added substrates, exhibited respiration rates greater than the controls incubated at 38°C. Anaerobic glycolysis was unaffected by hyperthermia.

Respiration and anaerobic glycolysis, in normal liver of rats, was unaffected during hyperthermia at 42°C, both with and without the presence of additional substrates.

The respiration rate of regenerating rat's liver was higher than that of normal liver and only marginally affected during hyperthermia at 42°C, both with or without substrates. However, if the rate of respiration was measured after hyperthermia exposure, the respiration rate was unaffected by

even 3.5 hours at 44°. The rate of anaerobic glycolysis, higher than in the normal lines, was unaffected by hyperthermia.

A minimum deviation 5123, hepatoma of the rat exhibited a rate of anaerobic glycolysis, less than that of the normal liver, that was insensitive to hyperthermia. Similarly the rate of respiration during hyperthermia was not affected by temperatures of 43° both with and without substrates. However, if the respiration rate was measured at 38°C after 3.5 hours at 43°C, there was a significant depression.

A Novikoff hepatoma of the rat exhibited no effect of hyperthermia on respiration during incubation at 42°C, but exhibited a significant depression after a 90 minute exposure at 43°. If the cells were heated anaerobically there was no effect on anaerobic glycolysis either during or after exposure at 43°C. However, if the exposure at 43°C was under aerobic conditions, a 25% reduction in anaerobic glycolysis was observed.

It was observed for the Novikoff hepatoma that, if the cells were heated at 38°C and 43°C and then disrupted and homogenized, a differential effect on oxygen uptake still existed. In contrast, if the cells were disrupted and homogenized before exposure to either 38° or 43°C, oxygen uptake was observed, but there was no differential for the two temperatures.

I 1.2 The Effects of Hyperthermia on Nucleic Acid and Protein Synthesis

Synthetic activity is of obvious importance to the reproductive integrity of the cell. Protein synthesis occurs to replace proteins that are continuously denatured at environmental temperatures. Some of these proteins, as enzymes, catalyse the biochemical reactions in the cell. The acid hydrolases catalyse the replication of DNA required for division and the formation of the various RNAs required for protein synthesis in the first place. This synthetic system is then a feedback system in which effects in one stage of the feedback loop necessarily affect the other stages.

Dickson and Shah (1972), investigating a malignant cell line, derived from a chemically induced rat breast carcinoma, observed significant reductions in the incorporation of labelled precursors of RNA, DNA, and protein, after exposure to elevated temperatures. The effect of hyperthermia was most severe on cells that were actively traversing the cell cycle. Six hours at 42° resulted in an inhibition of DNA, RNA and protein synthesis. Three hours at 42°, however, resulted in an inhibition of RNA synthesis only. Despite DNA and protein levels being unaffected there was no cell division until RNA synthesis had returned to near control levels.

Palzer and Heidelberger (1973 a) using HeLa cells determined that, during a 2 hour exposure at 42°C, the incorporation of DNA, RNA and protein precursors was inhibited. In contrast to Dickson's

(1972) observations, they observed that DNA synthesis was the most affected, protein the least, and RNA was intermediate.

Levine and Robbins (1970) measured precursor uptakes during heating at 42° in 2 heteroploid lines; HeLa and KB, and 5 human diploid lines. For HeLa cells after two hours, only the DNA precursor uptake was low, RNA and protein precursors being above the control level. After six hours, RNA synthesis had only marginally decreased. After 24 hours at 42° , all three synthesis rates were about 10% of control levels.

The precursor uptakes of the contact-inhibited human diploid lines were markedly different. After 48 hours at 42° , one of the lines exhibited a marginal depression of DNA and protein synthesis. After five days at 42° , all three precursor uptake rates were at about 25% of control levels. After nine days at 42° , DNA synthesis was at control levels, RNA synthesis exceeded control levels, and only protein synthesis remained low at 22% of the control value.

If the human diploid lines were heated while still actively dividing, they exhibited a response "between that given for HeLa and contact-inhibited diploids."

Mondovi et. al. (1969) investigated nucleic acid and protein synthesis during and after hyperthermic exposure of normal and neoplastic tissue of the rat and a human osteosarcoma. A depression of precursor

uptake was observed, both during and after hyperthermic exposure in the Novikoff hepatoma. Measurements made on the minimal deviation 5123 hepatoma and a human osteosarcoma after hyperthermic exposure demonstrated similar depression of synthetic activity. Regenerating liver cells exposed at 43° for two hours, in contrast, showed increased thymidine and amino acid uptake and less than a 10% depression of uridine uptake.

A cell free homogenate exhibited unchanged uptake of thymidine after exposure at 43° for two hours, in contrast to the intact cells.

The effects of a number of inhibitory and stimulatory drugs on hyperthermic response add additional insight. Giovanella and Heidelberger (1968) observed that FUDR, a DNA inhibitor, increased Ll210 cells' resistance to hyperthermia. L-erythro- $\alpha\beta$ -dihydroxybutyraldehyde doubled DNA synthesis at 42° and sensitized regenerating liver cells to 42° exposures.

BUDR, an analogue of thymidine, is synthesized in DNA molecules. The incorporation of BUDR sensitizes cells to radiation, but Schindler et.al. (1966) reported that BUDR did not sensitize cells to hyperthermia.

Palzer and Heidelberger (1973 a,b) observed that some chemicals, that inhibited DNA and protein synthesis, protected HeLa cells from hyperthermia at 42°C. All chemicals tested that inhibited RNA synthesis, sensitized the cells to 42°C.

McCormick and Penman (1969) observed a rapid disaggregation of polyribosomes in HeLa cells incubated at 42°C. The breakdown of the polyribosomes, observed

by ultracentrifugation of cytoplasmic extracts in sucrose gradients, was associated with a decrease in protein synthesis, as measured by electrophoretic separation of labelled proteins. After about 60 minutes at 42°, polyribosomes were observed to reform and the rate of protein synthesis returned to the control rate. If the cells were cooled to 37° after 10 minutes (maximum disaggregation) at 42°, polyribosomes were observed to reappear independently of RNA synthesis, determined by adding Actinomycin D, an inhibitor of RNA polymerase, after the hyperthermia insult. However, if Actinomycin D was added while the cells were at 42°, the reformation of polyribosomes and subsequent restoration of protein synthesis was not observed.

Warocquier and Scherrer (1969), also investigating HeLa cells exposed to temperatures of 42°C, observed that a particularly stable form of RNA, thought to be ribosomal RNA, is not formed, although labelled uridine is incorporated at a near normal rate. Using sucrose gradient techniques, they observed that labelled 45S rRNA precursor was not being converted to functional 28S and 18S forms at the elevated temperature, whereas non-ribosomal RNA appeared in the cytoplasm at the normal rate.

Heine et.al (1971) investigated changes in the RNA components of HeLa cells after hyperthermic exposure. At 41°C there was little effect on either the cytology or in the distribution of RNA components.

At 42° - 43°C, electron microscopy revealed a partial loss of the granular component of the nucleolus and that the polyribosomes had disaggregated. Formation of 45S precursor rRNA was only partially inhibited at 43°C, but the conversion to the active forms was inhibited, whether or not the 45S form was synthesised at 43° or 37°. After 24 hours, the cells had regained their original cytological characteristics.

Simard and Bernhard (1967), investigating nucleolar lesions due to hyperthermic exposure of BHK cells, observed a loss of granular component which they identified as ribonucleoprotein. They observed a loss of intranucleolar chromatin and a disappearance of the nucleolar reticulum. High resolution auto-radiography revealed that labelled uridine, incorporated after 60 minutes at 43°, was only marginally incorporated into the nucleolus, whereas the nuclear incorporation was only down by 20%. Uridine being present 30 minutes before heating resulted in normal nucleolar labelling at both 37° or 43°. The authors hypothesized that hyperthermia inhibited the nucleolar synthesis of rRNA precursor and that this synthesis was DNA dependent.

Simard (1969) and Almaric (1969), together with Zalta, observed similar results in ascites tumour cells of the rat. They attributed the disappearance of the granular ribonucleoprotein and the resulting inhibition of the 45S - 30S transition occurring at 45°, to a thermodynamic equilibrium between the fibrillar and granular forms.

Love, Soriano, and Walsh (1970) observed similar cytological changes in HeLa cells, BHK 21 cells, and three lines of human diploid cells after exposure to 46°C for 15 to 60 minutes. They noted the disappearance of nucleolar DNA. The granular component of the nucleolus disappeared while the fibrillar component became diffusely distributed. Again, polyribosome disaggregation was observed. They observed cytoplasmic inclusions in cells that contained nucleoli and hypothesized that these were derived from the nucleoli due to the similar appearance of the inclusions and the nucleoli.

Similar observations have been made on several species of protozoa. Schiebel et.al (1969) observed a disaggregation of polyribosomes and an associated decrease in protein synthesis for exposure of *Physarum polycephalum* to a temperature of 40°C for 10 or 30 minutes. The normal incubation temperature was 27°C.

Levy et.al (1969) observing the effect of a temperature of 34°C on *Tetrahymena pyriformis*, observed the disappearance of the rough endoplasmic^m reticulum and an associated inhibition of protein synthesis. Again *Tetrahymena* reproduces at 27°C.

Byfield and Scherbaum (1966 a, b; 1967a,b), investigating hyperthermic treatments of *Tetrahymena pyriformis*, observed a temperature dependent decay of acid insoluble RNA within the cell. At 34°C, as opposed to a growth temperature of 29°C, RNA synthesis was not greatly inhibited. If Actinomycin D was

was administered, stopping RNA synthesis, RNA levels in cells at 29°C remained constant, but at 34° a decay of RNA was observed. Bernstein and Zeuthen (1966) observed an inhibition of RNA synthesis at 34° for Tetrahymena.

The observations on the protozoa are not inconsistent with and in some instances, are identical with the observations made on mammalian cells, despite the hyperthermic temperature being 10°C lower for the protozoan observations. This fact coupled with the two observations by Mondovi et.al (1969) and Cavaliere et.al. (1967), that DNA synthesis and oxygen uptake of cell free homogenates of Novikoff hepatoma are unaffected by hyperthermia, suggests that rather than being the result of a pure thermodynamic effect on a physico-chemical equilibrium the observed effects, as suggested by Mondovi, are the result of disruption of cellular organization.

I 1.3 The Effects of Hyperthermia on Membranes and Lysosomes

Cellular membranes are thought to be composed of lipids and possibly proteins. In the older literature a theory of "lipoid liberation" was put forward as a mechanism for heat injury. This theory proposed that heat injury comes about as a result of melting the lipid components of the membrane. Lipids do in fact show crystalline to liquid-crystalline to liquid transitions at temperatures related to the degree of unsaturation in hydrocarbon chains, but the temperature at which these occur varies by more than 70°C for different types of lipids. It is further thought that membranes may actually require liquid lipids (Chapman 1967).

The effect of hyperthermia on lysosomes has been included in this section on the supposition that lysosomal action is regulated by the permeability and integrity of the lysosomal membrane.

Turano et.al. (1970) investigated the thermal lability of lysosomes isolated from normal and neoplastic tissues of rats. While the isolated lysosomes were labile at 38°C, incubation at 43°C increased the rate of release of RNAase, cathepsins, acid phosphatase, and DNAase. The lysosomes from Novikoff hepatoma cells were more sensitive than either normal or regenerating liver cells, both at 38° and 43°C. Damaging the lysosomes by photolysis, while depressing the respiration of intact Novikoff hepatoma cells, did not prevent a further inhibition of respiration by hyperthermic exposure.

Similarly inhibition of the lysosome action by trypan blue did not prevent respiratory inhibition by hyperthermia.

Overgaard and Overgaard (1972b) measured the amounts of acid phosphatase and cathepsin D in a homogenate from a mouse mammary tumour. An immediate increase of the acid hydrolases after 30 minutes at 42.5°C, was observed, in contrast to slightly reduced levels after a radiation dose of 800 rads.

Levine and Robbins (1970) observed no cytological change in the appearance of the lysosomes in HeLa cells after 42° exposures. Contact-inhibited human diploid lines took up choline and linoleic acid, presumably for lipid synthesis, at a higher rate at 43° than at 37°C. Burger and Fuhrman (1964b) found very little acid phosphatase accumulation in normal rat tissue at temperatures from 38° to 42°C, but observed potassium leakage at these temperatures. Dickson and Shah (1972) observed cellular leakage of lactate dehydrogenase in SDB cells after 3 hours at 42°C. Hahn, Braun, and Har-Kedar (1975) observed that at 43°C the drugs, Adriamycin and Bleomycin penetrated the cellular membrane of HAL cells more readily.

Levy, Gollon, and Elliott (1969) observed that after *Tetrahymena pyriformis* were exposed at 34°C 7° above the optimum growth point, there was no gross evidence of an effect on lysosomal enzymes, in that 80% of acid phosphatase and proteinase remained bound. Byfield and Scherbaum (1967b) observed that, in contrast to the decreased protein synthesis at 34°C of *Tetrahymena*, labelled glycerol incorporation into lipids was enhanced. Rosenbaum,

Beach, and Holz (1966) found that in a strain of *Tetrahymena*, adapted for full growth at 37°, the addition of phospholipid or neutral lipids, but not phospholipid precursors, to the medium enabled the organisms to divide at 40°C.

Dye exclusion tests for cell viability reflect the competence of certain cellular membranes. Harris (1966) demonstrated that staining with either trypan blue or erythrosin B, after hyperthermia, indicated higher viability than was obtained by a direct assay of colony formation. Similar observations have been made with Ll2l0 cells in an in vitro - in vivo assay with VX-2 tumour in vivo, and SDB cells in vitro (Giovanella, Lohman, and Heidelberger 1970; Muckle and Dickson 1971; Dickson and Shah 1972).

I 1.4 The Effects of Hyperthermia on the Mitotic Cycle and Mitosis

An agent that brings about a decrease in reproductive integrity must necessarily have a gross effect on the mitotic cycle and mitosis. Hyperthermia has been demonstrated to have very marked effects even for sublethal doses. The effects of mitotic activity and the cell cycle position on cellular sensitivity have been noted above. Effects on the duration of the mitotic cycle, the duplication fidelity, the induced delay before mitosis have also been reported.

Rao and Engelberg (1965), observing HeLa cells, and Siskin (1965) observing human amnion cells in vitro, noted an increase in the duration of the complete mitotic cycle for temperatures above or below the normal growth temperature of 37°C . In both cases, the duration of mitosis was most critically affected. Siskin further observed, of the various stages of mitosis, that metaphase was the most sensitive, prophase was intermediate, and the duration of anaphase was virtually independent of the temperature from 34° to 40°C .

Ostertag (1964) exposed human epidermis cells in culture to a temperature of 56°C for 1 hour. The 95% diploid line, after one month, was observed to be over 50% tetraploid and 20% octoploid. After six months the cell line had returned to its original ploidy, presumably due to a decreased division probability of the polyploid cells.

Kase and Hahn (1975) subjected normal and virus-transformed embryonic lung fibroblasts to a temperature of 43°C. They observed that, 24 hours after a four hour exposure at the elevated temperature, a large proportion of the normal cells contained approximately double the DNA content of unheated normal cells. The transformed cells had a high incidence of tetraploidy before heating, but 46 hours after a one and a half hour exposure, the tetraploid population increased with a corresponding decrease in diploid numbers. Westra and Dewey (1971) found that six minutes at 45.5°C induced 90% tetraploidy in CHO cells.

Westra and Dewey also observed that there was delay of about one mitotic period before cell division commenced. Similar observations have been made (Dickson and Shah 1972; Palzer and Heidelberger 1973; Leeper and Henle 1974; Kal, Hatfield, and Hahn 1975). Wang (1974) observed that temperature sensitive mutant CH cells were blocked in metaphase at 39°C. The mitotic figures, being similar in appearance to those observed after a Colchicine block, suggested that hyperthermia may be affecting the mitotic spindle.

Several investigations of the application of repeated hyperthermia exposures as an inducer of synchronous division have been reported (Martin and Schloerb 1964; Bernstein and Zeuthen 1966; Sapozink, Deschner, and Hahn 1973; Dietzel 1974).

Evidence from these and the preceding reports suggests that there is a gross effect of hyperthermia on important cellular mechanisms, and that normal tissues are less sensitive than neoplastic tissues. It has not been demonstrated that these are primary, as opposed to abscopal, effects of hyperthermia.

I 2 The Effects of Hyperthermia on Chromosomes and the Repair of DNA Damage

Chromosome aberrations, microscopically visible defects in condensed chromatin, have been well correlated with lethality in at least one x-radiation system (Dewey, Furman, and Miller 1970; Dewey, Miller, and Leeper 1971). That is, a radiation dose that reduced the survival to e^{-1} produced on average one chromosome aberration per cell irrespective of cell phase or sensitization with Colcemid or BUdR. The same authors (Dewey, Westra, Miller and Nagasawa 1971), in contrast, observed that chromosome aberrations were well correlated only during S phase after heat treatment at 45.5°C . Both during M and G_1 phase the number of chromosome aberrations was too low to account for the lethality observed. This, however, does not rule out damage to the DNA as the principle target of inactivation since there may be more subtle damage involved that has not, as yet, been demonstrated.

Ben-Hur and Elkind (1974b) investigated the effect of hyperthermia on the repair of DNA damage due to radiation. Using a technique of ultracentrifugation of lysed DNA in a sucrose density gradient, they were able to separate different molecular weight fractions of the DNA present in irradiated cells. Small radiation doses (17Gy) are sufficient to break-down a fraction with a molecular weight of approximately ten times that of single stranded DNA. The authors refer to this fraction as the DNA complex. Larger doses cause breaks in the single strands resulting in even smaller fractions to be separated.

Interestingly enough, incubation at 42°C after radiation (58Gy) resulted in faster repair of single strand breaks compared to repair at 37°C .

The V79 cells were capable of rejoining approximately 90% of the single strand breaks. At 42° this was complete in 40 minutes, however further incubation at this temperature to 5 hours resulted in the reappearance of a small molecular weight fraction indicating further degradation of the DNA.

After small radiation doses (17Gy), repair of the complex at 37° was complete in 45 minutes as evidenced by the disappearance of the single strand peak and reappearance of the complex peak at the bottom of the gradient. At 42°C, after 90 minutes, the single strand DNA peak had disappeared, but reformation of the complex was judged to be atypical, due to the non-reappearance of a single complex peak.

A comparable dose at a low dose rate, (.12Gy/min) resulted in little effect on the complex at 37°, but a complete disappearance of the complex at 42°. This illustrated that at low dose rates repair of the complex was occurring and hyperthermic exposure suppressed this repair. This further supported their contention that the effect of hyperthermia on radiation sensitivity is due in part to a suppression of repair of sublethal damage. (Ben-Hur, Bronk, Elkind 1972).

Similar investigations of the interaction of hyperthermia and methyl methanesulfonate, MMS, a radiomimetic alkylating agent, have been reported (Ben-Hur and Elkind 1974a ; Bronk, Wilkins and Regan 1975). The authors did not investigate the drug intracellular concentration (Hahn et.al. 1975) or the activation enthalpy for the drug reactions (Johnson and Pavelec 1973) so that the mechanism

of synergistic action is disputable. The authors however suggest that the interaction arises, in part, due to a suppression of SLD repair and corroborate this with effects on the repair of single strand breaks and of the complex at elevated temperatures, which are similar to those previously examined. They did observe, however, that the extent of repair of DNA was not well correlated with cell survival.

II Materials and Methods

II 1 Cell Media and Reagents

The media below were made exclusively from Gibco-Biocult products. Each item is listed with the Gibco reference number (1976/1977 catalogue).

Hams F10

500 ml Hams F10 W L-Glutamine	(155)
88 ml Newborn Calf Serum	(601)
1.5 ml Phenol red	(502)

Hams F12

40 ml Hams F12 10 x	(Special)
10 ml 1M Hepes-Buffer	(Special)
5.6 ml NaHCO ₃ 7.5%	(508)
5 ml L-Glutamine	(503)
5 ml Non-essential Amino Acids	(114)
80 ml Newborn Calf Serum	(601)
360 ml Distilled Deionized Water	

The special formulation of Hams F12 reproduces the 10x medium originally supplied by Bio-cult, but no longer produced by the amalgamated firm Gibco-Biocult. The special Hepes-buffer (pH-8) compensates for the decreased pH of the F12 medium. This combination was found to give better pH stability than the standard Gibco-Biocult 1x Hams F12 (176) and Hepes-buffer (563)

Miscellaneous Reagents

Trypsin - EDTA 10x	(540 G.B.)
Earles Balanced Salt Solution (Ca and Mg free)	(416 G.B.)
Phosphate Buffered Saline 10x	(406 G.B.)
Gentamycin	(Biocult)
Colchicine	(27805 BDH Chemicals Ltd.)
Me- ³ H thymidine	(TRA 120 Radiochemical Centre, Amersham)

II 2 Trypsinization Procedure

The flasks containing the attached cells were rinsed once and then incubated at 37° in five ml of Trypsin - EDTA solution. Three minutes were sufficient to release the cells from the plastic. The trypsin was inactivated by the addition of 5 ml of growth medium. The resultant suspension was repeatedly pipetted until a monodispersed cell suspension was obtained.

II 3 Chromosome Preparations

Mitotic cells were collected at metaphase after a 2 hour incubation with Colchicine (1 μ g/ml). These cells were harvested by gentle shaking, and washed once with PBS. The nuclear membrane was burst by a hypotonic treatment in 0.7% sodium citrate for 13 minutes. The cells were fixed twice with cold Carnoy's fixative, spread on chilled, wet microscope slides, dried over a flame and stained with Aceto-Orcein stain for 5 minutes.

The mitotic index was determined by treating the cells as above, except that Colchicine was ^{not} used. The cells were stored at 4°C for approximately 25 minutes after harvesting and before hypotonic shock.

II 4 Labelling Index

For autoradiography 10^4 cells per flask were plated and pulse labelled with (^3H) TdR for 15 minutes at the concentration of 5 μ Ci/ml. After labelling, the cells were washed with PBS and fixed twice with Carnoy's fixative for 15 minutes. The bottoms of the T30 flasks were cut off and coated with Kodak NTB-3 nuclear emulsion. Plates were exposed for five days at room temperature in a light-tight, dessicated container. The plates were developed and then stained in 10% carbol fuchsin for 5 minutes. Labelling index determinations were made by counting at least 400 cells per point.

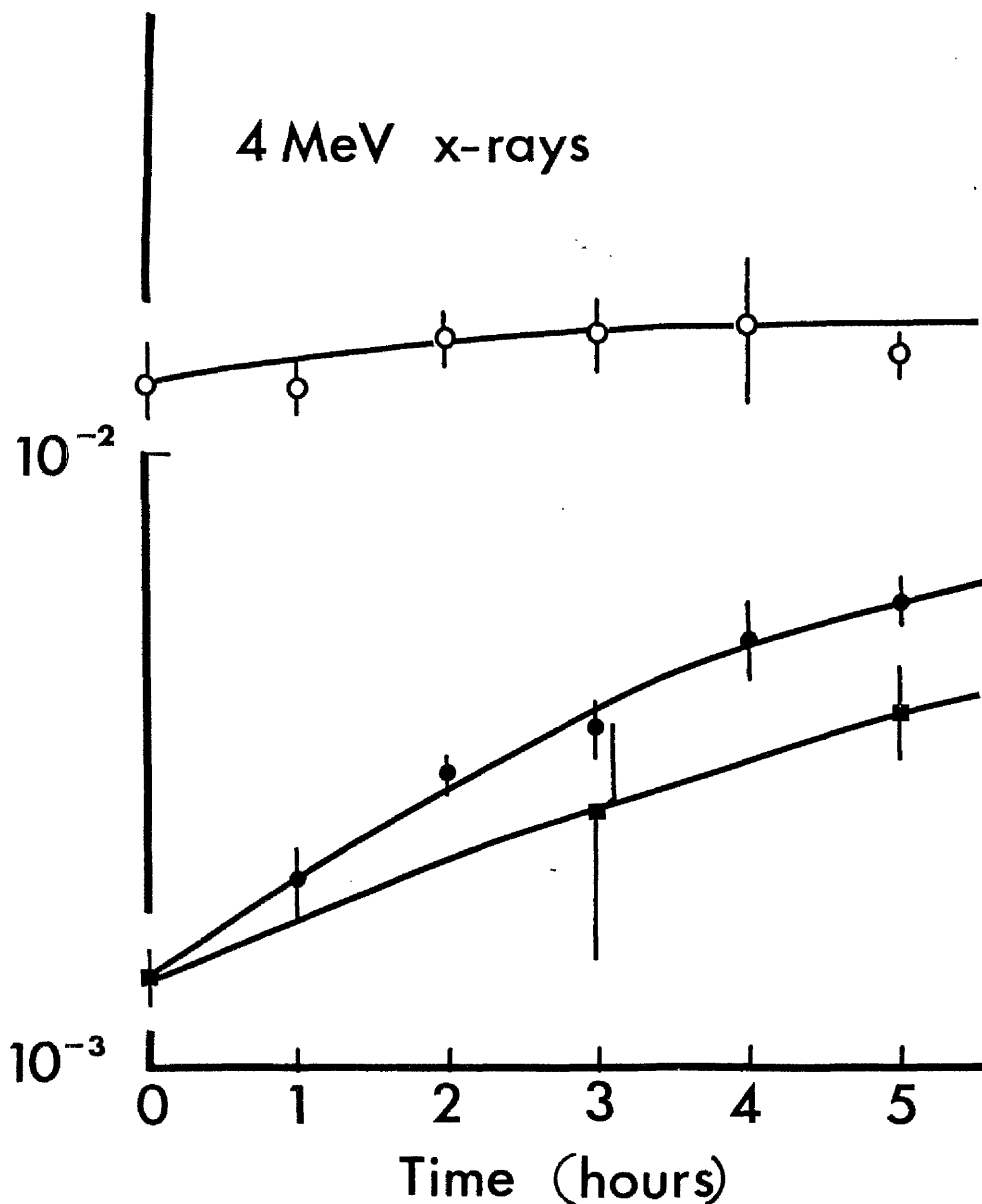


Figure III.1. The effect of hyperthermia on Elkind repair.
 Unheated cells 6.00Gy - t - 3.00Gy
 ● 60 min 42°C H - 30min - 4.75Gy - t - 2.75Gy
 ■ 60 min 42°C H - 30min - t - 7.50Gy
 The cells were maintained at room temperature, after hyperthermia, until five minutes after the second radiation dose. Data points represent the mean and standard error of three observations.

III Miscellaneous Observations

III 1 The Effect of Hyperthermia on Elkind Repair

The data in figure 3.5 suggest, due to the enhanced extrapolation numbers observed for cells heated to 46° before irradiation, that hyperthermia might actually enhance the apparent ability to repair sublethal damage. To test this hypothesis, the following experiment was performed.

CHO cells in Hams F12 were plated into T30 flasks, and incubated at 37°C for two hours. Half of the flasks were immersed in a 42°C waterbath for 60 minutes. Thirty minutes after the hyperthermia exposure was terminated, all of the heated flasks, except for the hyperthermia controls, were irradiated simultaneously with 4 MeV x-rays, at a dose rate of 0.95 Gy/min, to a total dose of 4.75 Gy. These flasks then received a further 2.75 Gy immediately, or at 1 hour intervals, during which time they were maintained at room temperature. Concurrently, unheated flasks were given split doses of 6 + 3 Gy, again being maintained at room temperature between doses. The plates were incubated at 37°C five minutes after the second radiation exposure terminated. The results are illustrated in figure III.1. The first experiment did not include the heated single dose points at three and five hour separations. These were included in the second and third experiment when the large recovery factor for the heated cells was noted. The recovery factors, corrected for the increase in heated-single dose survivals, are 1.3 and 1.6 respectively. This difference is not significant.

The results of this type of experiment are difficult to analyse, as mentioned in the introduction, in as much as the first radiation dose may be inhibiting the repair of hyperthermia ISD thereby reducing the apparent repair capability.

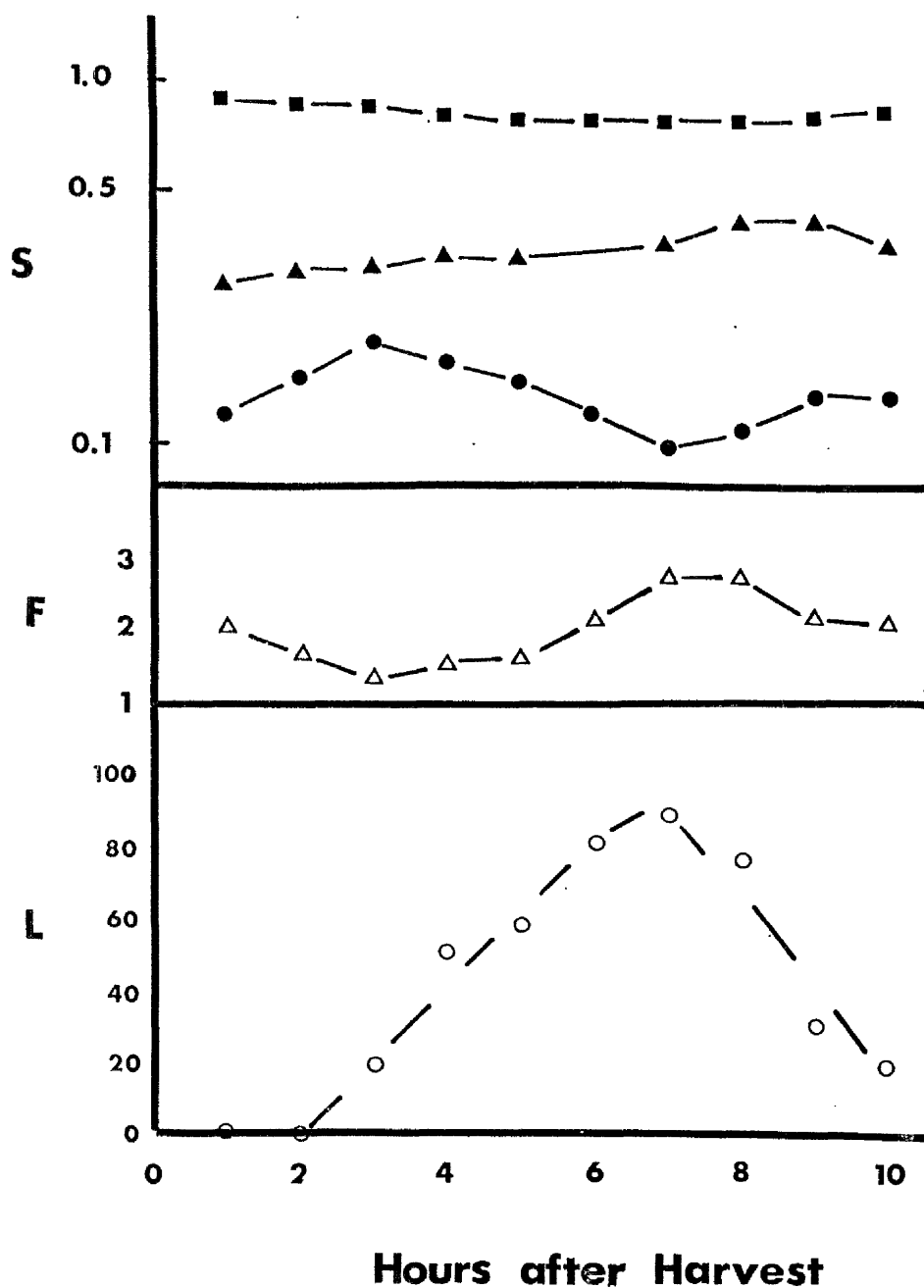


Figure III.2. Radiation and hyperthermia interaction as a function of cell age. Cell survival, S, for 60 minutes at 42°C, ■, for 4.5Gy γ radiation, ▲, and for 4.5 Gy γ followed five minutes later by 60 minutes at 42°C, ●. The sensitization factor, F, is the ratio of the product ■ and ▲ to ●. The labelling index, L, is the percent of TdR labelled cells at a given time after harvesting mitotic cells. Data points represent a single experiment. All irradiations were carried out at room temperature.

III. 2 The Effect of Cell Age on Interaction

Mammalian cells exhibit a complementary dependency on cell age in their response to radiation and hyperthermia (Westra and Dewey 1972). This complementary response, in which a cell of a particular age is sensitive to one agent, but not the other, may result in an apparent sensitization by population selection despite the absence of a genuine interaction.

Mitotic CHO cells were harvested from an exponentially growing culture by gentle shaking and plated into T30 flasks, at a concentration of 1000 cells/flask. The mitotic index at harvest was found to be 88%.

At hourly intervals, replicate flasks were either given a radiation (^{60}Co , .96 Gy/min) dose of 4.5 Gy, at room temperature, a heat exposure of 60 minutes at 42°C , or a radiation dose of 4.5 Gy followed five minutes later by a heat exposure of 60 minutes at 42°C .

The result of a single experiment is illustrated in figure III.2. It is observed that the interaction is cell age dependent, but occurs to some degree for all cell ages. The interaction is observed to be greatest at S phase, determined by the labelling index. The results are in partial agreement with those observed by Gerweck et.al. (1975) and Ben-Hur et.al. (1974) who observed that S phase CHO cells and V79 cells were sensitized to the greatest extent, but, however, remained the least sensitive age group. The synchronization procedures used by these authors might explain the discrepancy. Ben-Hur used hydroxyurea, and Gerweck used the shaking method coupled with storage at 4°C , to obtain the higher cell yields required for their experiments.

While it has been determined and affirmed that there is an interaction independent of cell age effects, one cannot rule out a cross sensitivity effect. Therefore in order to appreciate the magnitude of this cross sensitivity effect a numerical model of a hypothetical interaction system was analysed.

As a simple model, cells were assumed to be distributed uniformly about the cell cycle and that the cell survival parameters were smooth sinusoids.

Survival for cells of age, θ , after a dose, D_1 , from the first agent is described by

$$S_1(D_1, \theta) = 1 - (1 - e^{-D_1 / (1 + a \cdot \sin(\theta))^{2 + b \cdot \sin(\theta)}}) \quad \text{III.1}$$

Survival for cells of age, θ , after a dose, D_2 , from the second agent is described by

$$S(D_2, \theta, \Phi) = 1 - (1 - e^{-D_2 / (1 + a \cdot \sin(\theta + \Phi))^{2 + b \cdot \sin(\theta + \Phi)}}) \quad \text{III.2}$$

Survival in the asynchronous population to a dose D_1 and D_2 is then described by

$$S(D_1, D_2, 0) = 1/2 \oint S_1(D_1, \theta) \cdot S_2(D_2, \theta, \Phi) \cdot d\theta \quad \text{III.3}$$

The parameter θ is the cell age parameter, while Φ is the phase angle between the sensitivity patterns for the two agents. Thus when Φ is zero, the sensitivity patterns are identical and when Φ is 180° the sensitivity patterns are exactly opposite

(i.e. cells that are most sensitive to D_1 are the most resistant to D_2). Observe that the mean D_0 for both agents is 1 and the mean extrapolation number is 2.

Equation III.2 was numerically integrated on a digital computer to yield survival data for values of D_1 of 1, 2, 3, 4, and 5 units. (1 unit = D_0). The gradient of the logarithm of survival, $d\ln S/dD_1$ was determined by a linear least squares fit to the calculated survival data. This was repeated for values of D_2 from 0 to 5 units yielding the following sensitization curves.

The result of this computation for the situation in which only the value of D_0 changes with cell age is illustrated in figure III.3. The amplitude of the variation is 0.3 (i.e. D_0 changes from 0.7 to 1.3) for both agents. It is observed that when the phase angle between the sensitivity functions is zero (i.e. identical cell age sensitivity pattern) the effect of increasing D_2 is to apparently protect against the killing effects of D_1 as indicated by the decrease in $d\ln S/dD_1$. When Φ is 90° there is no interaction between the agents for any dose D_2 . When Φ is 180° the apparent interaction is synergistic. Figure III.4 illustrates the effect of a change only in extrapolation number with cell age. This is observed to be virtually without effect for other than a small sensitizing dose. Figure III.5 illustrates the effect of combined changes in sensitivity and extrapolation number. Figure III.6 illustrates the effect of varying the amplitude of

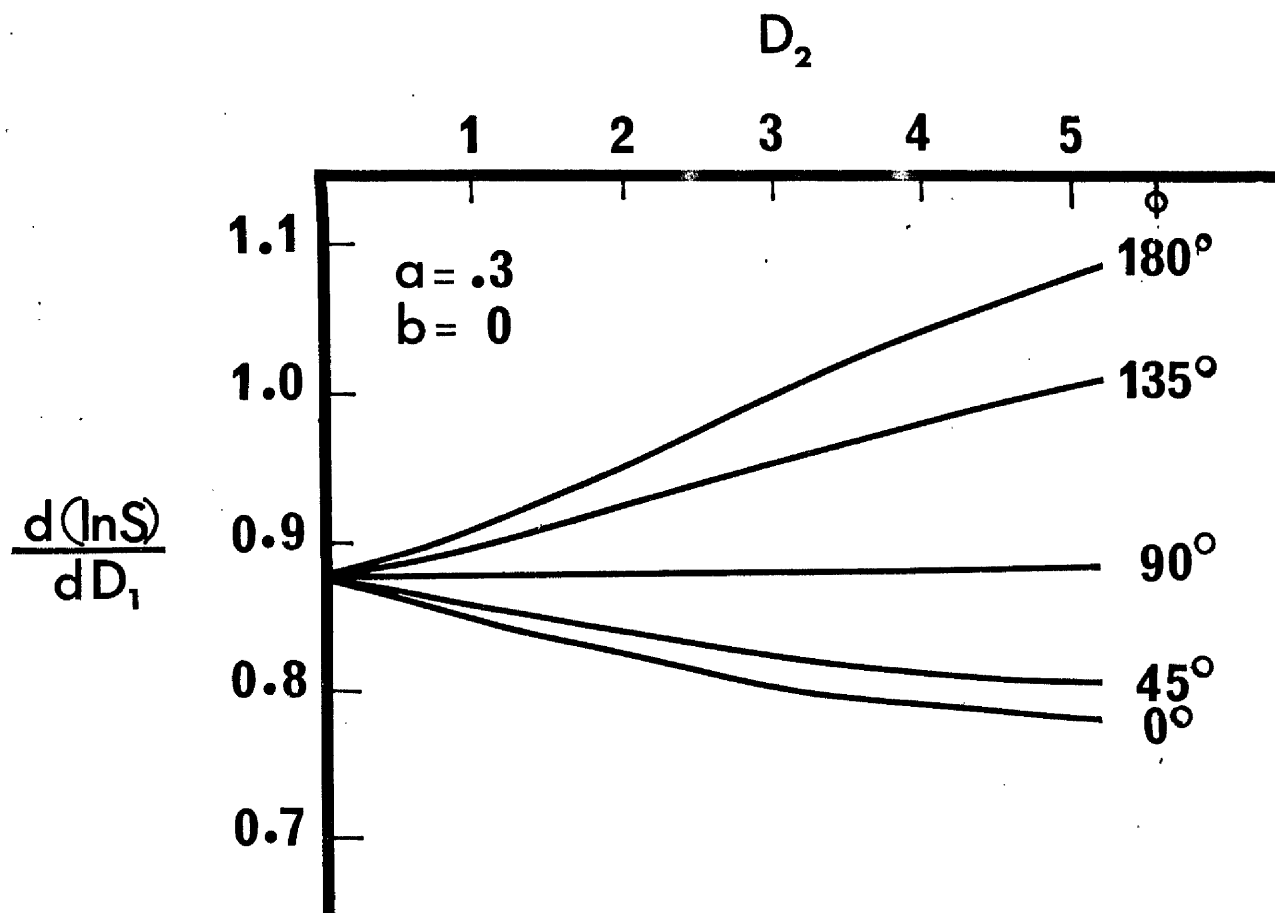


Figure III.3. Sensitization curves illustrating the effect of phase angle assuming a constant extrapolation number and varying sensitivity.

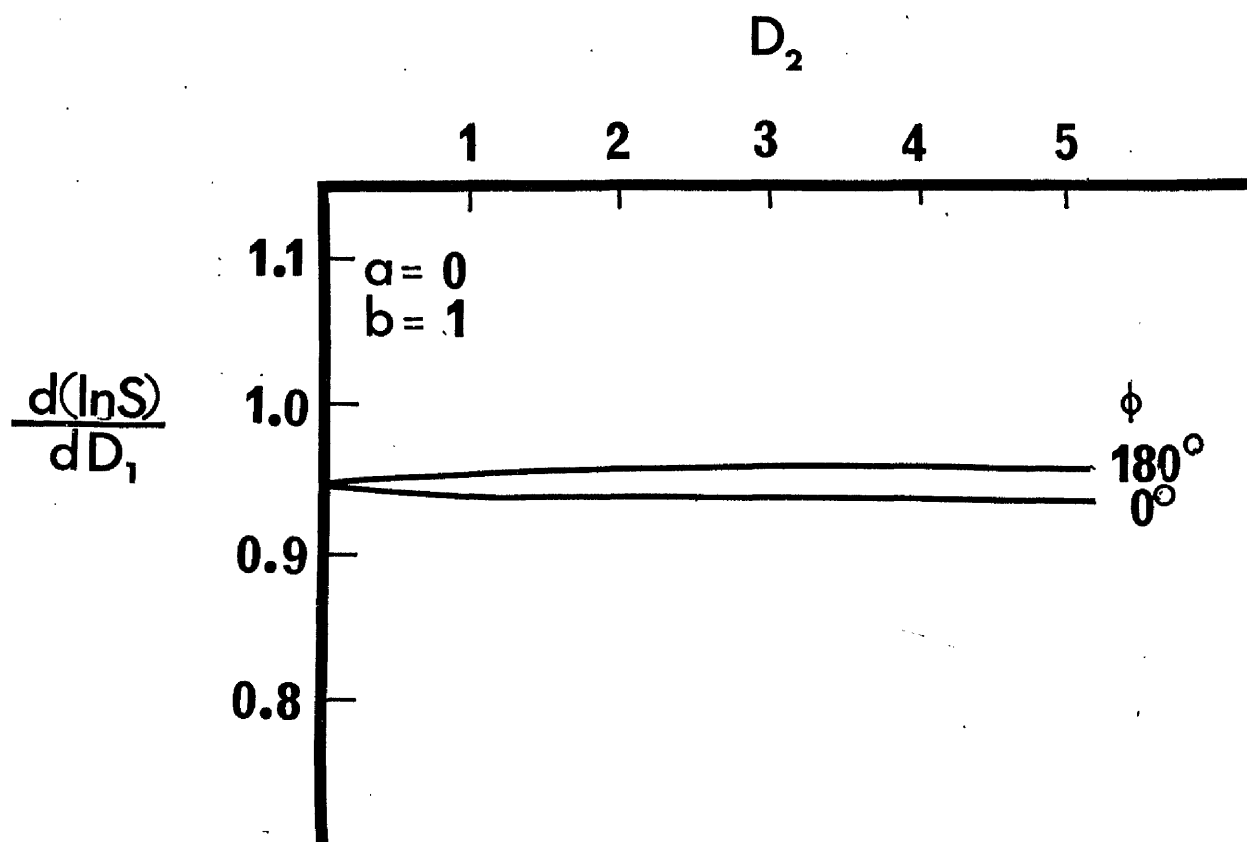


Figure III.4. Sensitization curves illustrating the effect of phase angle assuming a constant sensitivity and varying extrapolation number.

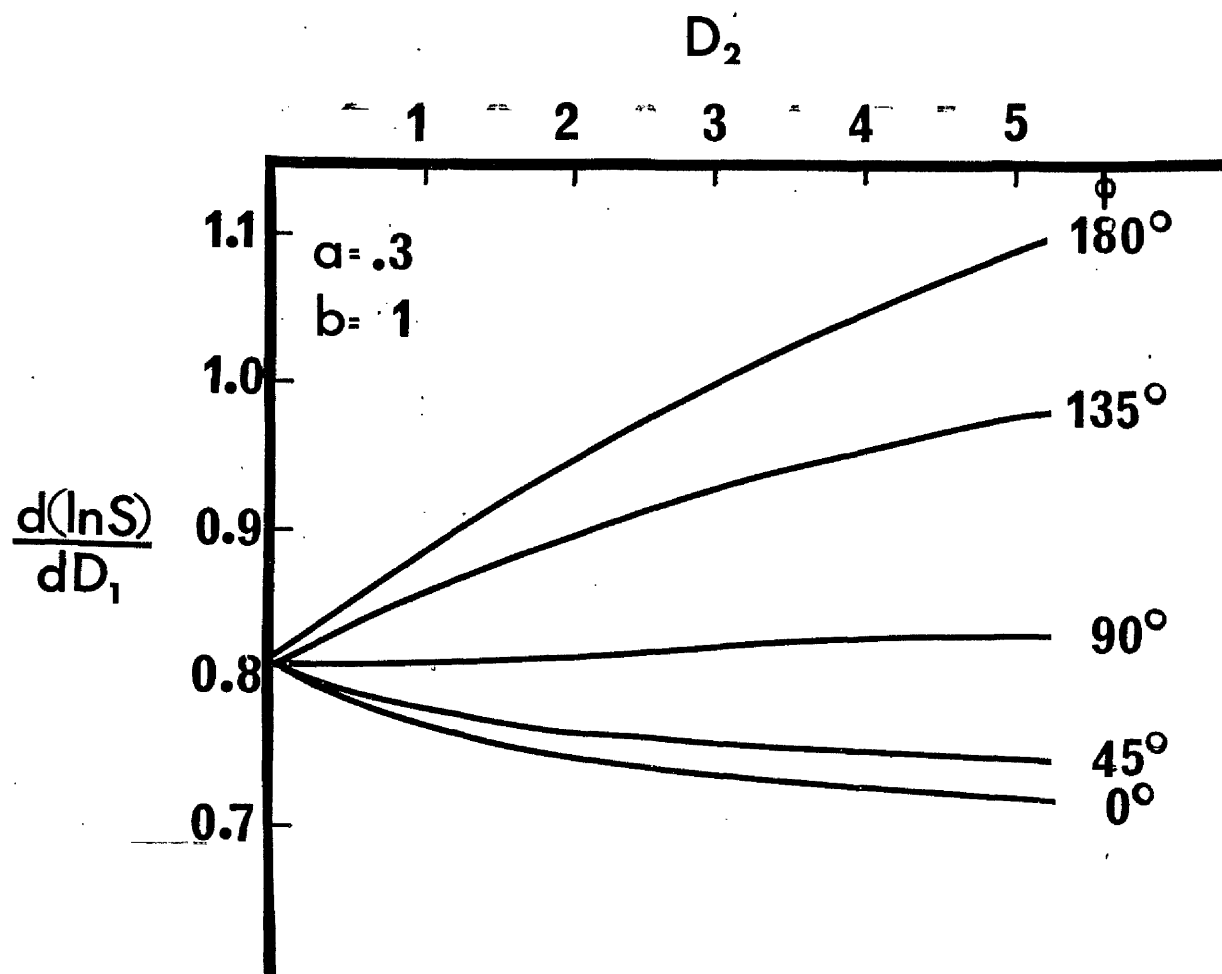


Figure III.5. Sensitization curves illustrating the effect of phase angle assuming both a varying sensitivity and a varying extrapolation number.

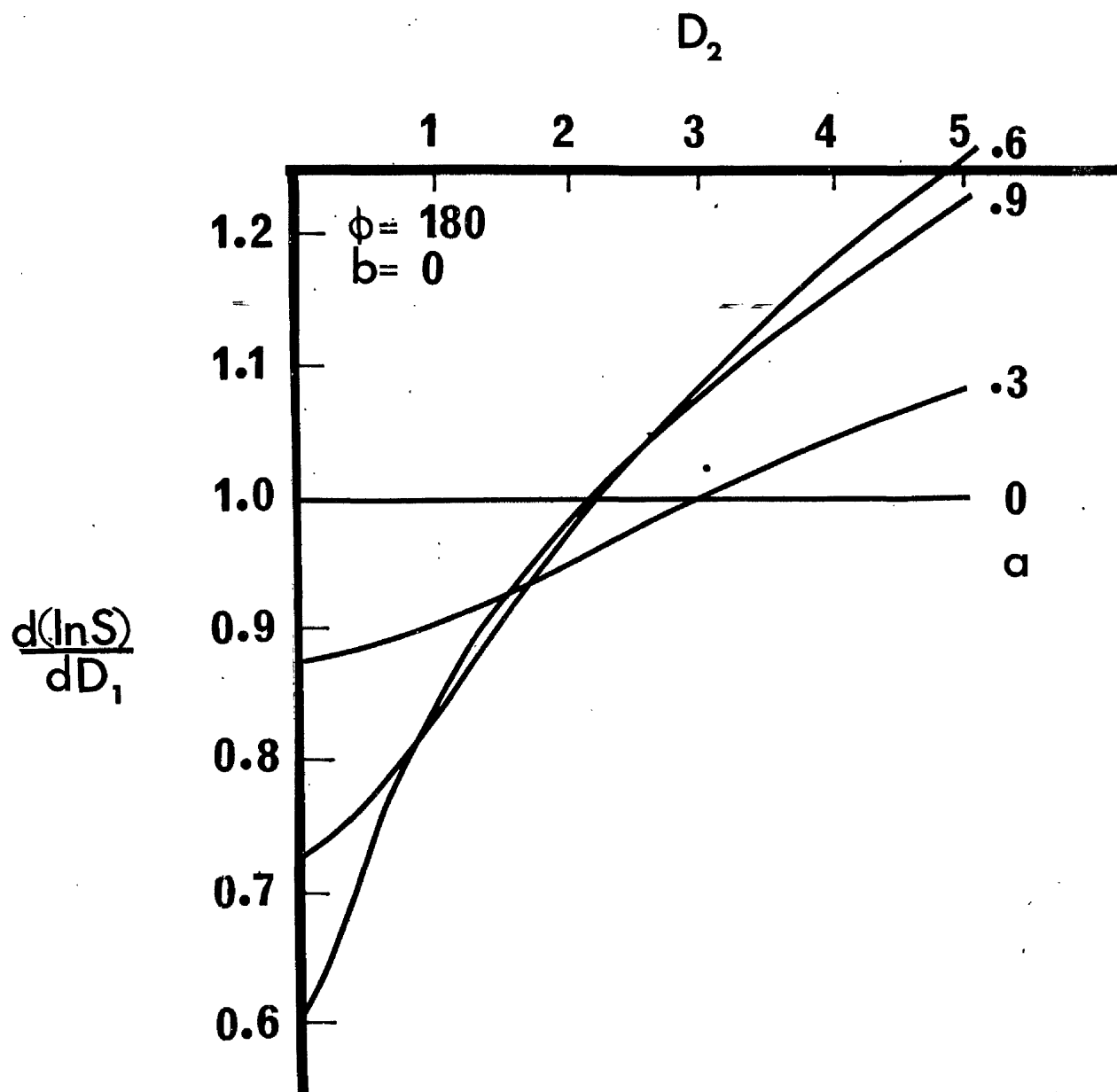


Figure III.6. Sensitization curves illustrating the effect of the amplitude of variation in sensitivity assuming the sensitivity spectrums are 180° out of phase.

variation insensitivity for sensitivity patterns 180° out of phase.

The experiments described in chapters four to six demonstrated that it was possible to double or triple the sensitivity due to radiation or hyperthermia with a hyperthermia or radiation dose corresponding to 3 or 3.5 D_0 's. An examination of figure III.5 reveals that this degree of sensitization would require an amplitude of .9 (i.e assuming a mean D_0 of 2 Gy the variation in D_0 would be from .2 to 3.8 Gy). This amplitude seems unrealistic and if we assume a more reasonable value of .3 which roughly corresponds to that observed by Terasima & Tolmach (1963) the cross sensitivity could account for no more than a 25% sensitization.

IV Simplex Program

The data obtained from the matrix experiments were stored in digital form on paper tape and magnetic disc. Various routines were used to manipulate and analyse these data. These have not been included as part of this thesis since these represent non-essential and unsophisticated programming that could be easily duplicated by anyone desiring to do so.

The nonlinear dose transformations required for equation 4.11 and the large number of parameters necessitated a very efficient iterative search technique. Such a technique was suggested by Nelder and Mead (1965) and implemented in BASIC by the author. This technique allowed the minimization of chi-square for 7 parameters and 70 data points in approximately one hour of computer time. A listing of a simplified version, that does not include the disc input-output routines, follows.

```

0001 REM PROGRAM SIMPLEXFIT GENERAL NONLINEAR ITERATIVE FIT
0002 REM BASIC IMPLEMENTATION OF MOVING SIMPLEX ITERATIVE SEARCH
0003 REM NELDER, J.A. & MEAD, R., (1965)
0004 REM A SIMPLEX METHOD FOR FUNCTION MINIMIZATION.
0005 REM THE COMPUTER JOURNAL, 7, 308-313.
0015 GOTO 1050
0020 LET N=2
0025 LET N3=25
0030 DIM A(N+1,N+1),B(N+1),C(N+1),E(N+1)
0040 MAT A=CON
0050 MAT A=(1E+10)*A
0060 FOR I=1 TO N
0070   PRINT I
0080   PRINT "STARTING VALUE PARAMETER " ; I
0085   INPUT B(I)
0090   LET E(I)=B(I)
0100 NEXT I
0110 GOSUB 0900
0120 GOSUB 0690
0130 FOR J1=1 TO N
0140   LET E(J1)=8*B(J1)/9
0150   GOSUB 0900
0160   GOSUB 0690
0170 NEXT J1
0200 FOR I=1 TO N
0210   LET C(I)=0
0220   FOR J=2 TO N+1
0230     LET C(I)=C(I)+A(I,J)
0240   NEXT J
0250   LET C(I)=C(I)/N
0260 NEXT I
0270 REM CALCULATE T=2C-W AND EVALUATE
0280 FOR I=1 TO N
0290   LET B(I)=2*C(I)-A(I,1)
0300   LET E(I)=B(I)
0310 NEXT I
0320 GOSUB 0900
0330 LET B(N+1)=E(N+1)
0340 IF B(N+1)<A(N+1,2) THEN GOTO 0500
0350 IF A(N+1,1)<B(N+1) THEN GOTO 0430
0360 FOR I=1 TO N
0370   LET E(I)=.5*(B(I)+C(I))
0380 NEXT I
0390 LET N3=N3-1
0400 GOSUB 0900
0410 GOSUB 0690
0420 GOTO 0860
0430 FOR I=1 TO N
0440   LET E(I)=.5*(A(I,1)+C(I))
0450 NEXT I
0460 LET N3=N3-1
0470 GOSUB 0900
0480 GOSUB 0690
0490 GOTO 0860
0500 IF B(N+1)<A(N+1,N+1) THEN GOTO 0520
0510 GOTO 0600
0520 FOR I=1 TO N
0530   LET E(I)=2*B(I)-C(I)
0540 NEXT I
0550 GOSUB 0900
0560 IF E(N+1)>A(N+1,2) THEN GOTO 0600

```



```

0570 LET N3=N3+1
0580 GOSUB 0690
0590 GOTO 0860
0600 FOR I=1 TO N+1
0610   LET E[I]=B[I]
0620 NEXT I
0630 GOSUB 0690
0640 GOTO 0860
0650 GOSUB 0900
0660 REM SORT PARAMETER MATRIX
0670 GOSUB 0690
0680 GOTO 0860
0690 FOR J=2 TO N+1
0700   IF E[N+1]<A[N+1,J] THEN GOTO 0750
0710   FOR I=1 TO N+1
0720     LET A[I,J-1]=E[I]
0730   NEXT I
0740   RETURN
0750   FOR I=1 TO N+1
0760     LET A[I,J-1]=A[I,J]
0770   NEXT I
0780   IF J<N+1 THEN GOTO 0830
0790   FOR I=1 TO N+1
0800     LET A[I,J]=E[I]
0810     PRINT E[I],
0820   NEXT I
0825   PRINT N3
0830 NEXT J
0840 RETURN
0850 PRINT N3
0860 IF N3>0 THEN GOTO 0200
0865 PRINT "SEARCH COMPLETE --- PARAMETER MATRIX"
0866 REM BEST FIT PARAMETERS IN COLUMN N+1
0870 MAT PRINT A
0875 PRINT "FOR LONGER SEARCH INCREASE VALUE OF N3 STATEMENT 25"
0880 CLOSE
0890 STOP
0900 LET E[N+1]=0
0901 REM E(1)=1ST PARAMETER
0902 REM E(2)=2ND PARAMETER
0903 REM E(N)=NTH PARAMETER
0904 REM E(N+1)=CHI SQUARE OR ANY OTHER VARIABLE TO BE MINIMISED
0905 REM D(I,1)=ITH DOSE
0906 REM Y(I,1)=ITH NUMBER OF CLONES COUNTED
0908 REM W(I,1)=ITH NUMBER OF CELLS PLATED
0909 REM E(1)=KR, E(2)=DQ
0910 FOR I=1 TO N1
0990   REM EXAMPLE OF SIMPLE SHOULDERED SURVIVAL CURVE
0995   REM CHANGE STATEMENT 20 TO REFLECT TOTAL NUMBER OF PARAMETERS
1000   LET D1=D[I,1]-E[2]
1002   IF D1<0 THEN LET D1=0
1004   LET S=W[I,1]*EXP(-D1*E[1])
1010   LET E[N+1]=E[N+1]+(Y[I,1]-S)*(Y[I,1]-S)/S
1030 NEXT I
1040 RETURN
1050 DIM Y[100,1],D[100,1],W[100,1]
1055 PRINT "INPUT DATA"
1060 INPUT " # OF POINTS",N2
1070 FOR I=1 TO N2
1080   INPUT "DOSE ? CELLS ? CLONES ?",D[I,1],W[I,1],Y[I,1]
1090 NEXT I

```

```

0900 LET E[N+1]=0
0905 REM ROUTINE FOR FIRST ORDER INTERACTION MODEL EQ.4.11
0910 FOR I=1 TO N1
0920 LET D1=D[I,1]-E[4]
0930 LET D2=D[I,1]-E[6]
0940 LET T1=T[I,1]-E[5]
0950 LET T2=T[I,1]-E[7]
0960 IF D1<0 THEN LET D1=0
0970 IF D2<0 THEN LET D2=0
0980 IF T1<0 THEN LET T1=0
0990 IF T2<0 THEN LET T2=0
1000 LET S=W[I,1]*EXP(-D1*E[1]-T1*E[2]-T2*D2*E[3])
1010 LET E[N+1]=E[N+1]+(Y[I,1]-S)*(Y[I,1]-S)/S
1030 NEXT I
1040 RETURN

```

REFERENCES

- Adams, W.R. & Pollard, E. (1952)
Combined thermal and primary ionization effects
on a bacterial virus.
Archives of Biochemistry and Biophysics, 36, 311-322.
- Airas, K.R. (1972)
Thermal inactivation and reactivation of an
enzyme in vitro.
Biochemical Journal, 130, 111-119.
- Alfieri, A.A., Hahn, E.W. & Kim, J.H. (1975)
The relationship between the time of fractionated
and single doses of radiation and hyperthermia
on the sensitization of an in vivo mouse tumour.
Cancer, 36, 893-903.
- Almaric, F., Simard, R. & Zalta, J.P. (1969)
Effect de la temperature supra-optimal sur les
ribonucleoproteins et la RNA nucleolaire.
Experimental Cell Research, 55, 370-377.
- Auersperg, N. (1966)
Differential heat sensitivity of cells in tissue culture.
Nature, 209, 415-416.
- Bacq, Z.M. & Alexander, P. (1955)
Fundamentals of Radiobiology.
London: Butterworth Scientific.
- Barnes, R., Vogel, H. & Gordon, I. (1969)
Temperature of compensation: Significance for virus
inactivation.
Proceedings of the U.S. National Academy of Science,
62, 263-270.
- Belehradek, J. (1957)
Physiological aspects of heat and cold.
Annual Review of Physiology, 19, 59-82.
- Belli, J.A., & Bonte, F.J. (1963)
Influence of temperature on the radiation response
of mammalian cells in culture.
Radiation Research, 18, 272-276.

BenHur, E., Bronk, B.V. & Elkind, M.M (1972)
Thermally enhanced radiosensitivity of cultured
Chinese Hamster cells.
Nature, 238, 209-211.

BenHur, E. & Elkind, M.M. (1974a)
Thermal sensitization of Chinese Hamster cells to
methyl methane-sulphonate; Relation of DNA damage
and repair to survival response.
Cancer Biochemistry Biophysics, 1, 23-32.

BenHur E. & Elkind, M.M. (1974b)
Thermally enhanced radioresponse of cultured Chinese
Hamster cells; Damage and repair of single-stranded
DNA and DNA complex.
Radiation Research, 59, 484-495.

BenHur, E., Elkind, M.M. & Bronk, B.V. (1974)
Thermally enhanced radioresponse of cultured
Chinese Hamster cells: Inhibition of repair of
sublethal damage and enhancement of lethal damage.
Radiation Research, 58, 38-51.

BenHur, E. & Elkind, M.M. (1976)
DNA damage and its repair in hyperthermic mammalian
cells: Relation to enhanced cell killing.
Radiation Research, (in press).

Bergan, P. (1960)
Blocking of mitosis by heat shock
Nature, 186, 905-906.

Bernstein, E. & Zeuthen, E. (1966)
The relationship of RNA synthesis to temperature as
an inducer of synchronous division.
Compte Rendu Des Travaux Du Laboratoire
Carlsberg, 35, 501-517.

Bowler, K., Duncan, C.J., Gladwell, R.T. & Davison, T.F.
Cellular heat injury.
Comparative Biochemistry Physiology, 45, 441-450.

Brannen, J.P. (1975)
A temperature and dose rate-dependent model for the
kinetics of cellular response to ionizing radiation.
Radiation Research, 62, 379-387.

- Bronk, B.V., Wilkins, R.J. & Regan, J.D. (1975)
Thermal enhancement of DNA damage by an alkylating agent in human cells.
Biochemical Biophysical Research Communications, 52, 1064-1070.
- Burger, F.J., & Fuhrman, F.A. (1964a)
Evidence of injury to tissues after hyperthermia.
American Journal of Physiology, 206, 1062-1064.
- Burger, F.J. & Fuhrman, F.A. (1964b)
Evidence of injury by heat in mammalian tissue.
American Journal of Physiology, 206, 1057-1061.
- Busch, W. (1866)
Über den Einfluss welchen heftigere Erysipela
Zuweilen auf organisierte Neubildungen ausüben.
Verhandl Naturh Preuss Rhein Westphal, 23, 28-30.
- Buzzell, A. & Lauffer, M.A. (1952)
X-ray studies on T5 bacteriophage.
Archives of Biochemistry & Biophysics, 39, 195-204.
- Byfield, J.E. & Scherbaum, O.H. (1966a)
Temperature dependent RNA decay in tetrahymena.
Journal of Cellular Physiology, 68, 203-205.
- Byfield, J.E. & Scherbaum, O.H. (1966b)
Suppression of RNA and protein accumulation by
temperature shifts in a heat-synchronized protozoan.
Life Sciences, 5, 2263-2269.
- Byfield, J.E. & Scherbaum, O.H. (1967a)
Temperature dependent decay of RNA and of
protein synthesis in a heat synchronized protozoan.
Proceedings of the U.S. National Academy of
Science, 57, 602-606.
- Byfield, J.E. & Scherbaum, O.H. (1967b)
Temperature effect on protein Synthesis in
heat synchronized protozoan treated with actinomycin D.
Science, 156, 1504-1508.

Cater, D.B., Silver, I.A. & Watkinson, D.A. (1964)
Combined therapy with 220kV roentgen and 10cm
microwave heating in rat hepatoma.
Acta Radiologica Therapy Physics Biology, 2, 321-336.

Cavaliere, R., Ciocatto, E.C., Giovannella, C.,
Heidelberger, C., Johnson, R.D., Margottini, M.,
Mondovi, B., Moricca, G. & Rossi-Fanelli, A. (1967)
A selective heat sensitivity of cancer cells.
Cancer, 20, 1351-1381.

Cerino, L.E., Ackerman, E. & Jones, J.M. (1966)
Effects of heat and ultrasound on VX-2
carcinoma in bones of rabbits.
Journal of the Acoustical Society of America,
40, 916-918.

Chapman, D. (1967)
The effect of heat on membranes and
membrane constituents.
In Thermobiology, ed. Rose, A.H.
123-145, London: Academic Press.

Chen, T.T. & Heidelberger, C. (1969)
Quantitative studies on the malignant transformation
of mouse prostrate cells in carcinogenic hydrocarbons
in vitro.
International Journal of Cancer,
4, 166-178.

Clarke, P.R., Hill, C.R. & Adams, K. (1970)
Synergism between ultrasound and x-rays in
tumour therapy.
British Journal of Radiology, 43, 97-99.

Cockett, A.T.K., Kazmin, M., Nakamura, R.,
Fingerhut, A. & Stein, J.J. (1967)
Enhancement of regional bladder cancer using
local bladder hyperthermia.
Journal of Urology, 97, 1034-1039.

Coley, W.B. (1893)
The treatment of malignant tumours by repeated
inoculations of erysipelas with a report of
ten original cases.
American Journal of Medical Sciences, 105, 487-511.

- Crile, G. Jr. (1961)
Heat as in adjunct to the treatment of cancer.
Cleveland Clinic Quarterly, 28, 75-89.
- Crile, G. Jr. (1962)
Selective destruction of cancers after
exposures to heat.
Annals of Surgery, 156, 404-407.
- Crile, G. Jr. (1963)
The effects of heat and radiation on
cancers implanted on the feet of mice.
Cancer Research, 23, 372-380.
- DeFlora, S. & Badolati, G. (1973)
Thermal inactivation of untreated and gamma
irradiated A2/AICHI/2/68 influenza virus.
Journal of General Virology. 20, 261-265.
- Dennis, J.A. (1971)
Energy loss characteristics of heavy ions
in nitrogen, carbon dioxide, argon,
hydrocarbon gases and tradescantia tissue.
AERE -M 2346
- Dertinger, H. & Jung, H. (1970)
Molecular Radiation Biology
New York: Springer-Verlag.
- Dewey, W.C., Furman, S. & Miller, H.H. (1970)
Comparison of lethality and chromosomal
damage induced by x-rays in synchronized
Chinese hamster cells.
Radiation Research, 43, 561-581.
- Dewey, W.C., Miller, H.H. & Leeper, D.B. (1971)
Chromosomal aberrations and mortality of X
irradiated mammalian cells: Emphasis on repair.
Proceedings of the U.S. National Academy of
Sciences, 68, 667-671.
- Dewey, W.C., Westra, A., Miller, H.H., Nagasawa, H. (1971)
Heat induced lethality and chromosomal damage in
synchronized Chinese Hamster cells treated with 5-
bromodeoxyuridine.
International Journal of Radiation Biology, 20,
505-520.

Dewey, W.C. (1972)

Confirmation of lesions having the potential for forming chromosomal aberrations. International Journal of Radiation Biology, 22, 95-97.

Dickson, J.A. & Muckle, D.S. (1972)

Total body hyperthermia versus primary tumour Hyperthermia in the treatment of the rabbit VX-Z carcinoma. Cancer Research, 32, 1916-1923.

Dickson, J.A. & Shah, D.M. (1972)

The effects of H.T. 42°C on the biochemistry and growth of a malignant cell line. European Journal of Cancer, 8, 561-571.

Dickson, J.A. & Ellis, H.A. (1974)

Stimulation of tumour cell dissemination by raised temperature (42°C) in rats with transplanted Yoshida Tumours. Nature, 248.

Dickson, J.A. & Suzangar, M. (1974)

In vitro in vivo studies on the susceptibility of the solid Yoshida sarcoma to drugs and hyperthermia (42°C) Cancer Research, 34, 1263-1274.

Dietzel, F. (1974)

Tumour synchronization by microwaves animal experiments concerning susceptibility of proliferation kinetics of the tumour in vivo to non ionizing radiation Strahlentherapie, 148, 531-542.

Dietzel, F. (1975)

Tumor und Temperatur
Urban & Schwarzenborg: Munchen.

Dietzel, F. (1975)

Hyperthermal treatment of malignant tumours: possibilities and limitations Therapiewoche, 25, 2341-2349.

Dietzel, F., Seibert, G. & Klobe, G. (1975)

The influence of a high frequency hyperthermia on the Erlich ascites carcinoma in the mouse. Strahlentherapie, 149, 105-117.

DiGioia, G.A., Licciardello, J.J., Vickerson, J.T.R. & Goldblith, S.A. (1970)
Thermal inactivation of Newcastle Disease Virus.
Applied Microbiology, 19, 451-454.

DiGioia, G.A., Licciardello, J.J., Vickerson, J.T.R. & Goldblith, S.A. (1970)
Effect of temperature on radiosensitivity of
Newcastle Disease Virus.
Applied Microbiology, 19, 455-457.

Doemin, N.N. & Blokhina, V.D. (1961)
Radiation-induced disturbances of the lipids
of cellular microstructures
In The Initial Effects of Ionizing Radiation on Cells
ed. Harris, R.J.C., 141-152,
London: Academic Press.

Elkind, M.M. & Sutton, H. (1959)
X-ray damage and recovery in mammalian
cells in culture.
Nature, 184, 1293-1295.

Elkind, M.M. & Sutton, H. (1960)
Radiation response of mammalian cells grown in
culture 1. Repair of x-ray damage in surviving
Chinese Hamster cells.
Radiation Research, 13, 556-593.

Elkind, M.M., Sutton, H., Gilbert, Moses, W.B.,
Alescio, T. & Swain, R.W. (1965)
Radiation response of mammalian cells grown in
culture part v temperature dependence.
Radiation Research, 25, 359-376.

Elkind, M.M., Swain, R.W., Alescio, T., Sutton, H. &
Moses, W.B. (1965)
Oxygen nitrogen recovery and radiation therapy
In Cellular Radiation Biology
442-466, Baltimore: William and Wilkins.

Elkind, M.M. & Whitmore, G.F. (1967)
The Radiobiology of Cultured Mammalian Cells
London: Gordon and Breach.

Erresa, M. & Forssberg, A. (1960)
Mechanisms in Radiobiology
Academic Press: New York

Euler, J., Priesching, A. & Wenzl, J. (1974)
Hyperthermia peritoneal perfusion in rats with
ascites tumour.

Wein Klinische WSCHR, 86, 220-225.

Evans, P.R. & Bowler, K. (1973)
Thermal death and the denaturation
of proteins.
Sub-cellular Biochemistry, 2, 91-95.

Evans, R.G., Li, G.C. & Hahn, G.M. (1975)
Modification of repair of potentially lethal
x-ray damage by hyperthermia.
Radiation Research, 62, ABST 6D-3.

Exner, O. (1964)
Concerning the isokinetic relationship.
Nature, 201, 488-490.

Eyring, H. (1935)
The activated complex in chemical reactions.
Journal of Chemistry and Physics, 3, 107-115

Gerner, E.W. & Schneider, M.J. (1975)
Induced thermal resistance in HeLa cells.
Nature, 256/5517, 500-502.

Gerweck, L.E., Gillette, E.L. & Dewey, W.C. (1975)
Effect of heat and radiation on synchronous
Chinese Hamster cells: Killing and repair.
Radiation Research, 64, 611-623.

Gerweck, L.E., Gillette, E.L. & Dewey, W.C. (1974)
Killing of Chinese Hamster cells in vitro by heating
under hypoxic or aerobic conditions.
European Journal of Cancer, 10, 691-693.

Gilchrist, R.K., Medal, R. & Shorey, W. (1957)
Selective heating of lymph nodes.
Annals of Surgery, 146, 596-606.

- Giles, N.H. Jr., Beatty, A.V. & Parkes, R.H. (1951)
The relation between the effects of temperature
and of oxygen on the frequency of x-ray induced
chromosome aberrations in *tradesantia* microspores.
Genetics, 36, 552-553. ABST
- Giovanella, B.C., Morgan, A.C., Stehlin, J.S. &
Williams, L.J. (1973)
Selective lethal effects of supranormal temperatures
on mouse sarcoma cells.
Cancer Research, 33, 2568-2578.
- Giovanella, B.C., Lohman, W.A. & Heidelberger, C. (1970)
Effects of elevated temperature and drugs on the
viability of L1210 leukemia cells.
Cancer Research, 30, 1623-1631.
- Giovanella, B.C., Mosti, R. & Heidelberger, C. (1969)
Further studies of the lethal effects of heat
on tumours.
Cancer Research, 29, ABST 29.
- Giovanella, B.C. & Heidelberger, C. (1968)
Biochemical and biological effects of heat
on normal and neoplastic cells.
Proceedings of the American Association for
Cancer Research, 9, ABST 92
- Ginoza, W. & Zimm, B.H. (1961)
Mechanisms of inactivation of
deoxyribonucleic acids by heat.
Proceedings of the U.S. National Academy
of Sciences, 47, 639-652.
- Ginoza, W. (1958)
The kinetics of heat inactivation of
ribonucleic acid of TMV.
Nature, 181, 958-961.
- Goldenberg, D.M. & Langner, M. (1971)
Direct and absopal antitumour action of
local hyperthermia.
Zeitschrift Fur Naturforschung, 26b, 359-361.
- Greer, S. & Zamenhof, S. (1962)
Studies on depurination of DNA by heat.
Journal of Molecular Biology, 4, 123-141.

- Hahn, G., Braun, J. & Har-kedor, I. (1975)
Thermochemotherapy: Synergism between hyperthermia (42-43°) and adriamycin (or bleomycin) in mammalian cell inactivation.
Proceedings of the National Academy of Sciences, 72, 937-940.
- Hahn, G.M. (1974)
Metabolic aspects of the rate of hyperthermia in mammalian cell inactivation and their possible relevance to cancer research.
Cancer Research, 34, 3117-3123.
- Hahn, E.W., Alfieri, A.A. & Kim, J.H. (1974)
Increased cures using fractionated exposure of x-irradiation and hyperthermia in the local treatment of the Ridgeway osteogenic sarcoma in mice.
Radiology, 113, 199-202.
- Hahn, E.W., Canada, T.R., Alfieri, A.A. & McDonald, J.C. (1974)
The radiation enhancement factor (REF) of hyperthermia in combination with fast neutrons on local tumour response.
Radiation Research, 59, ABST. B-35-5.
- Hahn, E.W., Feingold, S.M. & Kim, J.H. (1974)
The effect of radiation and hyperthermia on growing bone.
Radiation Research, 59, ABST. D-12-5.
- Harisiadis, L., Hall, E.J., Kraljevic, U. & Borek, C. (1975)
Hyperthermia: Biological studies at the cellular level.
Radiology, 117/2, 447-452.
- Hall, E.J. (1976)
Response of cultured cells to hyperthermia with special reference to thermal tolerance and hypoxia.
E.I.R. work in progress meeting, May 21, 1976.
- Hall, E.J. (1973)
Radiobiology for the Radiologist.
Hagerstown: Harper and Row.
- Hall, E.J., Bedford, J.S. & Oliver, R. (1966)
Extreme hypoxia: its effects on the survival of mammalian cells irradiated at high and low dose rate.
British Journal of Radiology, 39, 302-307.

Hall, E.J., Novak, J.K., Kellner, A.M., Rossi, H.H.,
Marino, S. & Goodman, L.J. (1975)
RBE as a function of neutron energy
1. Experimental observations.
Radiation Research, 64, 245-255.

Hall, R.R. (1974)
The effects of hyperthermia on bladder cancer.
British Medical Journal, 2, 593-594.

Hamlick, P.E. (1973)
Thermal denaturation of DNA exposed to 2450 mhz c.w.
microwave radiation.
Radiation Research, 56, 400-404.

Harris, M. (1969)
Growth and survival of mammalian cells under
continuous thermal stress.
Experimental Cell Research, 56, 382-386.

Harris, M. (1967)
Temperature resistant variants in clonal
populations of pig kidney cells.
Experimental Cell Research, 46, 301-314.

Harris, M. (1966)
Criteria of viability in heat treated cells.
Experimental Cell Research, 44, 658-660.

Haurowitz, F. (1950)
Chemistry and Biology of Proteins.
Academic Press Inc. New York.

Hayflick, L. (1965)
Tissue cultures and mycoplasma.
Texas Reports on Biology and Medicine.
23, 285-303.

Heine, U., Suerek, L., Kondratich, J. & Bonar, R.A. (1971)
The behaviour of HeLa-S₃ cells under the influence of
supranormal temperatures.
Journal of Ultrastructure Research, 34, 375-396.

- Henderson, M.A. & Pettigrew, R.T. (1971)
Induction of controlled hyperthermia in
treatment of cancer.
The Lancet, 1, 1275-1277.
- Henle, K.J. & Leeper, D.B. (1976)
The interaction of hyperthermia and radiation
in CHO cells - Recovery kinetics of sublethal damage.
Radiation Research, (in press).
- Henle, K.J. & Leeper, D.B. (1975)
Temperature dependence of the interaction
of radiation and hyperthermia damage in
mammalian cells.
Radiation Research, ABST. GD-1.
- Henriques, F.C. Jr. (1974)
Studies of thermal injury: The predictability
and significance of thermally induced rate
processes leading to irreversible epidermal injury.
Archives of Pathology, 43, 489-502.
- Howard, A. & Pele, S.R. (1953)
Synthesis of deoxyribonucleic acid in normal and
irradiated cells and its relation to chromosome breakage.
Heredity, 6, 261-273.
- Hofer, K.G. (1975)
Effect of hyperthermia on the radiosensitivity
of L1210 leukemia and Erlich ascites cells in vivo.
Radiation Research, 62, ABST. GD-6.
- ICRU Report 13 (1969)
Neutron Fluence, Neutron Spectra and Kerma.
International Commission on Radiation
Units and Measurements, Washington D.C.
- ICRU Report 85 (1965)
Physical Aspects of Radiation.
International Commission on Radiation
Units and Measurements, Washington D.C.
- Johnson, F.H., Eyring, H. & Palissor, M.J. (1954)
The Kinetic Basis of Molecular Biology.
London: Chapman and Hall.

- Johnson, F.H. (1974)
The Theory of Rate Processes in Biology and Medicine
 London: John Wiley & Sons.
- Johnson, H.A. & Pavelec, M. (1972a)
 Thermal injury due to normal body temperature.
 American Journal of Pathology, 66, 557-564.
- Johnson, H.A. & Pavelec, M. (1972b)
 Thermal noise in cells: A cause of "spontaneous"
 loss of cell function.
 American Journal of Pathology, 69, 119-130.
- Johnson, H.A. & Pavelec, M. (1973)
 Thermal enhancement of thio-tepa cytotoxicity.
 Journal of The National Cancer Institute, 50, 903-908.
- Johnson, H.J. (1940)
 The action of short radiowaves on tissue III.
 A comparison of the thermal sensitivities of
 transplantable tumours in vivo and in vitro.
 American Journal of Cancer, 38, 533-550.
- Joly, M. (1965)
A Physico-Chemical Approach to the Denaturation
 of Proteins
 London: Academic Press.
- Kachani, Z.F.C. & Sabin, A.B. (1969)
 Reproductive capacity and viability at higher
 temperatures of various transformed hamster
 cell lines.
 Journal of The National Cancer Institute, 43, 469-480.
- Kal, H.B., Hatfield, M. & Haln, G.M. (1975)
 Cell cycle progression of murine-sarcoma cells
 after x-irradiation or heat shock.
 Radiology, 117/1, 215-217.
- Kaplan, H.S. (1974)
 On the relative importance of hypoxic cells
 for the radiotherapy of human tumours.
 European Journal of Cancer, 10, 275-280.

- Kase, K. & Hahn, G.M. (1975)
Differential heat response of normal and transformed human cells in tissue culture.
Nature, 255, 228-230.
- Katz, R., Ackerson, E., Homayoonfar, M. & Sharma, S.C. (1971)
Inactivation of cells by heavy ion bombardment.
Radiation Research, Vol. 47, 402-425.
- Katz, R. & Sharma, S.C. (1974)
Cellular survival in a mixed radiation environment.
International Journal of Radiation Biology, Vol. 26, 143-
- Kim, J.H., Kim, S.H. & Hahn, E.W. (1974)
Thermal enhancement of the radiosensitivity using cultured normal and neoplastic cells.
American Journal of Roengenology Radium Therapy Nuclear Medicine, 121, 860-864.
- Kim, S.H., Kim, J.H. & Hahn, E.W. (1975)
The radiosensitization of hypoxic tumour cells by hyperthermia.
Radiology, 114/3, 727-728.
- Lai, P.K. & Ducoff, H.S. (1975)
Hyperthermia suppresses repair of sublethal radiation damage in the adult Flower Beetle, tribolum confusum.
Radiation Research, 62, ABST. GD-4.
- Lambert, R.A. (1912)
Demonstration of the greater susceptibility to heat of sarcoma cells.
Journal of The American Medical Association, 59, 2147-2148.
- Lappenbusch, W.L., Gillespie, L.J., Leach, W.M. & Anderson, G.E. (1973)
Effect of 2450 mhz microwaves on the radiation response of x-irradiated Chinese Hamsters.
Radiation Research, 54, 294-303.

- Leeper, D.B., Schneiderman, M.H. & Dewey, W.C. (1972)
Radiation-induced division delay in synchronized
Chinese Hamster ovary cells in monolayer culture.
Radiation Research, 50, 401-417.
- Leeper, D.B. & Henle, K.J. (1974)
The interaction of radiation and hyperthermic
damage in CHO cells.
Radiation Research, 59, ABST. B-35-2.
- Levine, E.M. & Robbins, E.B. (1970)
Differential temperature sensitivity of normal
and cancer cells in culture.
Journal of Cellular Physiology, 76, 373-380.
- Levy, M.R., Gollon, C.E. & Elliot, A.M. (1969)
The effects of hyperthermia on tetrahymena.
Experimental Cell Research, 55, 295-305.
- Love, R., Soriano, R. & Walsh, R. (1970)
Effect of hyperthermia on normal and neoplastic
cells in vitro.
Cancer Research, 30, 1525-1533.
- Lumry, R. & Rajender, S. (1970)
Enthalpy-entropy compensation phenomena in water
solution of proteins and small molecules:
A ubiquitous property of water.
Biopolymers, 9, 1125-1227.
- Malone, J.F., Porter, D. & Hendry, J.H. (1974)
The r.b.e. of Co⁶⁰ gamma rays with respect to
300 kvp x-rays for the survival of HeLa S3
and CHO cells, irradiated at different states of
proliferation.
International Journal of Radiation Biology, 26, 355-362.
- Martin, R.J. & Schloerb, P.R. (1964)
Induction of mitotic Synchrony by intermittent
hyperthermia in the Walker 256 rat carcinoma.
Cancer Research, 24, 1997-2000.
- Maxwell, K.R., Kempton, J.H. & Mosley, V.M. (1942)
Effect of temperature and time on the x-ray sensitivity
of maize seeds.
Journal of the Washington Academy of Sciences,
32, 18-24.

McCormick, W. & Penman, S. (1969)
Regulation of protein synthesis in HeLa cells:
Translation of T₂ levated temperature.
Journal of Moleccullar Biology, 39, 315-333.

McGee, A.R. (1967)
Apparent antagonism of vaccinia and wart viruses.
Cancer, 20, 1647-1653.

Miller, T.R. & Nicholson, J.T. (1956)
End results in reticulum cell sarcoma of
bone treated by bacterial toxin therapy
alone or combined with surgery and or
radiotherapy (47 cases) or with concurrent
infection (5 cases).
Cancer, 27, 524-548.

Mondovi, B., Agro, A.F., Rotilio, G., Strom, R.,
Moricca, G. & Rossi-Fanelli, A. (1969)
The biochemical mechanism of selective heat
sensitivity of cancer cells II. Studies on
nucleic acids and protein synthesis.
European Journal of Cancer, 5, 137-146.

Mondovi, B., Santoro, A.S., Strom, R., Faiola, R. &
Rossi-Fanelli, A. (1972)
Increased immonogenicity of Erlich ascites cells
after heat treatment.
Cancer, 30, 885-888.

Moressi, W.J. (1964)
Mortality patterns of mouse-sarcoma 180 cells
resulting from direct heating and chronic
microwave irradiation.
Experimental Cell Research, 33, 240-253.

Moritz, A.R., & Henriques, F.C. (1947)
Studies of thermal injury.
American Journal of Pathology, 23, 695-720.

Morowitz, H.J. (1968)
Energy Flow in Biology.
London: Academic Press.

- Muckle, D.S. & Dickson, J.A. (1971)
The selective inhibitory effect of hyperthermia
on the metabolism and growth of malignant cells.
British Journal of Cancer, 25, 771-778.
- Muckle, D.S. & Dickson, J.A. (1973)
Hyperthermia (42°C) as an adjuvant to radiotherapy
and chemotherapy in the treatment of the allogeneic
VX2 carcinoma in the rabbit.
British Journal of Cancer, 27, 307-315.
- Muckle, D.S. (1974)
Response of musculoskeletal tumour to
combined radiation therapy. An in vitro - in vivo
investigation.
Acta Radiologica Therapy Physics Biology, 13, 297-306.
- Mukherjee, P. & Bhattacharjee, S.B. (1972)
Studies on the recovery of heated bacteria.
Canadian Journal of Microbiology, 18, 539-540.
- Nauts, H.C., Fowler, G.A. & Bogatko, F.H. (1953)
A review of the influence of bacterial infections
and bacterial products (Coley's toxin) on malignant
tumours of men.
Acta Medica Scandinavica, 276, 1-103.
- Nelder, J.A. & Mead, R. (1965)
A simplex method for function minimization.
The Computer Journal, 7, 308-313.
- Oag, R.K. (1940)
Resistance of bacterial spores to dry heat.
Journal of Pathology and Bacteriology, 51, 137-141.
- Okada, C., Altman, K.I. & Gerber, G.B. (1970)
Radiation Biochemistry, Vol. I: Cells
London: Academic Press.
- Okumura, V., Morita, T., Matsuzawa, T. (1973)
The effects of temperature on the dying process of
lethally irradiated cultured mouse mammary carcinoma
cells.
Radiation Research, 55, 318-323.

- Ossovski, L. & Sachs, L. (1967)
 Temperature sensitivity of polyoma virus induction
 of cellular DNA synthesis and multiplication of
 transformed cells at high temperature.
 Proceedings of the U.S. National Academy of Sciences,
 58, 1938-1943.
- Ostertag, W. (1964)
 The change in ploidy of human cells in culture
 after temperature shock.
 Experimental Cell Research, 34, 194-198.
- Overgaard, K. & Overgaard, J. (1972a)
 Investigations on the possibility of a thermic
 tumour therapy I.
 European Journal of Cancer, 8, 65-78.
- Overgaard, K. & Overgaard, J. (1972b)
 Investigations on the possibility of a thermic tumour
 therapy II.
 European Journal of Cancer, 8, 573-575.
- Overgaard, K. & Overgaard, J. (1974)
 Radiation sensitizing effect of heat.
 Acta Radiologica Therapy Physics Biology, 13/6, 501-511.
- Overgaard, K. & Overgaard, J. (1975)
 Histologic and histochemical reactions in a
 mouse mammary carcinoma following exposure
 to combined heat roentgen irradiation.
 Acta Radiologica Therapy Physics Biology, 14, 164-176.
- Palzer, R.J. & Heidelberger, C. (1973a)
 Studies on the quantitative biology of hyperthermic
 killing of HeLa cells.
 Cancer Research, 33, 415-421.
- Palzer, R.J. & Heidelberger, C. (1973b)
 Influence of drugs and synchrony on the hyperthermic
 killing of HeLa cells.
 Cancer Research, 33, 422-427.
- Paul, I.J. & Zimmerman, A.M. (1973)
 Macromolecular synthesis and cell division in
 x-irradiated tetrahymena.
 Radiation Research, 55, 411-421.

Pettigrew, R.T., Galt, J.M., Ludgate, C.M. & Smith, A.N. (1974)
Clinical effects of whole body hyperthermia in advance malignancy.
British Medical Journal, 4, 679-682

Phillips, T.L., Kane, L.J. & Utley, J.F. (1975)
Thermal enhancement and oxygen enhancement ratios for EMTG carcinoma irradiated with gamma rays and neutrons.
Radiation Research, 62, ABST. GD-11.

Pinchus, G. & Fischer, A. (1931)
The growth and death of tissue cultures exposed to supranormal temperatures.
Journal of Experimental Medicine, 54, 323-329.

Pitot, H.C. (1966)
Some biochemical aspects of malignancy.
Annual Reviews of Biochemistry, 35, 335-368.

Pollard, E.C. (1966)
Physical considerations influencing radiation response.
In Radiobiological Basis of Radiotherapy, ed. E.E. Schwartz. London: Pitman Medical Publishing Co. Ltd. 1-30.

Pomp, H. (1974)
Clinical experiences with therapeutic hyperthermia in incurable gynecologic tumours.
Krebsgeschehen, 6, ABST. 15-16.

Powers, E.L., Webb, R.B. & Ehret, C.F. (1959)
Modifications of sensitivity to radiation in single cells by physical means.
Progress in Nuclear Energy (Series VI), 2, 189-198

Precht, H., Christophersen, J., Hensel, H. & Larcher, W. (1973)
Temperature and Life.
Berlin: Springer-Verlag.

Puck, T.T. & Markus, P.I. (1956)
Action of x-rays on mammalian cells.
Journal of Experimental Medicine, 103, 653-666.

- Rahn, O. (1945)
Physical methods of sterilization of micro-organisms.
Bacteriological Reviews, 1-47.
- Railton, R., Lawson, R.C., Porter, D. & Hannan, W.J. (1973)
Neutron spectrum dependance of r.b.e. and o.e.r. values.
International Journal of Radiation Biology, 5, 509-518.
- Railton, R., Lawson, R.C., Porter, D. & Hannan, W.J. (1974)
The oxygen enhancement ratio and relative biological effectiveness for combined irradiations of Chinese Hamster cells by neutrons and x-rays.
International Journal of Radiation Biology, 25, 121-127.
- Railton, R., Lawson, R.C. & Porter, D. (1975)
Interaction of x-rays and neutron effects on the proliferation capacity of Chinese Hamster cells.
International Journal of Radiation Biology, 27, 75-82.
- Rao, P.N. & Engelberg, J. (1965)
HeLa cells: effect of temperature on the life cycle.
Science, 148, 1092-1094.
- Reeves, O.R. (1972)
Mechanisms of acquired resistance to acute heat shock in cultured mammalian cells.
Journal of Cellular Physiology, 79, 157-170.
- Reid, C. (1957)
Excited States in Chemistry and Biology.
London: Butterworths
- Robinson, J.E. & Wizenberg, M.J. (1974)
Thermal sensitivity and the effect of elevated temperatures on the radiation sensitivity of Chinese Hamster cells.
Acta Radiologica Therapy Physics Biology, 13, 241-248.
- Robinson, J.E., Wizenberg, M.J. & McCready, W.A. (1974)
Radiation and hyperthermal response of normal tissue in situ.
Radiology, 113, 195-198.
- Robinson, J.E., Wizenberg, M.J. & McCready, W.A. (1974)
Combined hyperthermia and radiation suggest an alternative to heavy particle therapy for reduced oxygen enhancement ratio.
Nature, 251, 521-522.

- Rohdenburg, G.L. (1918)
Fluctuations in the growth of malignant tumours in man with special reference to spontaneous recession.
Journal of Cancer Research, 3, 193-225.
- Rohdenburg, G.L. & Prime, F. (1921)
The effect of combined radiation and heat on neoplasms.
Archives of Surgery, 2, 116-129.
- Rosenbaum, N., Beach, J.E. & Holz, C.G. (1966)
The induction of a phospholipid requirement and morphological abnormalities in tetrahymena pyriformis by growth at supraoptimal temperatures.
Journal of Protozoology, 13, 535-546.
- Rosenberg, B., Kemeny, G. & Switzer, R.C. (1971)
Quantitative evidence for protein denaturation as the cause of thermal death.
Nature, 232, 471-473.
- Sapozink, M.D., Deschner, D.D. Hahn, E.W. (1973)
Induction of mitotic synchrony by intermittent hyperthermia in Erlich carcinoma in vivo.
Nature 244. 299-300.
- Schiebel, W., Chayka, T.G., DeVries, A. & Rusch, H.P. (1969)
Decrease of protein synthesis and breakdown of polysomes by elevated temperatures in physarum polycephalum.
Biochemical and Biophysical Research Communications, 35, 338-345.
- Schindler, R., Ramseier, L. & Greider, A. (1966)
Increased sensitivity of mammalian cell cultures to radiomimetic alkylating agents following incorporation of 5-bromo deoxyuridine into cellular DNA.
Biochemical Pharmacology, 15, 2013-2023.
- Schrek, R. (1966)
Sensitivity of normal leukemic lymphocytes and leukemic myeloblasts to heat.
Journal of The National Cancer Institute, 37, 649-654.
- Selawry, O.S., Goldstein, M.N. & McCormick, T. (1957)
Hyperthermia in tissue-cultured cells of malignant origin.
Cancer Research, 17, 785-791.

- Selawry, O.S., Carson, J.C. & Moore, G.E. (1958)
Tumour response to ionizing rays at elevated temperatures.
American Journal of Roentgenology Radium Therapy
Nuclear Medicine, 80, 833-839.
- Setlow, R.B. (1952)
The inactivation of urease by deuterons and heat.
Archives of Biochemistry and Biophysics, 36, 328-335.
- Setlow, R.B. (1952)
Radiation sensitivity of catalase as a function of
temperature.
Proceedings of The U.S. National Academy of
Sciences, 38, 166-172.
- Shingleton, W.W., Bryan, F.A., O'Quinn, W.L. & Krueger,
L.C. (1962)
Selective heating and cooling of tissue in cancer
chemotherapy.
Annals of Surgery, 156, 408-416.
- Schulman, N. & Hall, E.J. (1974).
Hyperthermia: Its effect on proliferative and
plateau phase cell cultures.
Radiology, 113, 209-212.
- Simard, R. & Bernhard, W. (1967)
A heat sensitive cellular function located in the nucleolus.
Journal of Cell Biology, 34, 61-76.
- Simard, R., Almaric, F. & Zalta, J.P. (1969)
Effect de la temperature supra-optimale sur les
ribonucleo-proteines et le RNA nucleolaire.
Experimental Cell Research, 55, 359-369.
- Sisken, J.E., Morosca, L. & Kibby, S. (1965)
The effects of temperatures on kinetics of the
mitotic cycle of mammalian cells in culture.
Experimental Cell Research, 39, 103-116.
- Stehlin, J.S. (1969)
Hyperthermic profusion with chemotherapy for
cancers of the extremities.
Surgery Gynecology Obstetrics, 129, 305-

- Strom, R., Santoro, A.S., Crife, C., Bozzi, A., Mondouri, B. & Rossi-Fanelli, A. (1973)
The biochemical mechanism of selective heat sensitivity of cancer cells IV. Inhibition of RNA synthesis.
European Journal of Cancer, 9, 103-112.
- Suit, K.D. & Shwayder, M. (1974)
Hyperthermia: Potential as an anti-tumour agent.
Cancer, 34, 122-129.
- Suzuki, K. (1967)
Application of heat to cancer chemotherapy.
Nagoya Journal of Medical Science 30, 1-21.
- Szumiel, I. & Nias, A.H.W. (1976a)
Action of a platinum complex on Chinese Hamster ovary cells in vitro.
Chemical Biological Interaction (in press).
- Szumiel, I. & Nias, A.H.W. (1976b)
The effect of combined treatment with a platinum complex and ionizing radiation on Chinese Hamster ovary cells in vitro.
The British Journal of Cancer, Vol. 33, 450-458.
- Taylor, C.V. & Strickland, A.G.R. (1936)
Effects of high vacua and extreme temperature on cysts of colpoda cucullus.
Physiological Zoology, 9, 15-26.
- Thrall, D.E., Gillette, E.L. & Dewey, W.C. (1973)
Effect of heat on the C3H mouse mammary adenocarcinoma evaluated in terms of tumour growth.
European Journal of Cancer, 9, 871-875.
- Thrall, D.E., Gillette, E.L. & Dewey, W.C. (1975)
Effect of heat and ionizing radiation on normal and neoplastic tissue of the C3H mouse.
- Todd, P. & Schroy, C.B. (1974)
X-ray inactivation of cultures of mammalian cells: enhancement by ultrasound.
Radiology, 113, 445-447.
- Terasima, T. & Tolmach, L.J. (1963)
Variations in several responses of HeLa cells during the division cycle.
Biophysical Journal, 3, 11-33.

Turano, C., Ferraro, A., Strom, R., Cavaliere, R. & Rossi-Fanelli, A. (1970)
The biochemical mechanism of selective heat sensitivity of cancer cells - III studies on lysosomes. European Journal of Cancer, 6, 67-72.

Trujillo, R. & Dugan, V.L. (1972)
Synergistic inactivation of viruses by heat and ionizing radiation. Biophysical Journal, 12, 92-113.

Vermel, E.M. & Kuznetsova, L.B. (1970)
Hyperthermia in the treatment of malignant growths. Vaprosy Onkologii, 16, 96-102 (translation).

Vollmar, H. (1941)
Über den einfluss der temperatur auf normales gewebe und auf tumorgewebe. Zeitschrift Krebsforsch, 51, 71-99.

Von Ardenne, M. (1972)
Selective multiphase cancer therapy conceptual aspects and experimental basis. Advances in Pharmacology and Chemotherapy, 10, 339-380.

Wang, R.J. (1974)
Temperature sensitive mammalian cell line blocked in mitosis. Nature, 248, 76-78.

Warocquier, R. & Scherrer, K. (1969)
RNA metabolism in mammalian cells at elevated temperatures. European Journal of Biochemistry, 10, 362-370.

Warren, S.L. (1935)
Preliminary study of the effect of artificial fever upon hopeless tumour cases. American Journal of Roentgenology Radium Therapy. Nuclear Medicine, 33, 75-87.

Webb, R.B., Powers, E.L. & Ehret, C.R. (1960)
Thermorestitution of radiation damage in dry bacterial spores. Radiation Research, 12, 682-693.

- Westermarck, N. (1927)
The effect of heat upon rat tumours.
Skandinavisches Archiv Fur Physiologie, 52, 257-322.
- Westra, A. & Dewey, W.C. (1971)
Variation in sensitivity to heat shock during the
cell cycle of Chinese Hamster cells in vitro.
International Journal of Radiation Biology, 19, 467-477.
- Whitemore, G.F. & Till, J.E. (1964)
Quantitation of cellular radiobiological responses.
Annual Review of Nuclear Science, 14, 347-374.
- Winans, L.F., Dewey, W.C. & Dettor, C.M. (1972)
Repair of sublethal and potentially lethal x-ray
damage in synchronous Chinese Hamster cells.
Radiation Research, 52, 333-351.
- Wood, T.H. (1954)
Influence of temperature and phase state on
x-ray sensitivity of yeast.
Archives of Biochemistry and Biophysics, 52, 157-174.
- Woodhall, B., Pickrill, K.L. & Georgiade, N.G. (1960)
Effect of hyperthermia upon cancer chemotherapy.
Application to external cancer of head and face structures.
Annals of Surgery, 151, 750-759.
- Wurst, G. & Prang, L. (1973)
The effect of hyperthermia on the growth of a
heterotransplanted human sigma carcinoma.
Zeitschrift Krebsforsch, 79/3, 204-211.
- Yerushalmi, A. & Har-Kedar, I. (1974)
Enhancement of radiation effects by heating of the
tumour.
Israel Journal of Medical Science, 10, 772 776.
- Yerushalmi, A. (1975)
Cure of a solid tumour by simultaneous administration
of microwaves and x-ray irradiation.
Radiation Research, 64, 602-610.